İSTANBUL TECHNICAL UNIVERSITY ★ INSTITUTE OF SCIENCE AND TECHNOLOGY

HETEROLOGOUS EXPRESSION OF TWO PUTATIVE GLUTAMATE SYNTHASE SUBUNITS FROM *PYROCOCCUS HORIKOSHII*

M.Sc. Thesis by

Hande AKÇE, B.Sc.

Department : Advanced Technologies

Programme: Molecular Biology - Genetics and Biotechnology

JUNE 2006

İSTANBUL TECHNICAL UNIVERSITY ★ INSTITUTE OF SCIENCE AND TECHNOLOGY

HETEROLOGOUS EXPRESSION OF TWO PUTATIVE GLUTAMATE SYNTHASE SUBUNITS FROM *PYROCOCCUS HORIKOSHII*

M.Sc. Thesis by

Hande AKÇE, B.Sc.

(721031210)

Date of submission : 8 May 2006

Date of defence examination: 15 June 2006

Supervisor (Chairman): Assoc. Prof.Dr. Benan DİNÇTÜRK BOTOFTE

Members of the Examining Committee Assist. Prof.Dr. Eda TAHİR TURANLI (İ.T.Ü.)

Prof.Dr. Abdul Rezzak MEMON (TUBİTAK-GMBAE)

JUNE 2006

İSTANBUL TEKNİK ÜNİVERSİTESİ ★ FEN BİLİMLERİ ENSTİTÜSÜ

PYROCOCCUS HORİKOSHİİ İKİ PUTATİF GLUTAMAT SENTAZ KÜÇÜK ALTÜNİTE HOMOLOGLARININ HETEROLOG EKSPRESYONU

YÜKSEK LİSANS TEZİ

Hande AKÇE, B.Sc.
(721031210)

Tezin Enstitüye Verildiği Tarih : 8 Mayıs 2006
Tezin Savunulduğu Tarih : 15 Haziran 2006

Tez Danışmanı :	**Doç.Dr. Benan DİNÇTÜRK BOTOFTE**
Diğer Jüri Üyeleri :	**Yrd.Doç.Dr. Eda TAHİR TURANLI (İ.T.Ü.)**
	Prof.Dr. Abdul Rezzak MEMON (TUBİTAK-GMBAE)

JUNE 2006

ACKNOWLEDGEMENT

Regarding this study, I would like to express my special thanks to Associate Professor Dr. H. Benan Dinçtürk Botofte for her help and advice throughout the realization of the project. She provided a motivating, enthusiastic and critical atmosphere during many discussions we had. It was a great pleasure for me to carry out this thesis under her supervision.

I would also like to thank Volkan Demir for his encouragement and constructive comments all through my research.

In addition, I am pleased to acknowledge the supports given by T.R. Prime Ministry The State Planning Organization through the Advanced Technologies in Engineering project in Istanbul Technical University and by TUBITAK Basic Sciences Research Group through the TBAG 1904 project.

May, 2006 Hande AKÇE

TABLE OF CONTENTS

ABBREVIATIONS

2-OG : 2-Oxoglutarate
AP : Alkaline Phosphatase
ATP : Adenosine Triphosphate
BCIP : 5-Bromo-4-Chloro-3-Indoyl Phosphate p-toluidine
BLAST : Basic Local Alignment Search Tool
BPB : Bromophenol Blue
CBB : Coomassie Brilliant Blue
CDD : Conserved Domain Database
DNA : Deoxyribonucleic acid
DTT : Dithiothreitol
EDTA : EthyleneDiamineTetraAcetic acid
EtBr : Ethidium Bromide
FAD : Flavin Adenine Dinucleotide
Fd : Ferredoxin
FMN : Flavin Mononucleotide
FNOR : Ferredoxin NADP Oxidoreductase
GAT : Glutamine Amidotransferase
GOGAT : Glutamine: 2-Oxoglutarate Aminotransferase
IOR : Indolepyruvate Oxidoreductase
IPTG : Isopropyl-b D- Thiogalactopyranoside
KGOR : 2-Ketoglutarate Oxidoreductase
LB- broth : Luria Bertani broth
LGT : Lateral Gene Transfer
LMP agarose : Low Melting Point agarose
MBG : Molecular Biology Grade
MCS : Multiple Cloning Site
MOPS : 3-(N-Morpholino) Propanesulfonic acid
NAD^+ : Nicotineamid Adenine Dinucleotide, oxidized form
NADH : Nicotineamid Adenine Dinucleotide, reduced form
$NADP^+$: Nicotineamid Adenine Dinucleotide, phosphate oxidized form
NADPH : Nicotineamid Adenine Dinucleotide, phosphate reduced form
NBT : p-Nitro Blue Tetrazolium Chloride (NBT)
NCBI : National Center for Biotechnology Information
Ni-NTA : Nickel-Nitrilotriacetic Acid
OD : Optical Density
PCR : Polymerase Chain Reaction
Pit : Phosphate Inorganic Transport
Pst : Phosphate Specific Transport
POR : Pyruvate ferredoxin oxidoreductase
PVDF : Polyvinylidine Difloride
RBS : Ribosome Binding Site
RNA : Ribonucleic Acid

RNase	: Ribonuclease
RT	: Room Temperature
SDS	: Sodium Dodecyl Sulfate
SDS-PAGE	: Sodium Dodecyl Sulfate Polyacrylamide Gel Electrophoresis
VOR	: 2-Ketoisovalerate ferredoxin oxidoreductase
TAE	: Tris Acetate EDTA
TBS	: Tris Buffered Saline
TCA	: Trichloroacetic Acid
TTBS	: %0.05 Tween in Tris Buffered Saline

LIST OF TABLES

LIST OF FIGURES

LIST OF SYMBOLS

A_{260}	**:** Absorbance at 260 nm
A_{600}	**:** Absorbance at 600 nm
bp	**:** Base pair
ClustalW	**:** A general purpose multiple sequence alignment program for DNA or proteins
Fd	**:** Ferredoxin
kb	**:** Kilobase
kDa	**:** Kilodalton
lacZ	**:** ß-galactosidase
pET	**:** Plasmid expression by T7 RNA polymerase
Tris	**:** Hydroxymethyl aminomethane
X-Gal	**:** 5-Bromo-4-chloro-3-indolyl-D-galactoside

HETEROLOGOUS EXPRESSION OF PUTATIVE GLUTAMATE SYNTHASE SMALL SUBUNIT HOMOLOGUES FROM *PYROCOCCUS HORIKOSHII*

SUMMARY

Glutamate synthase (often abbreviated as GOGAT) is a key enzyme in the early stages of ammonia assimilation in bacteria, algae and plants, catalyzing the reductive transamidation of the amido nitrogen from glutamine to 2-oxoglutarate to form two molecules of glutamate. The ammonia that enters this pathway can be supplied either by internal metabolic processes, such as photorespiration in plants as well as amino acid catabolism, or through the reduction of external nitrogen sources, such as nitrate and atmospheric dinitrogen.

The genomes of three *Pyrococcus* species, *P. horikoshii, P. furiosus* and *P. abyssi*, harbour two open reading frames which show homology with the small subunit of glutumate synthase (β subunit of GOGAT). There are no open reading frames which may be coding for a large subunit responsible for the glutamate formation in the genomes of *P. horikoshii* and *P. abysii*. The presence of two putative GOGAT small subunits raises the possibility of gene duplication. Evolution of glutamate synthase might have occurred via lateral gene transfer via the combination of two subunits in the higher organisms. It seems likely that these open reading frames are the early forms of an electron transfer domain in archaea which may have later contributed to many electron transfer enzymes.

To further analyze this hypothesis, two open reading frames PH0876 and PH1873, from *P. horikoshii*, have been cloned and successfully expressed in *E. coli* and the presence of the proteins have been confirmed with Western Blot analysis. In addition, these two proteins have been obtained in the soluble fraction of the cell and purified with the aid of His-Tag present upstream the coding region. The β subunit-like C terminal region of NADH-dependent glutamate synthase from *Medicago sativa* has also been cloned, expressed in *E. coli* to be used as a control in activity analysis.

PYROCOCCUS HORİKOSHİİ PUTATİF GLUTAMAT SENTAZ KÜÇÜK ALTÜNİTE HOMOLOGLARININ HETEROLOG EKSPRESYONU

ÖZET

Glutamat sentaz (GOGAT), bakteri, alg ve bitkilerde amonyak asimilasyonun ilk basamaklarında görev alan ve glutaminin amido azotunun 2-okzoglutarata transamidasyonu sonucu iki molekül glutamat oluşumunu katalizleyen önemli bir enzimdir. GOGAT tarafından kullanılan amonyak, bitkilerde fotorespirasyon, amino acid yıkımı gibi metabolik işlemler sonucu sağlanabildiği gibi, nitrat ve atmosferik diazot gibi dış azot kaynaklarının indirgenmesi yoluyla da sağlanabilir.

Pyrococcus cinsinden olan *P. horikoshii, P. furiosus* ve *P. abyssi'*nin genomlarında, glutamat sentazın küçük altünitesine benzerlik gösteren iki tane homolog bölge vardır. Bununla beraber *P. horikoshii* ve *P. abysii*'nin genomlarında, enzimin glutamat oluşumundan sorumlu olan büyük altünitesini kodlayan bir bölge bulunmamaktadır. İki tane putatif glutamat sentaz küçük altünite homoloğunun varlığı, gen duplikasyonu olasılığını düşündürmektedir. Glutamat sentazın evriminin, lateral gen transferi ve iki altünitenin yüksek yapılı canlılarda birleşmesi olaylarını kapsaması muhtemeldir. Bunlar ışığında, bu homolog bölgelerin, elektron transfer protein domeynlerinin arkealarda bulunan erken formları olabilecekleri ve daha sonradan evrim sürecinde elektron transfer enzimlerin yapısına katılmış olabilecekleri düşünülebilir.

Bu çalışmada, bu hipotezin gerçekliğini araştırmak için, *Pyrococcus horikoshii'* nin iki putatif glutamat sentaz küçük altünitesi homoloğu, PH0876 ve PH1873, klonlanmış ve *Escherichia coli*'de protein ekpresyonu gerçekleştirilmiştir. Elde edilen sonuç Western Blot analizi ile desteklenmiştir. Üretilen proteinler, HisTag füzyon proteini olmalarından faydalanılarak saflaştırılmıştır. Buna ek olarak, aktivite analizlerinde kontrol amaçlı kullanılacak olan *Medicago sativa*'ya ait NADH-bağımlı glumat sentazın, küçük altünite ile benzerlik gösteren bölgesi de ekpresyon vektörüne klonlanmış ve *Escherichia coli*'de protein ekpresyonu gerçekleştirilmiştir.

1. INTRODUCTION

1.1. Archaea and *Pyrococcus horikoshii*

1.1.1. Archaea

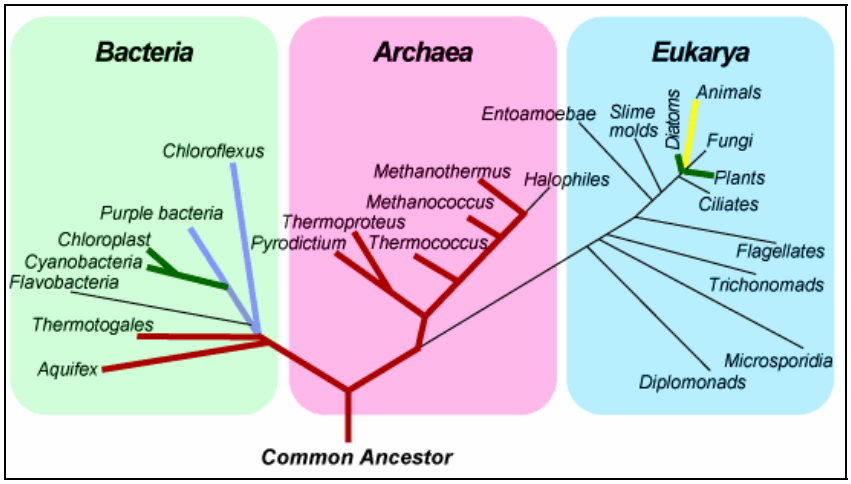

Figure 1.1: Three Domains of Life (Website of NASA Astrobiology Institute)

According to the biological classification based on 16S rRNA sequence comparisons, there are three distinct domains which are the *Bacteria*, the *Archaea* and the *Eukarya* (Figure 1.1) (Madigan, 2003).

The Archaea consist of three phylogenetically distinct groups which are Crenarchaeota, Euryarchaeota and Korarchaeota (Figure 1.2). Moreover, they can be categorized into three types according to their physiology: methanogens (prokaryotes that produces methane); extreme halophiles (organisms that live at high concentrations of salt; and extreme (hyper) thermophiles (organisms that live at very high temperatures). They can be either aerobic with oxygen as the terminal electron acceptor (e.g. *Sulfolobus*, *Pyrobaculum*, *Thermoplasma* and halophilic archaea) or anaerobic with alternating terminal electron acceptors, such as sulphur (*Thermoproteus*), nitrate (*Pyrobaculum*), sulphate (*Archaeoglobus*) or carbon dioxide (methanogens) (Madigan et. al., 2003). Archaea are prokaryotic organisms lacking distinct membrane-enclosed structures. They have features that distinguish them from bacteria such as lack of murein content in cell wall and ether-linked membrane

lipids (Madigan et. al., 2003). While archaea resemble bacteria, they consist of some characteristics that are more likely found in eukaryotes. For instance, despite the fact that transcription regulation in Archaea seems to involve bacterial-like proteins, there is a similarity between the archaeal and the eukaryotic transcriptional machinery. There is a homology between the basal transcription components of archaea and the eukaryotic RNA polymerase II system with regard to subunit complexity and sequence levels (Bell and Jackson, 2001). Moreover, there is a heavy selective pressure on archaeal proteins due to the extreme environments they live in so their proteins remained less changed in time. Thus, one would observe the evolution of an enzyme through time towards archaea, bacteria, plants and lower eukaryotes. They are declared as the "evolutionary clocks" (Cohen et al, 2003).

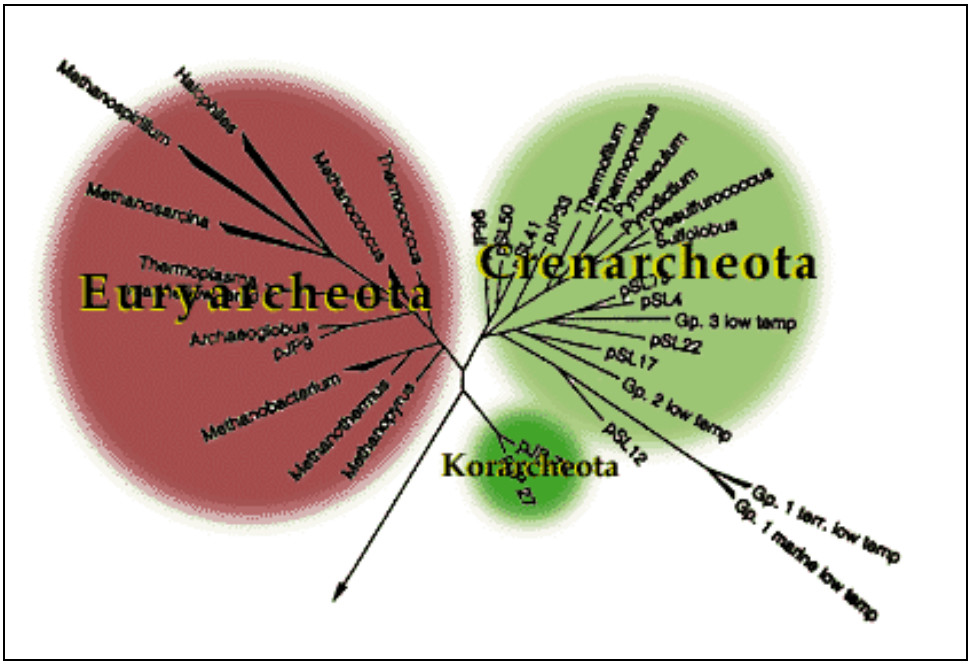

Figure 1.2: The phylogeny of archaeans (www.ucmp.berkeley.edu).

There are both autotrophic (methanogens, sulphur reducers and sulphate reducers) and heterotrophic (Pyrococci) representatives of archaea. Heterotroph representatives comprise most of the members of the hyperthermophilic archaea which use polypeptides as carbon and energy sources. Various geothermally heated environments are places from which hyperthermophiles are isolated. In addition, several modified sugar degrading pathways are also found in various members of heterotrophic archaeal species which are called to be saccharolytic such as *Pyrococcus furiosus*, *Pyrococcus glycovorans, Pyrococcus woesei, Thermococcus hydrathermalis, Desulfurococcus amylolyticus* (Verhees et al, 2003).

1.1.2. *Pyrococcus horikoshii*

1.1.2.1. Systematics, Ecology and Morphology of *Pyrococcus horikoshii*

Hydrothermal vents are sources for the isolation of the most of the archaea like *Pyrococcus horikoshii* OT3. *Pyrococcus horikoshii* is a hyperthermophilic archaea and belongs to the euryarchaeotal branch within the Archaea domain. *Pyrococcus horikoshii* OT3 was isolated in 1992 at a depth of 1395m in the Okinawa Trough lying between Japan and Taiwan in the Pacific Ocean (Gonzales et al, 1998). It is a hyperthermophilic, anaerobic heterotrophic archaebacterium which grows optimally at 98°C. The determination of the complete genome sequence of this microorganism is very important since its optimal growth temperature is near 100°C and its metabolism provides an alternative archaeal system to investigate biological processes in non-acidic high temperature environments (Gonzales et al, 1998; Kawarabayasi et al., 1998).

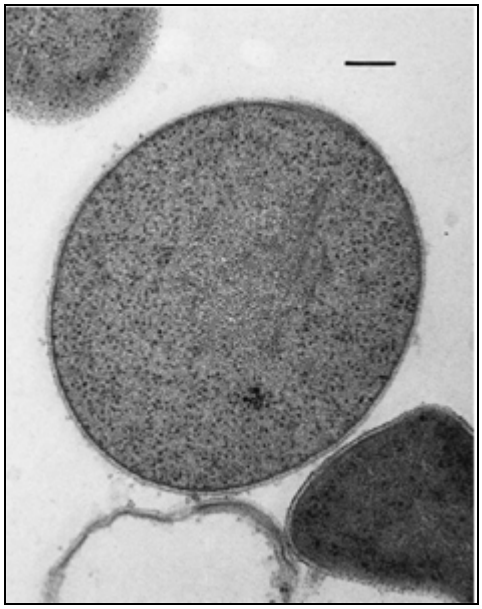

Figure 1.3: A photograph of the *Pyrococcus horikoshii* OT3 taken by a transmission electron microscope (Gonzales et al, 1998). Length of bar is 0.1 μm.

The taxonomic hierarchy of *P. horikoshii* and the degree of relationship of *P. horikoshii* to the related Euryarcheota on the unrooted phylogenetic tree of 16S rRNA sequences can be seen at Figure1.4 (Gonzales et al, 1998).

Table 1.1: The taxonomic hierarchy of *P. horikoshii* (Databases of genomes analyzed at NITE (National Institute of Technology and Evaluation, Japan).

Kingdom	*Archaeota*
Phylum	*Euryarhaeota*
Class	*Thermococci*
Order	*Thermococcales*
Family	*Thermococcaceae*
Genus	*Pyrococcus*
Species	*horikoshii*
Strain	OT3

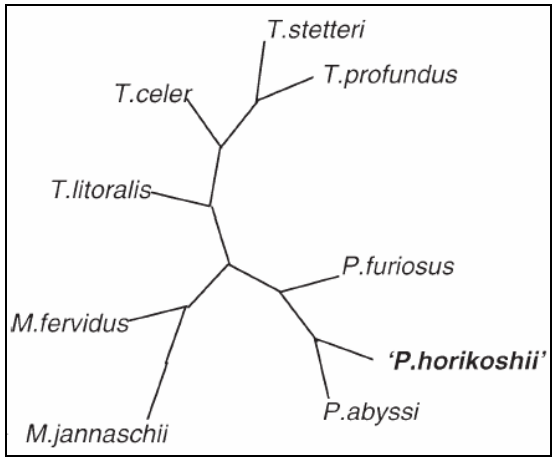

Figure 1.4: Unrooted phylogenetic tree of 16S rRNA sequences of related Euryarcheota. It which was done using Maximum Parsimony (Gonzales et al, 1998).

Cells of *P. horikoshii* have a shape of irregular cocci as seen at Figure 1.3 and their diameter vary according to growth conditions (0.8 and 2μ). They form pairs throughout the exponential phase which then accumulate to form aggregates during culture aging (Gonzales et al, 1998). It has a polar tuft of flagella. There is also a periplasmic space between the cell envelope and the cytoplasmic membrane (Figure 1.3). The growth of *P. horikoshii* is observed at different temperatures and at different growth media containing varying amounts of NaCl and H^+ ions. The corresponding generation times of *P. horikoshii* can be seen at Figure 1.5 (Gonzales et al, 1998). Growth is observed from pH 5-8 whereas the optimum pH for growth is 7. Optimum temperature that allows growth is 98°C whereas growth is also observed between 80°C and 102°C (Figure 1.5) (Gonzales et al, 1998). Moreover, optimum NaCl concentration that allows growth is 2.4% whereas growth is observed at concentration ranges from 1-5 % (Figure 1.5). The shortest doubling time is 32 min (Gonzales et al, 1998).

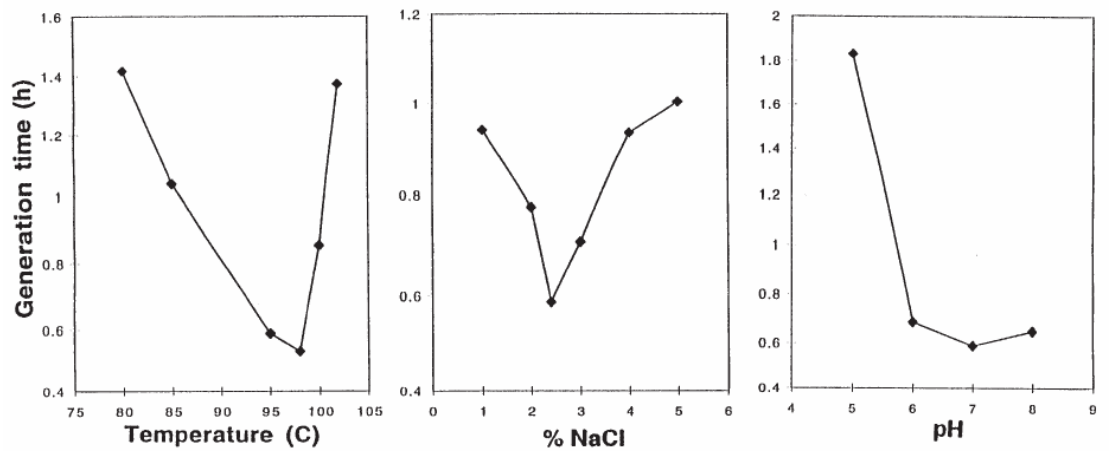

Figure 1.5: Generation times versus temperature, % NaCl and pH. Effect of temperature, NaCl concentration and pH on the growth of *P. horikoshii* (Gonzales et al, 1998).

Growth does not require elemental sulfur but the absence of S^0 has a significant negative effect on the growth rates. Likewise, it has a stimulatory effect and increases the growth yield. They can be cultivated heterotrophically on complex proteinaceous substrates like yeast extract, beef extract, peptone, tryptone, casein; and on casamino acids with an extra addition of tryptophan and vitamins (Gonzales et al, 1998). Moreover, growth can also be achieved on a mixture of 21 amino acids and vitamins (The 21. amino acid mentioned is selenocycteine). Tryptophan is a necessity for growth (Gonzales et al, 1998).

Similarity is observed between the cell envelopes of *P. horikoshii* and *P. furiosus* as a result of morphological studies. However, the cell envelope of *P. abysii* is different from that of *P. horikoshii*. A cellular compartment exists between the cytoplasmic membrane and the S-layer which is the outer layer of cellular envelope of *P. horikoshii* (Gonzales et al, 1998). However, considering that the most abundant portion of *P. horikoshii*'s cell envelope is the tetraether fraction, it is similar to *P. abysii* rather than *P. furiosus* with regard to membrane lipid composition (Gonzales et al, 1998).

1.1.2.2. Metabolism of *Pyrococcus* Species

Most of the hyperthermophilic archaea are heterotrophs which use polypeptides as carbon source. There are also some heterotroph representatives which comprise several modified sugar degrading pathways (Schut et al, 2003). Most of the information on *Pyroccoccus* genus is obtained from the studies on *Pyroccoccus*

furiosus. The principle metabolic pathway is peptide fermentation for *Pyrococcus* species (Cohen et al, 2003 and Schut et al, 2003). The excess reductants after the fermentation-type metabolic processes are got rid of in the form of H_2 or if S^0 is available in the form of H_2S (Adams et al, 2001). Interestingly, growth also occurs when *P. furiosus*, *P. woesei* and *P. glycovorans* are separately cultivated in a growth medium containing maltose as the main carbon source. Therefore, they are called as saccharolytic archaea (Verhees et al, 2003). However, *P. horikoshii* is not able to grow in that media since it is not able to grow on carbonhydrates. Various experiments were performed with *P. furiosus* which explains the effect of S^0 to the growth on peptides and on maltose (Schut et al, 2003). These experiments are also important for the understanding of the metabolism of *P. horikoshii* since peptide fermentation is the common pathway and since the comparisons explain the reasons for the lack of some genes in *P. horikoshii* which will mainly be discussed in the part focusing on genomic features of the *P. horikoshii* (Introduction, 1.2.2.3). The examination of the growth of *P. furiosus* was performed by Adams et al (2001) by using media containing different combinations of peptides (hydrolyzed casein), maltose and elemental sulfur (S^0). It was seen that only when S^0 is present, the effective utilization of peptides occurred (Adams et al, 2001). In addition, more growth was observed in medium containing peptides and S^0 together than only maltose containg medium. Results of these experiments also show that the prefered carbon source is peptides, which make the peptide fermentation the main catabolic pathway for Pyrococcus species (Adams et al, 2001). In addition, it can be concluded that peptide fermentation in these organisms requires S^0 to a great extent. The reason for that can be the withdrawal of the negative influence of H_2 gas on growth rate in the presence of sulfur. It is suggested that detoxification of H_2 is achieved by H_2S formation (Adams et al, 2001).

P. horikoshii was also examined for the growth on various substrates such as sucrose, glucose, maltose, cellobiose, citrate, pyruvate, glycerol, lactate, acetate, and olive oil. It was seen that these subsrates were not suitable for the growth of *P. horikoshii* (Gonzales et al, 1998). Among *Pyrococcus* species, *P. abysii*, *P. horikoshii, Pyrococcus sp. Strain GB-D (*isolated from the Guaymas Basin hydrothermal vents*)* can only grow on proteinaceous carbon sources (Erauso et al., 1993; Gonzales et al., 1998; Jannash et al., 1992).

Since all *Pyrococci* can grow on peptides, their pathway for utilization of peptides is expected to be roughly similar (Figure 1.6).

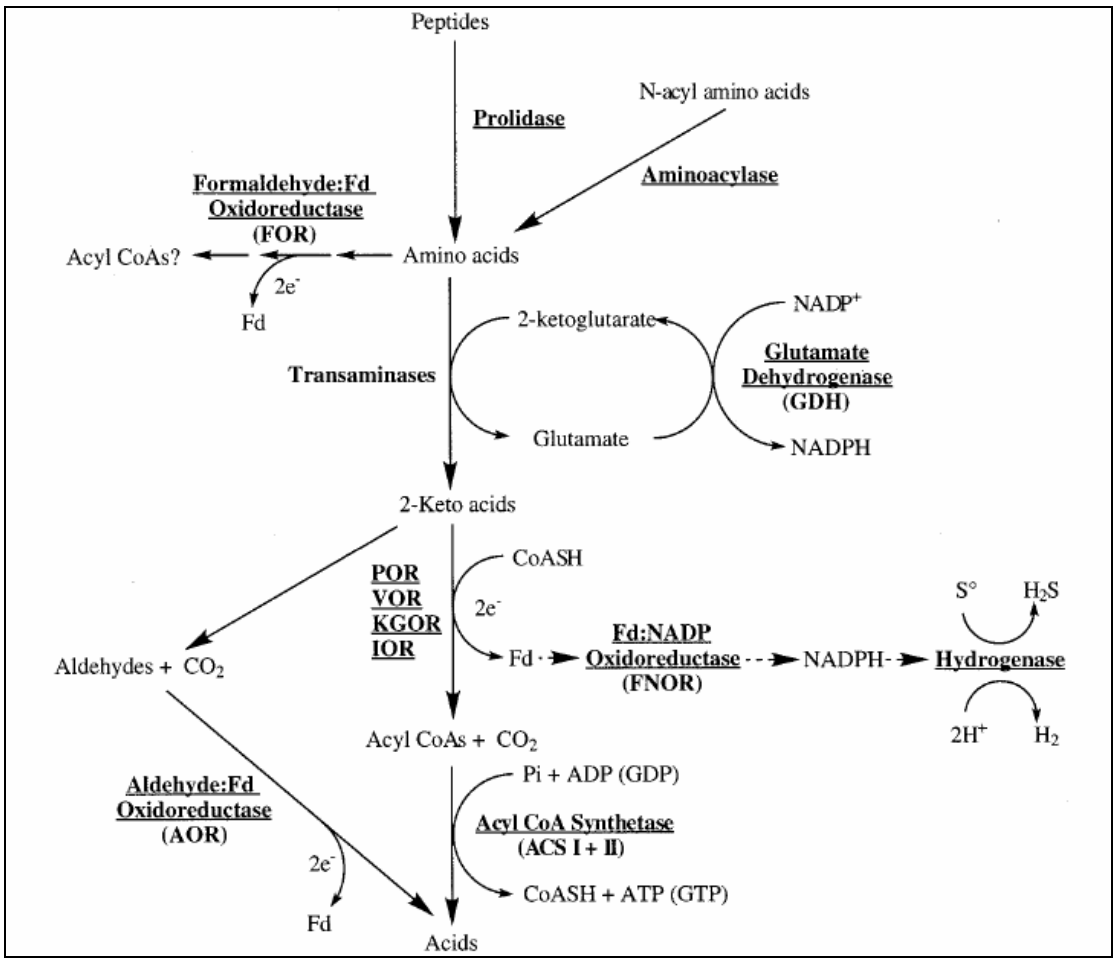

Figure 1.6: The proteolytic pathway which is suggested for *P. furiosus* (Adams et al, 2001).

The catabolism of peptides occurs as seen in the figure above in all three *Pyrococci* (*P. horikoshii, P. furiosus, P. abysii*) except some differences in the types of the used 2-ketoacid ferredoxin oxidoreductases (KORs). Peptides are transformed into 2-Ketoacids at the end of the amino acid deamination step with the contribution of transaminases (Figure1.6) (Adams et al, 2001, Schut et al, 2003). During the formation of 2-keto acids, glutamate is also produced from 2-ketoglutarate by glutamate dehydrogenase (GDH). After the deamination part, 2-keto acids are converted into acyl-CoAs by the reactions catalyzed by 2-ketoacid ferredoxin oxidoreductases (KORs) gene cluster products (POR: Pyruvate ferredoxin oxidoreductase; VOR: Utilizes 2-ketoacids derived from branched chain amino acids; KGOR: 2-ketoglutarate oxidoreductase; IOR: Indolepyruvate oxidoreductase) (Figure 1.6).

Adams et al. (2001) presented that KGOR, IOR and GDH show higher activities in *P. furiosus* cultures cultivated on media containing peptide and S^0 together than media containing only maltose. In addition, genes encoding the same enzymes were also upregulated in peptide grown cultures (Schut et al., 2003). However, the activity of POR was nearly same in all type of media (Adams et al., 2001). In addition, the expression level of POR was high in both cells growing in only peptide containing and in only maltose containing media. This is not surprising because pyruvate is also produced from glycolysis while cells are growing on maltose and POR also utilizes this pyruvate (Schut et al., 2003).

The enzyme which is responsible for the removal of aldehydes which can be produced from either peptidolytic (with IOR, POR, VOR) or sacchorylotic pathways (with POR) is Aldehyde: Fd oxidoreductase (AOR). The reductants, ferredoxin and NADPH, are produced from the conversion reaction of 2-keto acids to acyl-CoAs and the activity of GDH, respectively. These reductants are oxidized via ferredoxin NADP oxidoreductase (FNOR) catalyzed reaction (Adams et al., 2001 and Schut et al., 2003). During its catalysis, the electron acceptors of exterior sources such as elemental sulphur or polysulphide take the electrons that are donated from NADP (Silva et al., 2000 and Schut et al., 2003). It seems likely that the most important electron carrier in Pyrococci is ferredoxin. It is reduced throughout sugar or peptide utilization (Silva et al., 2000) (Figure 1.6).

The gene content difference of *Pyrococcus* species involves amino acid biosynthesis, maltose transport and phosphate uptake operon genes (Cohen, 2003).

In order for maltose to be utilized, it should be transported into the cell. In *P. furiosus*, a membrane protein called as MalE captures the maltose which is followed by transport through the membrane via the MalFG ATP-binding casette (ABC) membrane transporter complex. It is not surprising that there is not a homologue for *malEFG* in the genome of *P. horikoshii* since it is incapable of maltose fermentation (Schut et al, 1999).

Another gene level comparison is for the two important phosphate transporters which are called as Pst (Phosphate specific transporter) and Pit (Phosphate intake transporter) systems (Cohen et al, 2003). The Pit-system is the fast nonspecific uptake system for phosphate whereas Pst is the inducible high-affinity ABC-type

transport system and it allows specific movement of P_i into the cell. Both of them appear in the genomes of both *P. furiosus* and *P. abysii*. However, there is only the Pit system in the genome of *P. horikoshii* (Cohen et al, 2003). The operon named as *pstSCAB-phoU*, which is highly conserved, encodes the Pst transport system. The gene product of *phoU* is alkaline phosphatase which removes phosphate groups (Pi) from many biological molecules. The Pit system, involves the glycerol-3-phosphate transport system which is encoded from *ugpABCE* operon. (http://biology200.gsu.

edu/houghton/4595%20'04/lecture25.html).

Motility in *P. horikoshii* and *P. furiosus* is provided by flagellas. *P. horikoshii* contains bacteria-like methylated chemotaxis proteins (which are encoded from PH0478, PH0479, PH0481-PH0484, PH0491) whereas *P. furiosus* lack these proteins. However, the motility of the *P. furiosus* suggests that there should be another taxis system encoded in the *P. furiosus* genome (Maeder et al, 1999).

Amino acid biosynthesis is of importance to saccharolytic organisms like *P. furiosus* throughout growth on carbonhydrates such as maltose. Also, carbon supply to these amino acid biosynthesis reactions through metabolic intermediates is very important. There are three citric acid cycle enzymes responsible for carbon supply to this type of reactions such as citrate synthase, aconitase and isocitrate dehydrogenase (PF0201 to PF0203) (Schut et al, 2003). There are not any homologs of these three ORFs in *P. horikoshii* which lacks the ability to grow on carbonhydrates, consistent with the indirect contribution of these enzymes to the amino acid biosynthesis during growth on carbonhydrates (Schut et al, 2003). The carbon source for glutamate synthases is 2-ketoglutarate. Glutamate synthase encoding genes are in the form of an operon in *P. furiosus.* There is a more than 5 fold increase at the transcript levels of genes of that operon when *P. furiosus* cells are cultivated in maltose containing medium (Schut et al, 2003).

In addition, there is another operon containing ORFs PF0204-PF0206, which is present downstream of the operon encoding citric acid cycle enzymes. The genes in this operon are also upregulated during growth on maltose (Schut et al, 2003). Although ORF PF0205 was thought to be the large subunit of an NAD-dependent glutamate synthase, each ORF in this operon shows homology to the domains present in ferredoxin-dependent glutamate synthase protein which itself shows similarity to

α subunit of NAD-dependent glutamate synthase (Schut et al, 2003). In addition, 20 fold upregulation is also observed for the putative glutamine synthetase (PF0450) present in *P. furiosus* during growth on maltose. This is a consistent result, since glutamate synthase generally works with glutamine synthetase which is responsible for the conversion of glutamate and ammonia into glutamine in an ATP dependent manner (Schut et al, 2003).

There are no homologs for the ORFs PF0204-PF0206 in *P. abysii* and *P. horikoshii* genomes. Considering the fact that glutamine is the storage form of ammonia, and glutamate and α-ketoglutarate are biosynthetic precursors during amino acid biosynthesis, it is an expected condition since they can not grow in media containing maltose as the sole carbon source without peptides (Schut et al, 2003).

1.1.2.3. Genome of *Pyrococcus horikoshii*

The entire genome of *P. horikoshii* is 1,738,505 bp in length (Figure 1.7). There are 2061 open reading frames (ORFs) which are accepted as potential protein coding regions. 406 ORFs were annotated as genes with putative functions as a result of sequence similarity searches (Kawarabayasi et.al, 1998). However, now the number of ORFs annotated as genes have raised to 557 (27%) (Database of the Genomes Analyzed at Nite (National Institute of Technology and Evaluation, Japan) and the function of 455 (22%) ORFs are not known, hypothetic proteins. There is not any meaningful similarity between sequences in the database and the rest of the ORFs which comprises comprises 50, 89% (1049.ORFs). There are 46 tRNA genes two of which contains intron stuctures, one 16S-23S rRNA operon and two 5S rRNA genes. The direct analysis of the base composition revealed that the G+C content of the DNA 42% whereas it is 44%, according to the melting point method (Kawarabayasi et al, 1998).

There are intein elements in eleven ORFs in the genome of *P. horikoshii.* Inteins are regions of a polypeptide sequence generally encoding unique motifs of endo-nucleases and are removed via self splicing. Rearrangements of the polypeptide sequence via combination of exteins occur after the inteins are excised (Kawarabayasi et al, 1998).

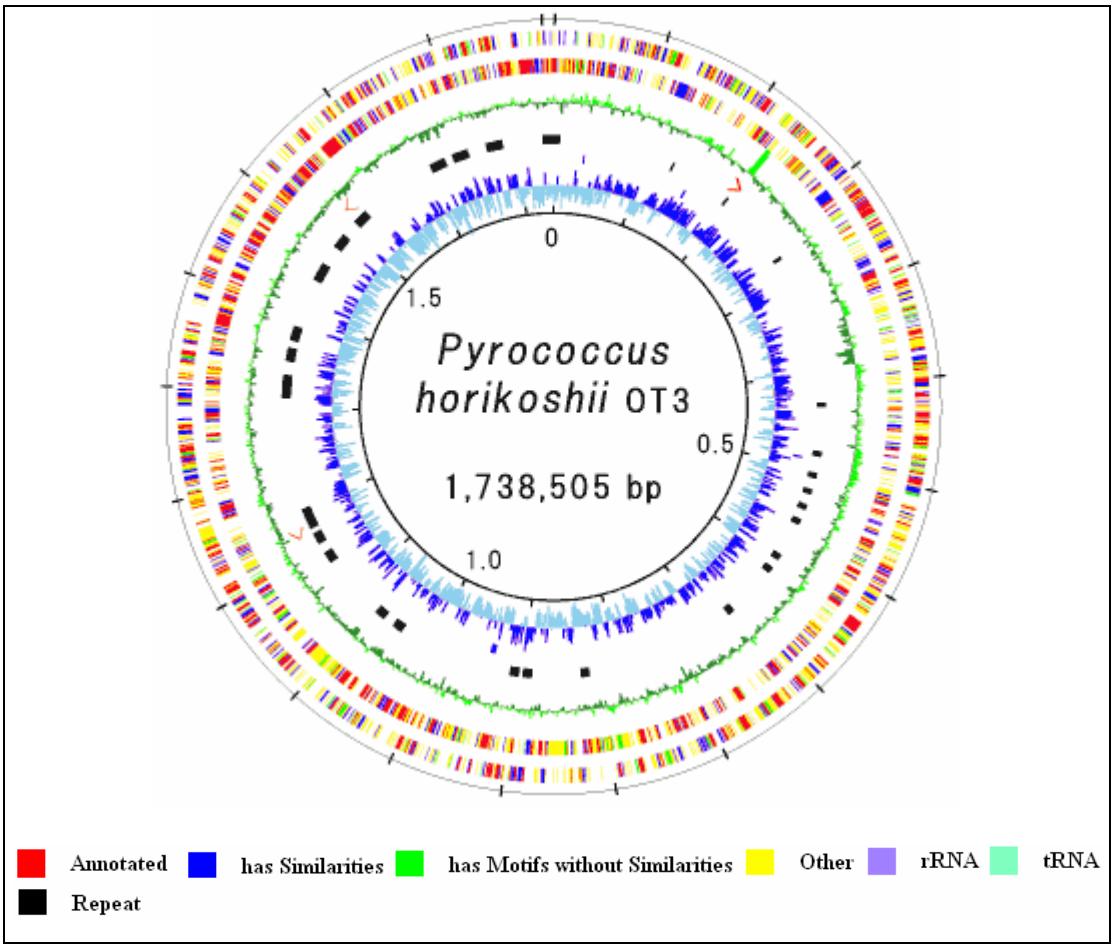

Figure 1.7: Physical map of *P. horikoshii OT3* genome the location of RNA genes. (http://www.bio.nite.go.jp/ dogan/MicroTop?GENOME_ID=ot3). Color key is as above.

There is a low similarity observed between the genomes of other *Pyrococcus* species and *P. horikoshii* as a result of DNA-DNA hybridization analysis (Table 1.2). The highest hybridization score belongs to *P. furiosus* (Maeder et al., 1999).

Table 1.2: DNA-DNA hybridization analysis of three species of the *Pyrococci* and *Thermococcus celer* (Gonzales et al, 1998). JA-1 is a strain type of *Pyrococcus horikoshii* like OT3.

Species or strain	% hybridization with the DNA of		
	JA-1	*P. furiosus*	*P. abyssi*
P. horikoshii JA-1	100	50	32
P. furiosus	63	100	36
P. abyssi	36	45	100
Thermococcus celer	25	50	36

Although the highest hybridization score belongs to *P. furiosus*, there are a lot of differences at gene level between *P. horikoshii* and *P. furiosus*. There is 170 kbp size difference between genomes of the two *Pyrococcus* species. The length of the *P. furiosus* genome is 1,908 Mbp, whereas the length of the *P. horikoshii* genome is 1,738 Mbp (Maeder et al., 1999).

1.1.3. Importance of Genome Comparisons Among Hyperthermophilic Archaea

There can be large scale insertion/deletion events among hyperthermophiles because of their unique feature of strong capacity for accelerated DNA repair systems. For instance, one of these enzymes which has an important role in DNA repair systems is reverse gyrase which is present in all hyperthermophilic genomes and which is absent from all mesophilic and thermophilic genomes (Forterre, 1995). Therefore, it is of significant importance since it is the only hyperthermophile-specific protein (Forterre, 2002). However, it has been claimed that the presence of reverse gyrase is not a necessity for hyperthermophilic life at least until the conditions below 90°C (Atomi et al., 2004). This enzyme increases the number of topological links between the two DNA strands by introducing positive supercoils and helps DNA to function at high temperatures (Atomi et al., 2004). As a result of this accelerated DNA repair systems; the occurance of gene gains, losses or replacements within hyperthermophiles can be expected significantly in also short period of genetic and geographical separations which are valid conditions for species separation. For this reason, genome sequencing experiments of even same type of genus, as in the case for Pyrococci, are required to understand what is happening at the genome level among species by a combinatory study of proteomics and genomics before increasing the complexity of interactions. In addition, genomes and proteomes of hyperthermophilic organisms belonging to same genus, provide information about the rates of protein replacements and function diversity formation of a protein at interspecies level. This makes it possible to trail the traces of molecular evolution of proteins belonging to organisms comprising huge amounts of gene rearrangements at the interspecies level. It is of importance since the tested organisms are annotated as "evolutionary clocks" as they live in environments bearing highly selective pressure forcing their proteins to remain unchanged. Also it can give rise to identification of common features of a genus (DiRuggiero et al., 2000).

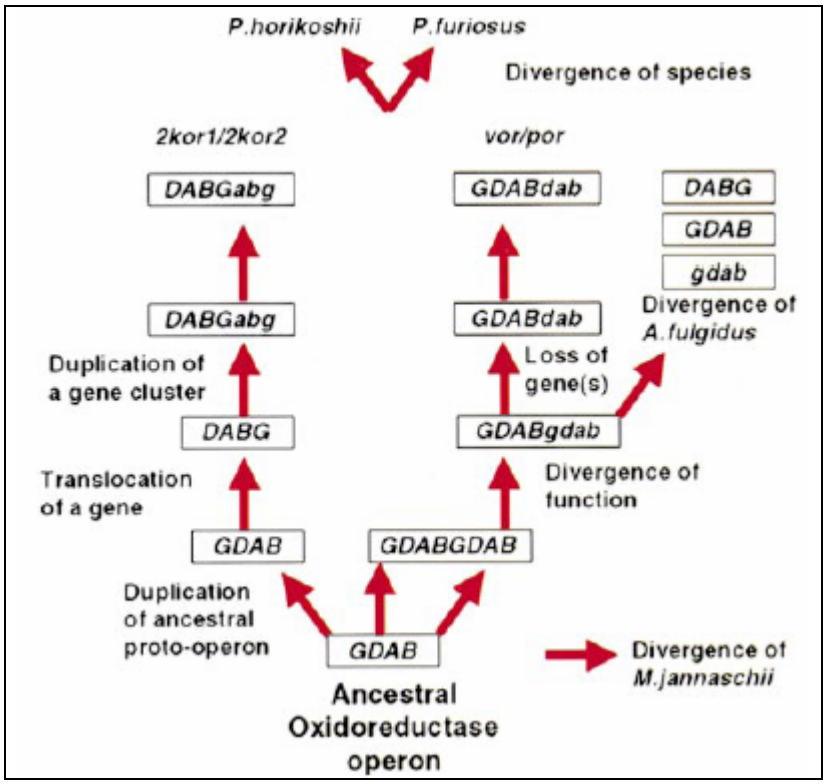

Figure 1.8: The rearrangement of the ferredoxin oxidoreductase gene clusters before the divergence of the two species: *P. horikoshii* and *P. furiosus*. There are four homologous genes belonging to that operon which are different from each other: *A, B, G, D* (Maeder et al., 1999).

The rearrangement of the ferredoxin oxidoreductase gene clusters is a very good example indicating the dynamic genomic rearrangements because of the events taking part during its evolution such as operon duplication, gene loss, and also gene translocation (Figure 1.8). 2-Ketoisovalerate ferredoxin oxidoreductase (VOR) and pyruvate ferredoxin oxidoreductase (POR) have vital roles for energy metabolism (Section 1.1.2.2) consistent with the fact that their genes are conserved among Pyrococci. It can be followed from the figure that the rearrangement events of this gene clusters occured before the divergence of the two species, *P. horikoshii* and *P. furiosus* (Maeder et al, 1999).

1.1.4. Possible Mechanisms of Speciation in *Pyrococcus*

Pyrococcus species, which live in similar hydrothermal habitats, share some genes but may differ from one another with their metabolism. Insertion sequences are suspected to play key roles that led to the evolutionary divergence of *P. furiosus* from *P. abysii* and *P. horikoshii* (Zivanovic et.al, 2002). Recent studies have shown interesting results which shed some light to the speciation of *Pyrococcus* species. *P.*

furiosus and *P. woesei,* which were isolated from the same hydrorthermal vent, seem to share the same metabolism and have 100% identity of 16S rRNA. However, the genome of *P. woesei* has not been elucidated yet. Hybridization of genomic DNA from *P. furiosus* and *P. woesei* showed that homologues of 105 ORFs are absent from the genome of *P. woesei*. MalI gene cluster, which is only present in *P. furiosus*, is flanked by direct repeats, *P. woesei* does not contain the MalI gene while the direct repeats are found in both species (Hamilton-Brehm et.al, 2005). This makes it likely that a genetic transfer via insertion elements may have occurred and insertion elements play an important role in shaping the genomes which share the same environment.

1.2. Glutamate Synthase

1.2.1. Glutamate Synthase Reaction

Amidotransferases are responsible for the distribution of the nitrogen to other compounds after the primary assimilation of nitrogen into glutamine and glutamate. It is one of the most important biochemical reactions in plants and bacteria, like in some yeast and fungi so that inorganic nitrogen is assimilated into carbon skeleton as ammonium (NH_4^+) later to be used in amino acid production. (Vanoni and Curti, 1999; Heuvel et al., 2003).

A single step conversion of 2-oxoglutarate into L-glutamate by the enzyme glutamate dehydrogenase in a NAD(P)H dependent manner, was generally thought to be responsible for the ammonia assimilation until 1970. In 1970, the existence of a glutamine synthetase (GS)/glutamate synthase (GOGAT) pathway was presented in *Aerobacter aerogenes* by the pioneering work of Tempest and co-workers (Tempest et al., 1970). This pathway is utilized in bacteria which are growing on ammonia limited media and in bacteria lacking glutamate dehydrogenases (GDH) or equivalent amino acid dehydrogenases. Later, the role of glutamine synthetase and GOGAT for primary and secondary ammonia assimilation was also presented in other bacterial species (Hummelt and Mora, 1980; Senior, 1975), in cyanobacteria (Marques et al., 1992), in yeast (Cogoni et al., 1995), in plants (Miflin et al., 1980, Anderson et al., 1989, Gosset et al., 1989) and in lower animals (Hirayama et al., 1998).

The GS/GOGAT pathway is very important for microbial and plant cells, since L-glutamine and L-glutamate, which are the products of the GS/GOGAT pathway, are the nitrogen donors for the biosynthesis of major nitrogen-containing compounds (such as nucleotides, other amino acids, chlorophylls, polyamines and alkaloids). The GOGAT enzyme of the GS/GOGAT pathway is refered as GltS. (Lea and Ireland, 1999, Reitzer, 2003).

Glutamate synthase (EC 1.4.1.13) and glutamine synthatase (GS, EC 6.3.1.2) catalyse the joint reactions which results in glutamate formation in a NAD(P)H or ferredoxin-dependent manner (Figure1.9). During the reaction, the amide group of the glutamine is transferred to the C(2) carbon of the 2-oxoglutarate (Figure1.9). The overall reaction catalysed by GS and GOGAT is similar to the reaction of glutamate dehydrogenase (Figure1.10). GS provides the assimilation of ammonia into the amide group of L-Gln and therefore it provides the substrate, L-Gln, to a wide range of biosynthetic reactions catalyzed by L-glutamine dependent amidotransferases like GltS (Curti et al., 1996, Zalkin and Smith, 1998).The difference between two reaction pathways is the expenditure of an extra molecule of ATP for each glutamate that is producedin GDH (Figure1.10). Glutamate dehydrogenase catalyses a reversible NADPH-dependent reaction during which glutamate is formed from ammonia and alpha-ketoglutarate as seen in Figure 1.10 (Chavez et al., 1999). There has been some discussion that this reaction rather works in the reverse direction of glutamate deamination. In overall, at the end of these amidotransferase reactions, this nitrogen atom becomes available for amino acid biosynthesis.

In addition, the glutamine synthetase (GS)/GltS (GOGAT) pathway is of importance, since it partipates in the ammonia assimilation into L-Glu at low intracellular ammonia concentrations. Each of the enzymes in the pathway has a low K_m value for its substrates. Thus, the other known glutamate synthetic reaction can be easily substituted by it particularly on media with low ammonia content (for instance: nitrogen fixation)

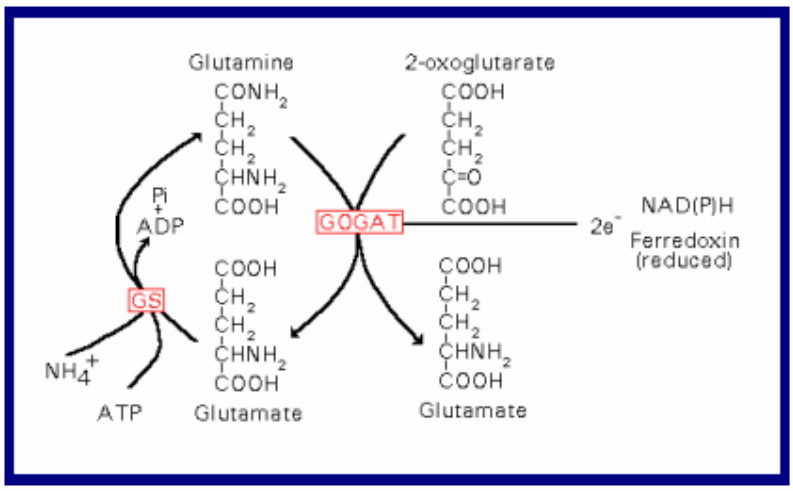

Figure1.9: Reaction catalyzed by Glutamate Synthase

GDH	NH_3 + 2-oxoglutarate + NADPH + H^+ ⇔ Glutamate + $NADP^+$
GS(Reaction 1)/ GOGAT(Reaction 2)	**1)** NH_3 + Glutamate + ATP ⇨ Glutamine + ADP + Pi **2)** Glutamine + 2-oxoglutarate + (NAD(P)H + H^+ or Fd_{ox}) ⇨ 2 Glutamate + ($NADP^+$ or Fd_{red})

Figure1.10: The reactions catalyzed by Glutamate Dehydrogenase (GDH) and Glutamine Synthatase/Glutamate Synthase (GS/GOGAT) Pathway (Curti,1995).

In bacteria, being involved in protein synthesis, being precursor for heme biosynthesis (Heuvel et al., 2002), being involved in maintanence of osmotic balance and being the amido nitrogen donor for transamidation reactions giving rise to another amino acids, are among the roles of L-Glu produced by *GltS*.

Moreover, cyanobacteria have an incomplete tricarboxylic acid cycle because of the lack of 2-oxoglutarate dehydrogenase and succinyl-CoA synthetase activities. Thus, the GS-GOGAT pathway in cynobacteria also represents the most important way in the utilization for 2-oxoglutarate (Navarro *et al.*, 2000).

In corporation of ammonia into the amino acids is mainly achieved by the GS/GOGAT pathway in plants. There are two GS isoforms (GS1 and GS2) found in most species, whose subcellular localizations are different. GS1 is found in cytosol and GS2 is found in plastids. The distribution and concentration of GS is not affected by ammonium. There are two molecular forms of GOGAT in plants which are Fd-dependent and NADH-dependent which are showed to be present in almost all tissues of the plants. Both forms of GOGAT are monomeric proteins and contain FMN and 3Fe-4S cluster as prosthetic groups. Ferredoxin (Fd)-dependent glutamate

synthase is solely found in plant chloroplasts but also in nonphotosynthetic plant tissues such as roots and shoots, whereas NADH-dependent GOGAT is found in plastids of roots and also in non-green and developing leaf blades (Tobin and Yamaya, 2001, Lea an Miflin, 2003). It was found that the amount of NADH-dependent GOGAT increased with the increasing concentration of ammonium in rice roots esspecially at the root tips whereas it had no effect on Fd-dependent GOGAT (Ishiyama et al, 1998). The NADH-glutamate synthase is responsible for the primary nitrogen assimilation (from N fixation) in roots. GOGAT is also very important during secondary ammonia assimilation in plants where photorespiration is done and a significant proportion of assimilated nitrogen is given as ammonia (Temple 1998). Toxicity of ammonia released through photorespiration is prevented by GltS. The primary function of Fd-glutamate synthase in leafs is the re-assimilation of ammonia released from the photorespiratory nitrogen cycle. In addition, Fd-glutamate synthase mutant plants are also photorespiratory mutants without exception, thus under atmospheric oxygen levels, they can not survive (Coschigano et al., 1998). Figure 1.11 indicates the localizations two isoenzymes GS and two molecular forms of GOGATs in plants and summaries the functions of them.

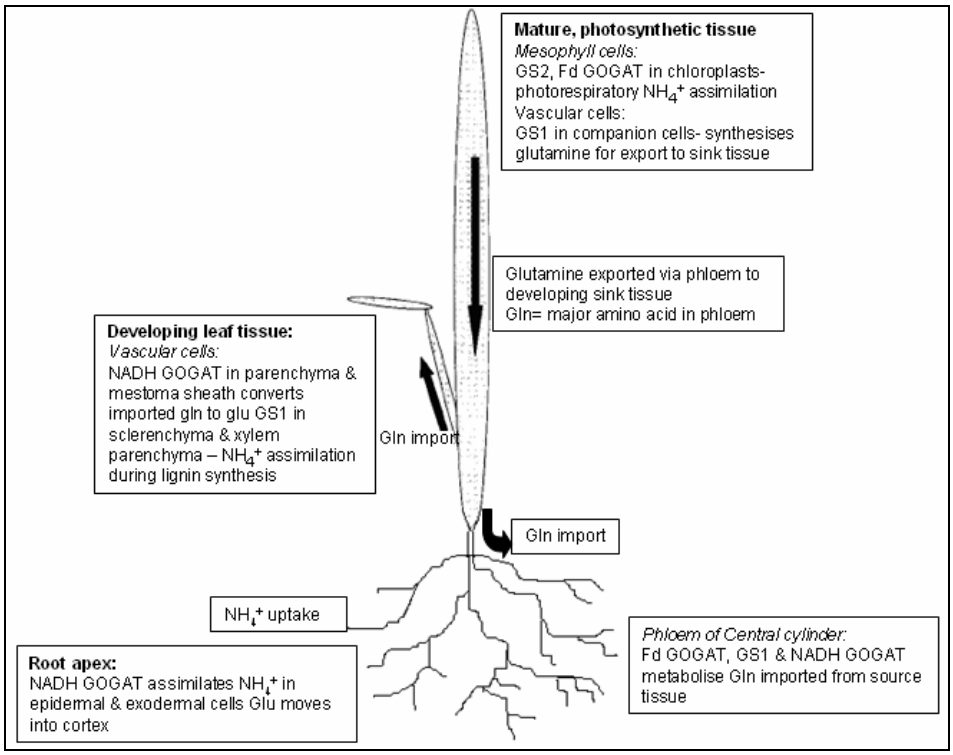

Figure 1.11: The localizations of GS and GOGAT isoenzymes in plants (Tobin and Yamaya, 2001)

1.2.2. Electron donor specifities and subunit compositions of glutamate synthases

There are three forms of glutamate synthase classified according to their electron donor specificities and subunit compositions in nature: NADPH-dependent GltS, NADH-dependent GltS and ferredoxin (Fd)-dependent GltS. There are many studies presenting the genes encoding GltS in a growing number of organisms ranging from bacteria to lower animals. NADPH-dependent αβ-heterodimer enzyme is found in bacteria such as *E. coli* (Miller and Stadtman, 1972) and *Azospirillum brasiliense* (Ratti et al., 1985) NADPH-dependent αβ-heterodimer is composed of a large α subunit and a smaller β subunit. There are two different forms of glutamate synthases in plants: NADH-dependent GltS and Fd-dependent GltS. An NADH-dependent enzyme consisting of a single protein chain exists in all higher plants as well as *Chlamydomonas* and *Neuspora crassa* (Gregerson et al., 1993). It is thought that putative fusion of the bacterial α and β subunits may have given rise to these monomeric enzymes (Gregerson et al., 1993).

Ferredoxin (Fd)-dependent glutamate synthase is a monomeric enzyme found in plant chloroplasts and cyanobacteria (Marques et al., 1992), green algae (Galvan et al., 1984), as well as nonphotosynthetic plant tissues such as roots and shoots (Sakakibara et al., 1991). As a result of sequence analysis, high homology was found between the Fd-dependent glutamate synthases and the α subunit of the bacterial enzymes. However, Fd-dependent GltS lacks sequences corresponding to the β subunit. There is a significant synchronization difference between catalytic centers of Fd-GltS and alpha-GltS, although the presence of this sequence homology (Heuvel et al., 2002).

Each group displays different subunit composition, cofactor content and physiological reductant, different distribution among different organisms and tissues.

I) NADPH-GltS (EC 1.4.1.13) These type of enzymes have a two subunit composition forming the active protomer (Figure1.11). Moreover, there are one flavin adenine dinucleotide (FAD), one flavin mononucleotide (FMN) and three different iron-sulfur (Fe/S) clusters in this structure. There have been better biochemically characterized enzymes in this group of enzyme such as the ones from *Klebsiella aerogenes*, *Escherichia coli*, *Bacillus subtilis* and *Azospirillum brasilense.*

Bacterial GltS is specific for NADPH except the GltS enzyme found in *B. subtilis* thus, bacterial form of GltS enzyme will be mentioned via the abbreviation NADPH-GltS (Binda et al, 2000).

II) Fd-GltS (EC 1.4.7.1) An Fd-dependent form of GltS is present in cyanobacteria and plants (Figure 1.12). In these organisms, Fd-GltS is reported to be mainly involved in re-assimilation of ammonia released during photorespiration (Petoukhov et al., 2003). The localization of this enzyme is plastids in plants and it is a single polypeptide chain similar to the α subunit of bacterial NADPH-GltS. However, it differs from the bacterial NADPH-GltS with a lower nonheme iron and acid-labile sulfur content. (Marques et al., 1992, Hirasawa et al., 1996). Most of the data about the biochemical properties of Fd-GltS depend on studies of the enzyme prepared from spinach (Hirasawa et al., 1996). In addition, characterization of preparations of Fd-GltS from *Chlamydomonas* (Galvan et al., 1984), *Synechococcus* (Marquez et al., 1992) and *Synechocystis* (Navarro et al., 2000) has also been done.

III) NADH-GltS (EC 1.4.1.14) There is also a pyridine nucleotide-linked form of GltS found in yeast, fungi, plants and lower animals (Figure 1.12). NADH-dependent GltS appears to be mainly responsible for primary ammonia assimilation in roots (Gregerson et al., 1993). The purification of the enzyme have been achieved from *Medicago sativa* (Anderson et al., 1989), *Saccharomyces cerevisiae* (Cogoni et al., 1995). In addition, NADH-dependent GltS has also been presented in silkworm (Hirayama et al., 1998). There have been many studies on cloning and sequencing of the genes or the complementary DNA (cDNA) encoding GltS in several eukaryotes. The eukaryotic pyridine nucleotide- dependent enzyme is found to be composed of a single polypeptide chain which is thought to be formed by the fusion of polypeptides corresponding to the α and β subunits of bacterial GltS. The electron donor of this enzyme was shown to be NADH-dependent. GltS is the least studied enzyme among enzymes of nitrogen metabolism. For instance, the eukaryotic NADH-dependent GltS has been studied very little because of a combination of factors like low amount levels and high instability of this enzyme. Fd-dependent GltS is more abundant so more studies has been performed on it (Binda et al., 2000).

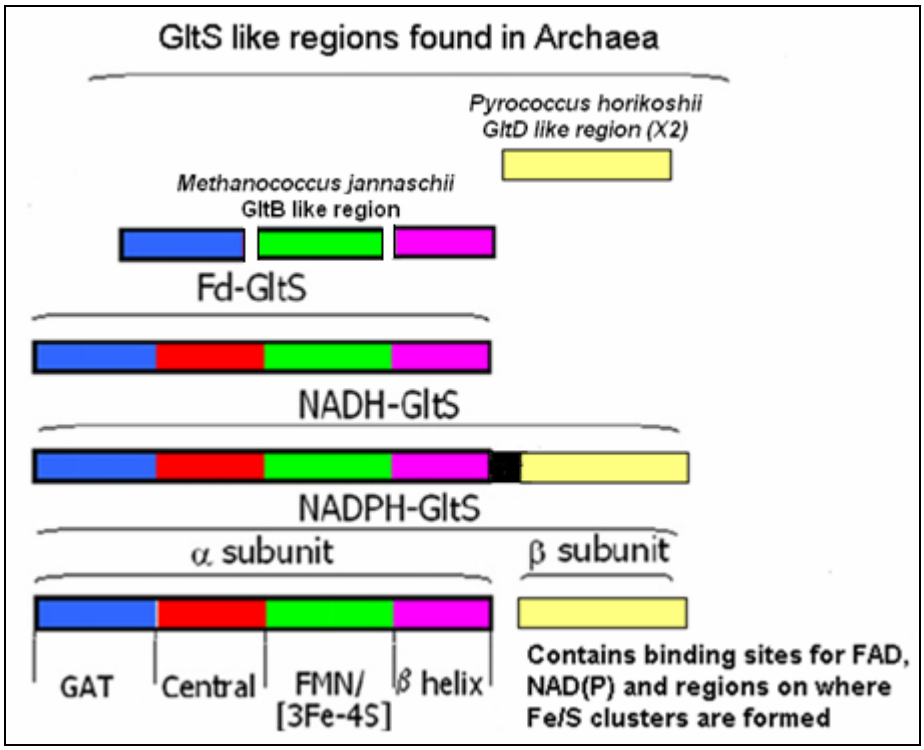

Figure 1.12: Eukaryotic, eubacterial and archaeal glutamate synthase and glutamate synthase-like proteins are showed with respect to their subunit compositions. Redrawn and changed from Vanoni and Curti (2005).

Mature proteins do not contain the regions indicated by black box in Figure 1.12 and the other regions indicate the similar regions among the proteins.

1.2.3. Catalytic Mechanism of Glutamate Synthase

Both α subunit of NAD(P)H-GltS and Fd-GltS consist of four domains which are the N-terminal glutamine amidotransferase (GAT) domain, the central domain, the flavin mononucleotide (FMN) -binding domain, and the C-terminal domain (Vanoni et al.,1992).

The reactions that take place in these domains are shown in Figure 1.13 (Nagradova, 2003).

The Glutaminase Domain	L-glutamine + H_2O → L-glutamate + NH_3
The FMN-binding Domain	2-oxoglutarate + NH_3 → 2-iminoglutarate + H_2O 2-iminoglutarate + FMN_{red} → L-glutamate + FMN_{ox}

Figure 1.13: The reactions taking place in the glutaminase domain and in the FMN-binding Domain which are present in the α subunit of glutamate synthase.

Different reactions give rise to reduction of FMN in Fd-GltS and NAD(P)H-GltS. The transmission of electrons from the reduced ferredoxin, present in the Fd-loop, to the FMN, present in the FMN binding domain, through the 3Fe-4S clusters results in FMN reduction (Vanoni et al.,1992).

$$Fd_{red} \xrightarrow{2e^-} \text{3Fe-4S cluster} \xrightarrow{2e^-} FMN_{red} \qquad \textbf{(1.1)}$$

On the contrary, αβ heterooligomer formation is required for the reduction of FMN, it can not be achieved only via the FMN- binding domain of alpha subunit of NAD(P)H-GltS. The β subunit of NAD(P)H-GltS catalyzes the reduction of the FAD and then, iron-sulfur clusters which are present in the αβ protomer take role during the transfer of the reducing equivalents to FMN (Vanoni et al., 1992).

$$NADPH + FAD_{ox} \rightarrow NADP^+ + FAD_{red} \qquad \textbf{(1.2)}$$

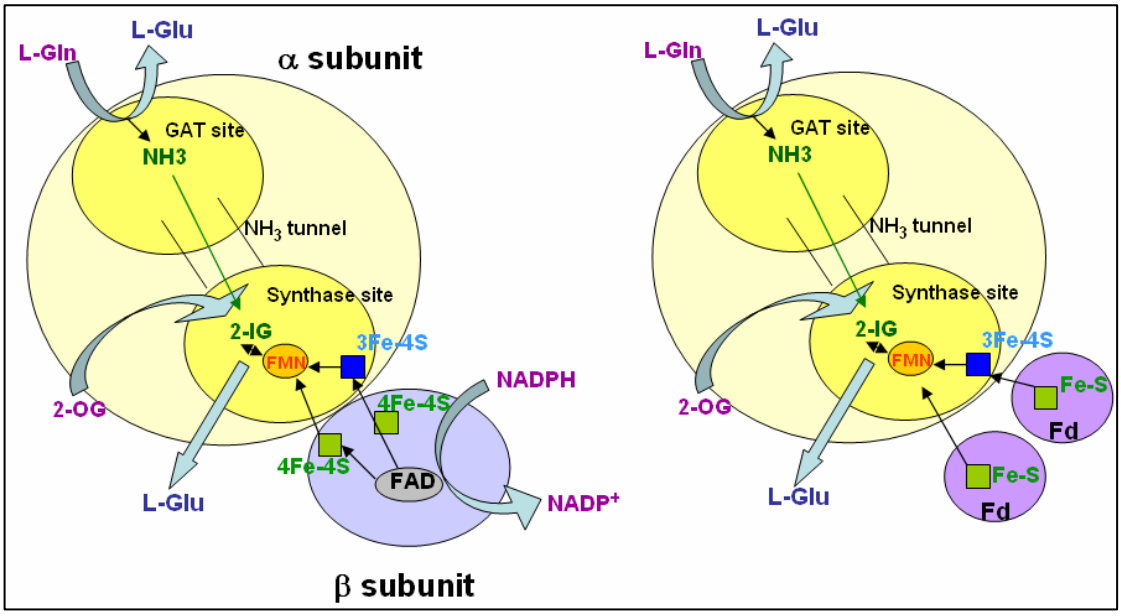

Figure 1.14: NADPH-dependent and Fd-dependent GOGAT reaction mechanisms (Vanoni and Curti, 2005).

In the Figure 1.14, [4Fe–4S] clusters of NADPH-dependent GOGAT and [2Fe–2S] center of Fd-dependent GOGAT are shown via cubes covered with small dashes. The possible electron transfer path from FAD (two linked ovals) to FMN (oval) through one of the [4Fe–4S] clusters (in the β subunit) and the [3Fe–4S] center of the α subunit of NADPH-GltS (cube) are shown with open headed arrows. Between FAD

and the [3Fe–4S] cluster, there is the second [4Fe–4S] of NADPH-GltS. A possible electron-transfer path between Fd and Fd-GltS is also presented (Vanoni and Curti, 2005).

1.2.3.1. Catalytic Mechanism of Fd-Dependent Glutamate Synthase

In Fd-dependent GltS, wasteful consumption of L-glutamine is prevented by its noticable characteristic of coordinating its catalytic centers when there is not any FAD and 2-oxoglutarate in the environment (Heuvel et al., 2002; Heuvel et al., 2003). The amidotransferase domain is only activated when the reduced FMN binding domain interacts with the reduced ferredoxin molecule and the ammonia acceptor subsrate 2-OG (Figure 1.14). The activation process is controlled by two enzyme conformations. The 2-OG, reduced cofactors and reduced ferredoxin stabilizes the active conformation of the enzyme (Heuvel et al., 2002). There is a strickly conserved polypeptide loop 4 (Figure 1.15) in the FMN binding domain providing organization between the catalytic centers and ferredoxin binding. This region of GltS protein is a strictly conserved part of the protein. As a result of the structural studies of the *Synechocystis* ferrodixin-dependent GltS, it has been found that there is a close proximity between the N-terminal region of loop 4 and the Fd loop and 3Fe-4S cluster. Moreover the OH of Tyr-987 (loop4) directly contacts with the OD1 of Asp-907 (Fd loop). Loop 4 also makes three hydrogen bonds with the substrate, 2-oxoglutarate. Moreover, it forms the walls of the ammonia tunnel at the C terminal part of itself (Figure 1.15). Stabilization of Cys-1 conformation via hydrogen bonding is achieved by its Glu-1013 C terminal residue (Heuvel et al., 2002).

A conformational change in loop 4 is thought to occur as Fd and 2-oxoglutarate are bound to the FMN binding domain of Fd-GltS. This conformational change may lead a hydrogen bond break between Cys-1 and Loop4 making a suitable condition for the L-glutamine to bind to Cys-1. This conformational change also triggers more changes that give rise to first molecule of L-glutamate and ammonia to be formed after the hydrolization of L-glutamine. The produced L-glutamate and ammonia is then sent through the channel to 2-oxoglutarate-binding site. In summary, after the interaction between the 2-oxoglutarate and FMN binding domain, a conformational change occurs in loop 4 and Cys-1 moves in the amidotransferase domain. The

simultaneous operation between Fd and Fd-dependent GltS provides these critical steps. As a result of this kind of simultaneous progression in the transfer of activatory signals which are Fd and 2-oxoglutarate, L-glutamine binding of the enzyme is achieved in a controlled manner (Heuvel et al., 2002).

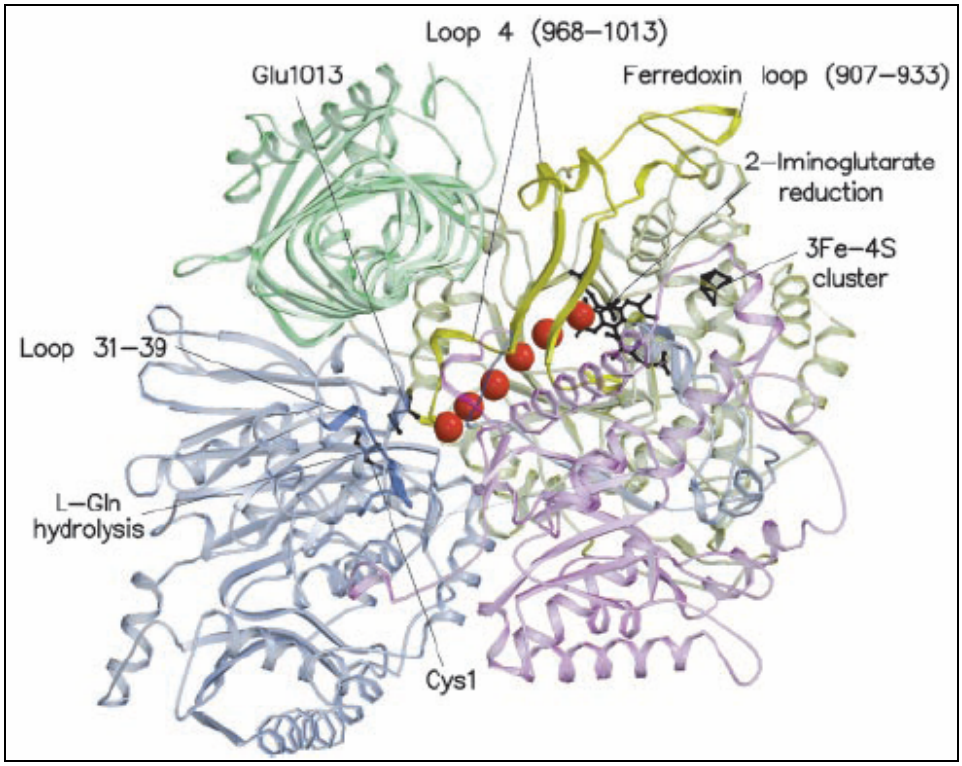

Figure 1.15: Three dimensional structure of Fd-dependent glutamate synthase of *Synechococcus* sp. PCC 6301 showing activatory signals transfers among domains leading simultaneous operation. The red balls indicate the location of the ammonia tunnel (Heuvel et al., 2002).

1.2.3.2. Catalytic Mechanism of NADPH-Dependent Glutamate Synthase

There are three different catalytic sites in the NADPH-GltS. Firstly, NADPH oxidation occurs at the pyridine nucleotide site which is present in the beta subunit, and then, hydroquinone form of FAD is produced as a result of its reduction (Figure 1.14). At least two of the three iron sulfur clusters of GltS (the [3Fe-4S] cluster in the α subunit and one of the two low potential [4Fe-4S] clusters in the holoenzyme) transmit reducing equivalents from FAD which is present on the beta subunit to FMN which is present on the alpha subunit (Vanoni et al., 1992, Vanoni et al., 1998, Ravasio et al., 2001). After ammonia addition, 2-iminoglutarate intermediate is produced from the bound 2-OG in the FMN domain of the α subunit (Figure 1.14). The N-terminal glutamine amidotransferase (GAT) domain of the GltS α subunit is the place where the ammonia is produced from the hydrolysis of glutamine (Figure

1.14). Intramolecular tunnel (Binda et al., 2000) is involved in the transfer of the ammonia to the FMN/2-OG-binding site. L-Glu is formed after the reduction of 2-iminoglutarate intermediate via the participation of FMN cofactor (Ravasio et al., 2001).

The crystal structures of the NADPH-GltS αβ protomer, of the isolated β subunit have not been elucidated yet, however, Binda et al. (2000) elucidated the three-dimensional structure of NADPH-GltS α subunit of *Azospirillum brasilense* (Figure 1.16).

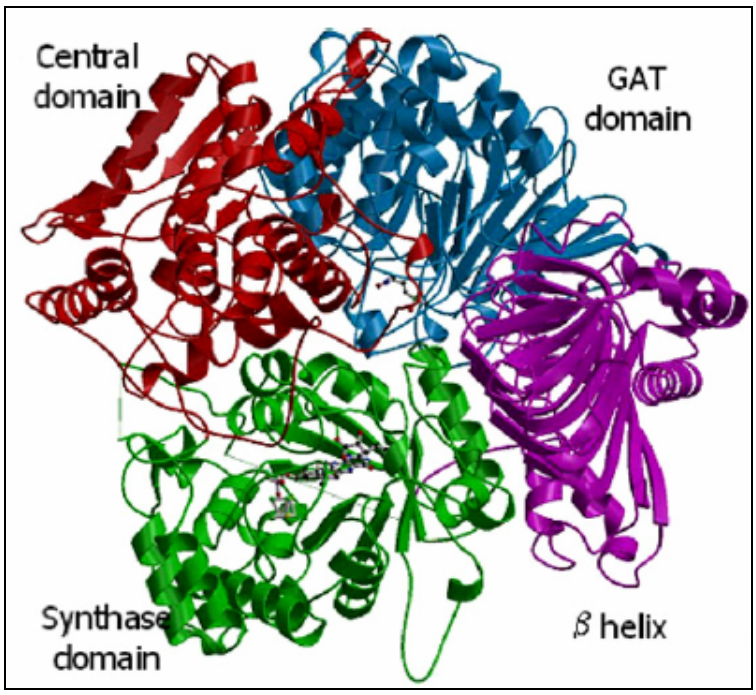

Figure 1.16: Three-dimensional structure of NADPH-GltS α subunit from *Azospirillum brasilense*.

In the Figure1.16, the enzyme glutamine amidotransferase site (blue) contains the bound L-Methionine sulfone which is presented via sticks. The synthase domain (green) includes FMN, the [3Fe–4S] cluster and 2-OG which are presented via sticks. The red part is the central domain and the purple part is the C-terminal β helix. (Binda et al., 2000)

1.2.4. Properties of GOGAT β subunit

The catalytic core is on the α subunit of GltS containing FMN cofactor and the 3Fe-4S cluster. This is the part where L-Gln hydrolysis, 2-iminoglutarate synthesis and reduction occur. On the contrary, briefly, transmisson of electrons produced as a

result of NADPH oxidation; to the FMN via using Fe-S clusters is the main function of the FAD containing β subunit (Binda et al., 2000)

It has been suggested that the interaction of the α subunit with β subunit to yield the holoenzyme, triggers conformational changes in the α subunit. This conformational changes lead to a tight link between glutamine hydrolysis at the glutamine amidotransferase (GAT) site and glutamate synthesis at the synthase site of the α subunit (Vanoni et al., 1998). Thus, the sole role of the β subunit of the enzyme does not seem to be reducing equivalents supply for the overall oxidoreduction reaction. This seems to be effective on the 3Fe-4S center and the FMN cofactor association and therefore is expected to be effective for the reactions to occur in a synchronic manner: amide transfer from glutamine to 2-oxoglutarate and L-glutamate production as a result of iminoglutarate intermediate reduction (Vanoni et al., 1996; Vanoni et al., 1998).

The interaction between α and β subunit triggers conformational change on the α subunit. Moreover, association between Fe/S centers II and III of GltS is likely to require the β subunit. The communication between the redox cofactors on the α subunit is provided by the centers II and III (Vanoni, 1998). At least one of the 4Fe-4S clusters of the GltS holoenzyme, is required for electron transfer between the flavin sites of the enzyme (Vanoni et al., 1992; Stabile et al., 2000)

The β subunit is the first identified member of a novel class of FAD-dependent NAD(P)H oxidoreductases. These classes of enzymes take role as a subunit or a domain of a complex enzyme. It seems that the decision of presence of low redox potential having Fe-S clusters is also achieved by the β subunit-like polypeptides. (Vanoni et al., 1999; Rosenbaum et al., 1998; Hagen et al., 2000)

Intramolecular electron transfer pathway can be determined via measuring the midpoint potential values. As a result of observations of the midpoint potential values , the association of the α and β subunits of the enzyme only has an influence on the midpoint potential of FAD which is taking a less negative value, indicating an environment that supports the reduction of GltS by NADPH (Ravasio et al.,2001). This result is conceivable with the supposed occurence of conformational changes after the combination of the two subunits in order to make an active holoenzyme. The electrons flow route is assumed to be from NADPH to FAD which is at GltS β

subunit and through FMN to the 2-iminoglutarate intermediate on the α subunit (Ravasio et al., 2001). This asumption is also conceivable with the caluculated midpoint potential values of GltS flavins and the 3Fe-4S cluster which takes part in the intramolecular electron transfer system (Ravasio et al., 2001).

1.3. Evolutionary Analysis of GOGAT

Most early studies assumed that species evolved only by vertical inheritance from parents. However, horizontal inheritance which is the process where genes are shared among genomes of different species due to lateral transfer (LGT) rather than vertical (inheritance) transfer is now considered to be quite common among bacteria and archaea. The term "tree of life" is exchanged with the term"web of life" in this perpective (Doolittle, 1999). Complete genome analyses are performed in order to search for the LGTs among organisms. For instance, it was discovered that over 200 lateral gene transfer processes occured between *E. coli* and *Salmonella sp.* 100 million years ago, which gave rise to 10 % of the present *E. coli* genome (Lawrence and Ochman, 1998). After the genome of *Thermotaga maritama* is sequenced, the high percentage similarity (24 %) of the *T. maritama*'s putative open reading frames to archaeal genes ratherthan to other bacterial genes, suggested the occurence of extensive lateral gene transfer between archaea and *T. maritama* (Nelson et al., 1999). Some of these ORFs are present as clusters at specific regions in the genome and these regions show a different GC pattern than other parts of the genome (Nelson et al., 1999).

Such differences in GC contents indicate that such clusters may have been laterally transferred. As a result of protein sequence analysis of GOGATs, eukaryotic NADH-GltS which is encoded by a single gene contains sequences resembling to both subunits of bacterial NADPH-GltS which are encoded by two separate genes, *gltB* and *gltD*. It has been seen that there is a high homology between the α subunit of the bacterial NADPH-GltS (GltB) and N-terminal region of eukaryotic NADH-GltS and also between the β subunit of the bacterial NADPH-GltS (GltD) and the C-terminal region of eukaryotic NADH-GltS (Figure 1.3) (Gregerson et al., 1993). Therefore, it can be speculated that there may be a common evolutinary origin among them suggesting an LGT event from prokaryotes to a eukaryotic ancestor. Furthermore, previously, it was thought that either a joining event of these two subunits or

separation of these two subunits from an ancestory single gene occured during evolution (Gregerson et al., 1993). However, a conserved gene pair changing into a single fused gene in eukaryotes would make it more favourable for eukaryotic organisms to control the gene regulation by leaving behind the operon structure (Andersson and Roger, 2002). Evolution scenarios about NADH-GOGATs involve a possible gene transfer from a prokaryotic endosymbiont to the nucleus. A gene transfer from prokaryotes to eukaryotic nucleus may also have occured when eukaryotes were feeding on prokaryotes. Such a mechanism could also explain the putative genetic exchange of glutamate synthase between a Gram-positive eubacterium to a single celled common ancestor of fungi, animals, and plants which later ended with the gene fusion of two subunit encoding genes (Andersson and Roger, 2002).

Moreover, the presence Fd-GOGAT (generally found in photosynthetic tissues like chloroplasts) together with NADH-GOGAT (generally found in non-photosynthetic tissues like roots and nodules) in plants is another factor to consider (Gregerson et al., 1993). The Fd-GOGAT is found in higher plants (maize, rice and *Arabidopsis*), two red algae species (*Porphyra purpurea and Antithamnion sp.*) and two cyanobacteria (*Synechocystis sp. and Plectonema boryanum*). The sequence analysis of these Fd-GOGATs revealed that there is a close relation between eukaryotic Fd-GOGAT and bacterial Fd-GOGAT. This finding supports the assumption that the eubacterial precursors of chloroplasts can be the ancestral sources for the genes encoding Fd-GOGATs (Temple et al., 1998). In addition, according to a widely accepted hypothesis, plastids may have evolved from endosymbiotic relationships between eubacteria and eukaryotic organisms. The presence of the Fd-GOGAT gene in the plastid genomes of the red algae supports this assumption (Temple et al., 1998). The fact that nuclear genome of higher plants containing GOGAT genes is consistent with the hypothesis of endosymbiont ancestral source of plastids and gene transfer between the endosymbiont genome and the host (Temple et al., 1998).

Furthermore, there are also some proteins containing the conservative sites of the glutamate synthase β subunit, and therefore called as GltS β subunit like proteins, however, their C-terminal and N-terminal parts show difference from one another. Moreover, there are no open reading frames, which may code for a large subunit adjacent to these small subunit homologue ORFs. The ORFs which are encoding

GltS β subunit like proteins are *DsrL* from *Allochromatium vinosum* (Dahl et al., 2005), *SudA* from *P. furiosus* (Schut *et al*., 2003), *GltA* from *Thermococcus kodakaerensis* (Jongsareejit et al., 1997), *GltX* from *C. saccharobutylicum* NCP262 (Stutz and Reid., 2004).

1.4. Properties of Glutamate Synthase β Subunit-like Proteins

Two flavin cofactors (FAD and FMN) and three distinct Fe-S centers: one [3Fe-4S] $^{0;1+}$ cluster (Center 1) and two [4Fe-4S]$^{1+;2+}$ clusters (Centers II and III) are among characteristics of glutamate synthase which is an iron sulfur flavoprotein (Reid and Stutz, 2004). The function of the β subunit is to transfer electrons into the α subunit for reductive glutamate synthesis (Vanoni et al., 1999). The reduction of FAD occurs as NAD(P)H binds to the β subunit. The Fe-S centers conduct electrons through to FMN, this transmission give rise to a reduction of this second flavin present on the α subunit (Vanoni et al., 1999). There are two consensus sequences for the formation of ADP-binding folds in the GltS β subunits, one of which is for NAD(P)H binding and the other is for FAD (Stutz and Reid, 2004).

Electron transfer between a reduced pyridine nucleotide and a second protein or protein domain is probably the role of GltS β subunits, putative β subunits and β subunit-like proteins as they contain conservative sites for FAD and Fe/S cluster(s) encoded from their N-terminal sequence. DNA sequence homology studies revealed many genes which are considered as glutamate synthase β subunit-like genes in Gene Bank databases. However, none of them are adjacent to a gene possibly encoding a GltS α subunit (Stutz and Reid, 2004).

Recently, an open reading frame showing striking homology with GOGAT small subunit from *Clostridium saccharobutylicum* NCP262 was cloned and named as *gltX* (Stutz and Reid, 2004). The translated gene product showed homology to GOGAT β subunits and β subunit-like genes varying from 27% to 77% homology at the protein level. This protein comprises all the basic structural characteristics of GOGAT β subunits. There are two N-terminal cysteines which may be the ligands for the [4Fe-4S] clusters; CX2CX4CX3P (residues 15-27) and CX3CX5CX3C (residues 62-76) (Vanoni et al., 1999, Pelanda et al., 1993, Curti et al., 1995). Moreover, this translated gene product contains possible ADP-binding regions involved in FAD and

NAD(P)H binding which are conserved in all GOGAT β subunits. There are also common sites between the *A. brasilense* GltS β subunit protein and GltX, differing from NADH GltS β subunit like region, which are proposed to be involved in NADPH binding. For instance, there is an A instead of G in the last position of the motif GXGXX(G/A/P) and an arginine residue at position 271. Moreover, there is a mismatch in the second position of the second consensus FAD binding sequence at the COOH-terminus of GltX like *S. cerevisiae* GltS β subunit (Stutz and Reid, 2004). There is not any α subunit homologue adjacent to GltX protein, and the transcription of *gltX* occurs independently. In addition, the hyperthermophilic *Aquifex aeolicus* (Deckert et al., 1998), and the archaeon *P. furiosus* (Schut et al., 2003) contain α and β subunit homologues of GOGAT, respectively. In both situations there is not an adjacent homologue of other subunit. However, enzyme activity assays have not been performed yet.

Because of the the striking homology between the predicted amino acid sequence of GltX and GOGAT beta subunit protein sequences, and because of the presence of predictable FAD and NADPH binding conserved regions, this protein is expected to be responsible for electron transmission utilizing NADPH and FAD. However, the Fe-S centres II and/or III which are forming second cystein-rich domains in the GltX does not comprise some highly conserved residues. As a result of the studies performed with *A. brasilense* GltS, it has been found that not only do the Fe-S centers II and III supply reducing elements for oxidoreduction reaction but also they were shown to be involved in the formation of accurate interaction between the two subunits of GltS which is important for conformational changes activating catalytic activities. These conformational changes lead to an association of the glutaminase and glutamate synthase activities and also electron transmission between the redox centers (Vanoni et al., 1999).

After enzyme activity assays were performed as described by Jongsareejit et.al. (1997), it has been shown that *gltX* product does not show a glutamate synthase activity (Stutz and Reid, 2004). GltX found in *C. saccharobutylicum* NCP262 is proposed to be a member of β subunit like proteins, which may have an electron transmission role (Stutz and Reid, 2004).

There is a controversial report that a small subunit-like ORF in *Thermococcus kodakaerensis* (formerly known as *Pyrococcus* KOD1*)* can show GOGAT activity without the large subunit by forming a homotetramer structure (Jongsareejit *et al*., 1997). Primers designed on the basis of conserved motifs in non-archaeal glutamate synthases were used in order to find the structural gene for this protein by Jongsareejit et al (1997). *Thermococcus kodakaraensis* small subunit-like ORF shows similarities ranging from 41% to 49% when compared to the small subunits of the NADPH-dependent bacterial glutamate synthases and to the second domain of the yeast, rice and alfalfa glutamate synthases.

It has been claimed that KOD1-*gltA* gene product shows GOGAT catalytic activity, only depending on the NADPH dependent electron transfer reaction and amino acid sequence homology (Jongsareejit *et al*., 1997). Such a result could not be repeated by any other group and the recently published *Thermococcus kodakaraensis* genome by the same group do not report the presence of a glutamate synthase large subunit gene within the genome (Fukui et.al, 2005).

```
SUDA            MPR--LIKDRVPTPERSVGERVRDFGEVNLGYSMELALREAERCLQCPVEYAPQIKQCPV 58
KOD1            MPRRKLIKERVPTPERPPEERIKDFKEVNLGYTFELAVKEAERCLQCPYEYAPCIKGCPV 60
                ***  ***:*******.  **::** ******::***::********* **** ** ***

SUDA            IHNIPGFIKALRENRDNPSKAVREALRIIWRDNTLPAITGRVCPQEEQCEGACVVGKVGD 118
KOD1            HINIPGFISKLVEYRDDPDKAVKEALNVIWACNSLPATTGRVCPQEDQCEMNCVMGKVGD 120
                ******. * * **:*.***:***.:**  *:*** ********:***  **:*****

SUDA            PINIGKLERFVADYAREHGIDDELLLEEIKGIKRNGEKVAIIGAGPAGLTCAADLAKMGY 178
KOD1            KINIGKLERFVADYAREKGIDEELLFEIIPKIEKKGQ-VAIIGAGPAGLTAAGELAKLGY 179
                ***************:***:***:* *  *:::*:.***********.*.:***:**

SUDA            EVTIYEALHQPGGVLIYGIPEFRLPKEIVKKELENLRRLGVKIETNVLVGKTITFEELRE 238
KOD1            DVTIYEALHEPGGVLMYGIPEFRLPKEIVNKEIEKLRKLGVKILTDHVVGRTVTIEELLQ 239
                :********:*****:*************:**:*:**:***** *: :**:*:*:*** :

SUDA            EYDAIFIGTGAGTPRIYPMPGVNLNGIYSANEFLTRINIMKAYKFPEYDTPIKVGKRVAV 298
KOD1            EYDAVFIGSGAGTPRLINAPGINLNGIYTANEFLTRVNLMKAYLFPEYDTPVYVGKKVIV 299
                ****:****:******:    **:******:*******:*:**** *******: ***:* *

SUDA            IGGGNTAMDAARSALRLGAEVWILYRRTRKEMTAREEEIKHAEEEGVKFMFLVIPKRFIG 358
KOD1            IGAGNTAMDAARSARRFGAEVTIAYRRGEEDVSARPEEVEHAKEEGIKFVY-VNPVEFIG 358
                **.********** *:**** * *** .::::******::**:***:**:: * * .***

SUDA            DENGNLKAIELEKMK-LGEPDESGRRRPIPTGETFIMEFDTAIIAIGQPTNKTFLETVPG 417
KOD1            DENGRVKAVKFEKMKALDERDARGKRKIVGTGEYVTLEADTVIIAIGKHPNRLIIN-TPG 417
                ****.:**:::**** *.* *  *:*: : *** . :* **.*****: .*: :::::.**

SUDA            LKVDEWGRIVVDENLMTSIPGVFAGGDAIRGEATVILAMGDGRKAAKAIHQYLSKEK--- 474
KOD1            LKVER-GKIVVDENLMTSIPGVFAGGDAIRGEATVILAMGDGRKAAKAIHEYLTKKRQEK 476
                ***:. *:*****************************************:**:*::

SUDA            ---
KOD1            ANA 479
```

Figure 1.17: The homology between α subunit of sulfide dehydrogenase (SudA) and KOD1-GltA.

A later report suggested that KOD1-*gltA* product is a not a glutamate synthase, but a part of the sulfide dehyrogenase (SudH) enzyme (Hagen *et al*, 2000) (Figure 1.17), which is also a ferrodoxin: NADP+ oxidoreductase (FNOR) (Schut et al., 2003). These enzymes are responsible for the interconvention of the reductants produced from amino acid catabolism: ferrodoxin and NAD(P)H. (Schut et al., 2003) SudH encoding gene is composed of two structural genes; α subunit, *sudA* and β subunit, *sudB*. Three Fe-S clusters which are one [2Fe-2S] cluster with asparagine as a ligand, one [3Fe-4S] cluster, one low potential [4Fe-4S] cluster and, two FADs and two putative binding sites for NADPH were identified as a result of sequence analysis of SudH (Hagen et al., 2000). One putative FAD binding site and a putative nucleotide binding site for NADPH, and a $[2Fe\text{-}2S]^{2+,+}$ prosthetic group is found in α subunit, SudA. As a result of the sequence analysis, *sudA* product showed high homology to GOGAT small subunit while SudB is highly homologous to HydG, the γ-subunit of *P. furiosus* sulfhydrogenase (Ni-Fe hydrogenase) which is another sulfide dehydrogenase (Hagen et al., 2000). There are also SudB subsequences in the genomes of hyperthermophilc archaea *Pyrococcus horikoshii* and *Pyrococcus abysii* and of the hyperthermophilic bacteria *Thermotoga maritima* and *Aquifex aelicus* (Hagen et al., 2000). The *sudA* product was shown to be one of the subunits of sulfide dehydrogenase enzyme (SudH), and it did not show any glutamate synthase activity. An ORF, which is highly homologous to *sudAB*, was also named as *sudXY* (PF1901 and PF1911) (Hagen *et al*, 2000). However, it was later reported that *sudAB* and *sudXY* was homologous only at the sequence level because microarray data showed different upregulation in carbohydrate and peptide grown cells (Schut *et al*., 2003). In addition, PF1852, which also shows homology to the small subunit, was upregulated in maltose-grown cells (Schut *et al*., 2003).

Another GltS β subunit-like open reading frame is *DsrL* from *Allochromatium vinosum* as it contains the conserved sites belonging to GltD (Dahl et al., 2005). There are two regions (GXGXXG/A/P, adenylate binding) which are expected to be involved in FAD and pyridine nucleotide factor binding (Vanoni et al., 1996; Morandi et al., 2000). NADP(H) binding proteins (Scrutton et al, 1990) contains an alanine or serine at the terminal position and, this feature is also seen in DsrL. There are two putative [Fe-S] clusters one of which is with four and the other is with three or four [Fe-S] binding cysteine residues at the N terminus of the small subunits of

glutamate synthases (Hagen et al., 2000). However, DsrL does not contain the second cysteine of the first cluster (Dahl et al., 2005). There is a ferredoxin extension at the C-terminal of DsrL unlikely to glutamate synthase beta subunit (*gltD* encoding protein) or SudA. Moreover, *dsrL* is not adjacent either to a *gltB*-like or to a *sudB*-like gene. Because of the two properties of DsrL together with results of the pyhlogenetic studies, it can be suggested that DsrL has a distinct catalytic activity than both glutamate synthase and from sulfide dehydrogenase (Dahl et al., 2005). According to its amino acid sequence, DsrL can most probably transfer electrons between NADPH /$NADP^+$ and an unknown acceptor/donor with the aid of FAD cofactor. The C-terminal ferredoxin domain may be involved in a NADPH: ferredoxin oxidoreductase reaction (Dahl et al., 2005).

1.5. Aim of the Study

According to the comparative analysis of protein primary structures, open reading frames (ORFs) which are encoding proteins similar to both α subunit domains and β subunits of GOGAT have been found in some archaea.

In *Methanocaldococcus jannaschii*, there are three ORFs (ORFs MJ1350-MJ1351-MJ1351.1) which are highly homologous to the three domains of the large subunit of GOGAT while no ORF has been detected for a small subunit homologue. MJ1351.1 shows homology to glutamine aminotransferase domain, MJ1351 to FMN binding synthase domain and MJ1350 to β-helix domain. However, the genomes of three *Pyrococcus* species, *P. horikoshii* (Figure 1.18), *P. furiosus* and *P. abyssi*, harbour two open reading frames which show homology with the small subunit of GOGAT.

The genomes of *Pyrococcus* species, *P. horikoshii, P. abyssi*, harbour two, *P. furiosus* three open reading frames which show homology to the small subunit of glutumate synthase (GOGAT). The regions encoding β-subunit like proteins in *P. horkoshii* are ORFs PH0876 and PH1873. There are no open reading frames which may be coding for a large subunit which is responsible for the glutamate formation in the genome of *P. horikoshii*. The presences of two putative GOGAT small subunits, which are showing high homology to each other (Figure 1.18), raise the possibility of gene duplication. Evolution of glutamate synthase might have occured via lateral gene transfer via the combination of two subunits in the higher organisms (Dinçtürk,

2001, Andersson & Roger, 2002). It seems likely that these open reading frames are the early forms of an electron transfer domain in archaea which may have later contributed to many electron transfer enzymes.

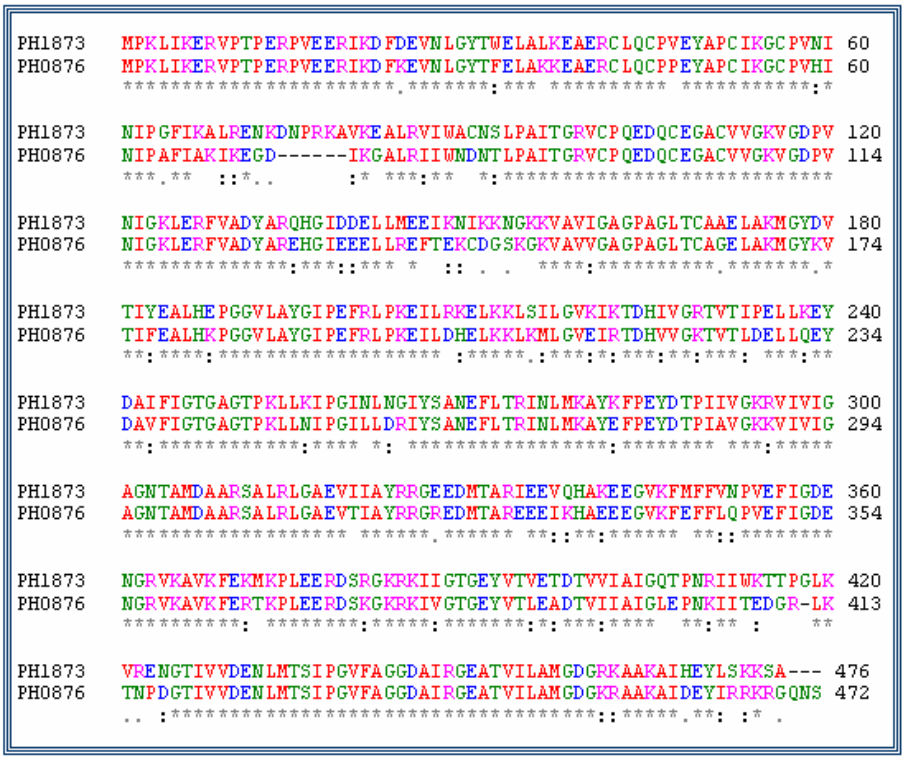

Figure 1.18: ClustalW multiple protein sequence alignment of PH0876 and PH1873. Identical residues are indicated by stars. Dashes indicate gaps introduced to maximize sequence similarity. The two putative GOGAT small subunits have raised the speculation of gene duplication since they show very high homology.

To further analyze this hypothesis, two open reading frames PH0876 and PH1873 from *P. horikoshii* have been cloned and successfully expressed in *E. coli* and the presence of the proteins have been confirmed with Western Blot analysis. Both proteins have been obtained in the soluble fraction of the cell and purified with the aid of His-Tag present upstream the coding region. The glutamate synthase small subunit of *Medicago sativa* has also been cloned and expressed in *E. coli* to be used as a control in activity analysis. Activity analyses are on progress to further characterize the proteins in our laboratory.

2. MATERIALS AND METHODS

2.1. Materials

2.1.1. Bacterial strains

- *Escherichia coli* strain XL1 Blue [*recA1 endA1 gyrA96 thi-1 hsdR17 supE44 relA1 lac* [F' *proAB lacI*^{q}*ZΔM15* Tn*10* (Tet^{r})]].
- *Escherichia coli* strain Rosetta(DE3)pLysS [F^{-} *ompT hsdS*$_B$(r_B^{-} m_B^{-}) *gal dcm lacY1* (DE3) pLysSRARE^2 (Cm^{R})] was purchased within the Rosetta™ Competent Cell Set from Novagen.

2.1.2. Bacterial culture media and antibiotics

2.1.2.1. LB broth medium

LB medium contains was prepared by dissolving 10 g tryptone, 5 g NaCl and 5 g yeast extract in 1 lt. distilled water. The pH was adjusted to 7.0-7.5 using 10 M NaOH..

2.1.2.2. LB agar medium

LB agar medium contains was prepared by addition of 15 gr agar to the recipe given for LB medium.

2.1.2.3. Antibiotics

Kanamycin, Chloramphenicol, Tetracycline and Ampicilin were used in this study at final concentrations of 50µg/ml, 34µg/ml, 12µg/ml and 100µg/ml, respectively.

2.1.3. Chemicals and Enzymes

2.1.3.1. Chemicals

Chemicals were obtained from Sigma and Fluka. Restriction enzymes were purchased from Fermentas and Takara.

2.1.3.2. Enzymes

Restriction Enzymes

The restriction enzymes used in this study and are shown below. They were purchased from Fermentas.

Table 2.1: Restriction enzymes used in this study

EcoRI	*5'* – G^AATTC – 3'	10 units/ µl, Fermentas
XbaI	5' – T^CTAGA –3'	10 units/ µl, Fermentas
*Bam*HI	5' – G^GATCC-3'	10 units/ µl, Fermentas
SacI	5'-GAGCT^C-3'	10 units/ µl, Fermentas
SalI	5'-G^TCGAC-3'	10 units/ µl, Fermentas

DNA Modifying Enzymes

TaKaRa *Ex Taq*™

The enzyme, which is 5 units/µl, was purchased from Takara Biomedicals Inc. It was preserved at -20°C in its storage buffer containing 20 mM Tris HCl (pH8.0), 100 mM KCl, 0.1 mM EDTA, 1 mM DTT, 0.5% Tween 20, 0.5% Nonidet P-40, 50% Glycerol. 10X reaction buffer containing 100 mM Tris-HCl (pH: 8.5), 500 mM KCl was used at 1X final concentration for the reaction.

***Pfu* DNA Polymerase**

The enzyme, which is 2.5u/µl, was purchased from Fermentas. It was preserved at -20°C in its storage buffer containing 20mM Tris-HCl (pH 8.2), 1mM DTT, 0.1mM EDTA, 100mM KCl, 0.1% (v/v) Nonidet P40, 0.1% (v/v) Tween 20 and 50% (v/v) glycerol. 10X reaction buffer containing 200mM Tris-HCl (pH 8.8 at 25°C), 100mM $(NH_4)_2SO_4$, 100mM KCl, 1% (v/v) Triton X-100, 1mg/ml BSA was used at 1X final concentration for the reaction.

T4 DNA Ligase

The enzyme, which is 5 units /µl, was purchased from Fermentas. It was preserved at -20°C in its storage buffer containing 20mM Tris-HCl (pH 7.5), 1mM DTT, 50mM KCl, 0.1mM EDTA and 50% (v/v) glycerol. 10X reaction buffer containing 400mM Tris- HCl (pH 7.8), 100mM $MgCl_2$ 100mM DDT, 5mM ATP. It was used at 1X final concentration for the reaction.

Lysozyme (from chicken egg white)

Lysozyme was supplied as a lyophilized powder from Sigma-Aldrich. 50 mg/ml lysozyme stock solutions were prepared and stored at -20°C.

2.1.4. pET30b Expression vector

There is an N-terminal His•Tag®/thrombin/S•Tag™/enterokinase configuration plus an optional C-terminal His•Tag sequence on this vector. The circular map (Figure 2.1.a) and the MCS are shown below (Figure 2.1.b). The vector is 5422 bp long.

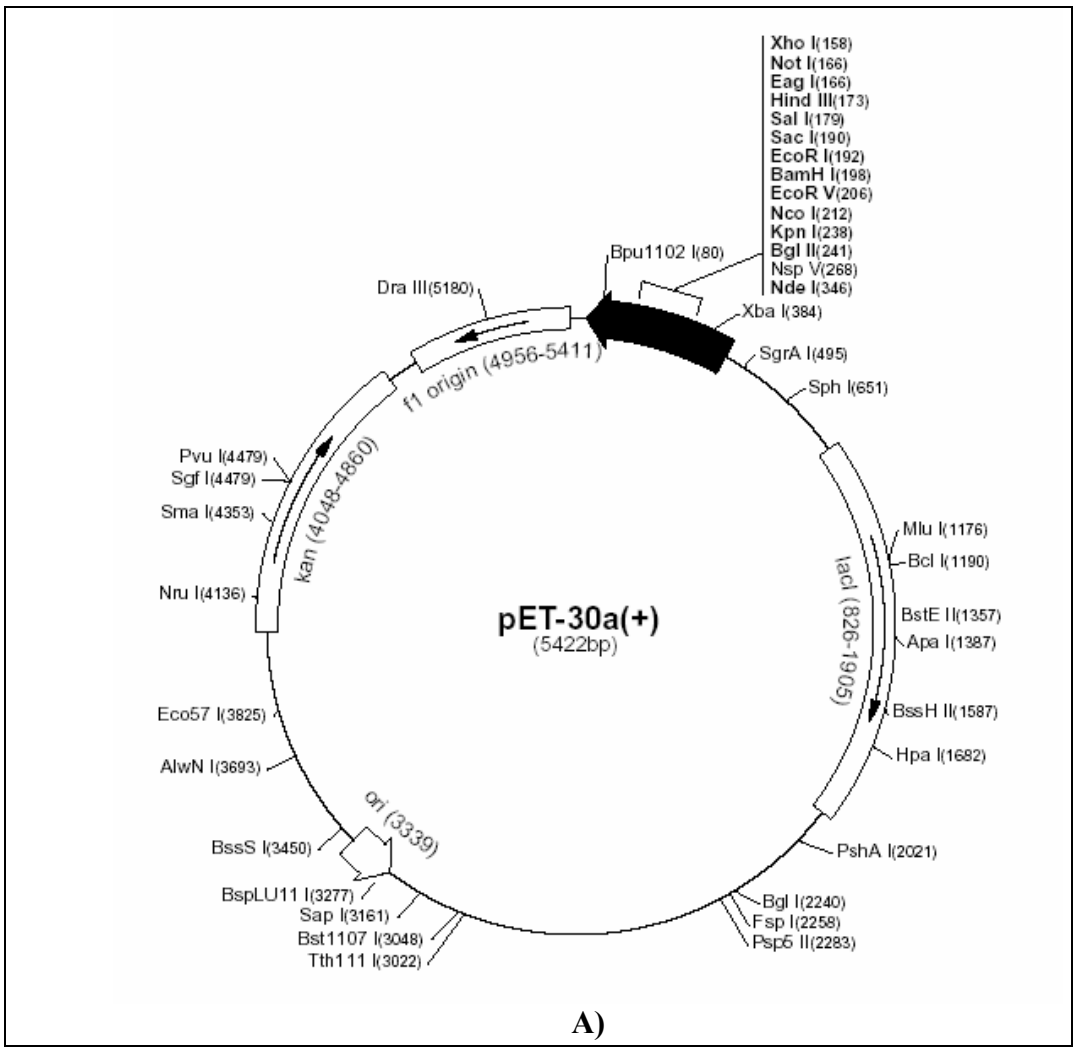

Figure 2.1: Vector map **(A)** and, cloning/expression region of the coding strand of pET30b **(B)** (http://www.novagen.com).

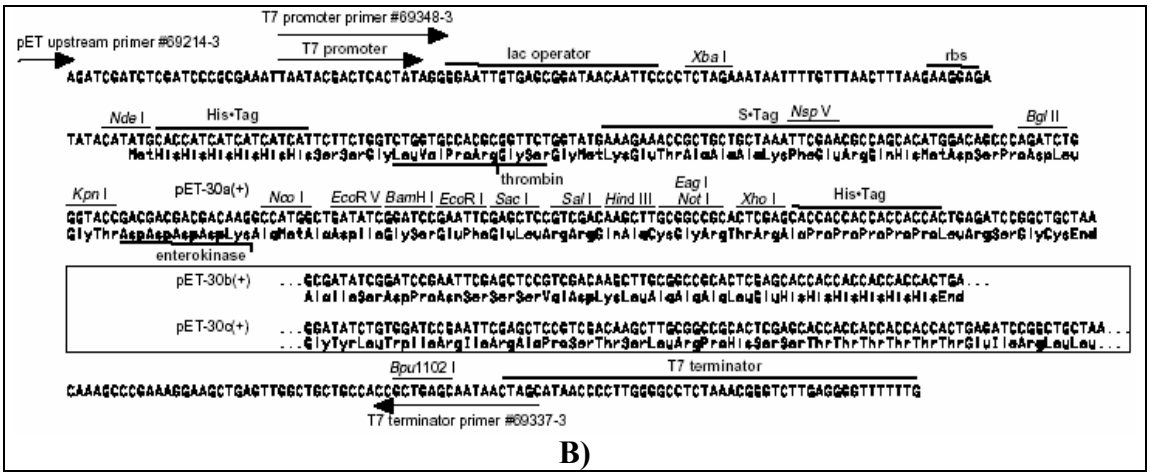

Figure 2.1: Continuing. Vector map **(A)** and, cloning/expression region of the coding strand of pET30b **(B)** (http://www.novagen.com).

2.1.5. T/A cloning vector pTZ57R/T

Plasmid pTZ57R/T, which is 2886 bp in length, has 3'-ddT overhangs at both ends. These 3'-ddT overhangs make it possible to directly ligate a PCR fragment with 3'-dA overhangs into this vector. InsT/Aclone™ PCR Product Cloning Kit including T/A cloning vector pTZ57R/T was purchased from Fermentas (Figure 2.2).

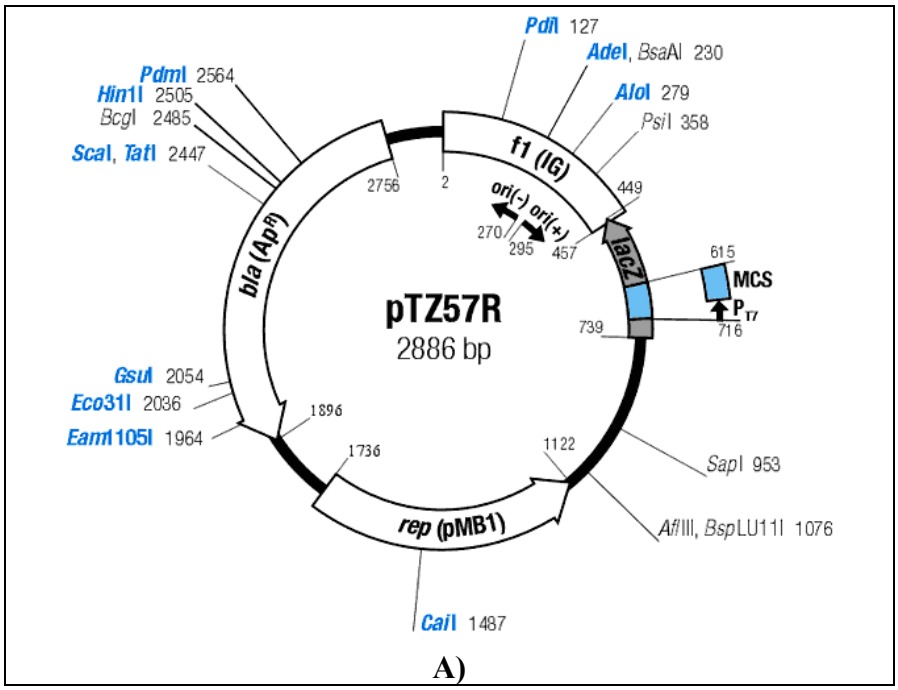

Figure 2.2: Vector map **(A)** and, multiple cloning site of pTZ57R/T **(B)** Source: http://www.fermentas.com.

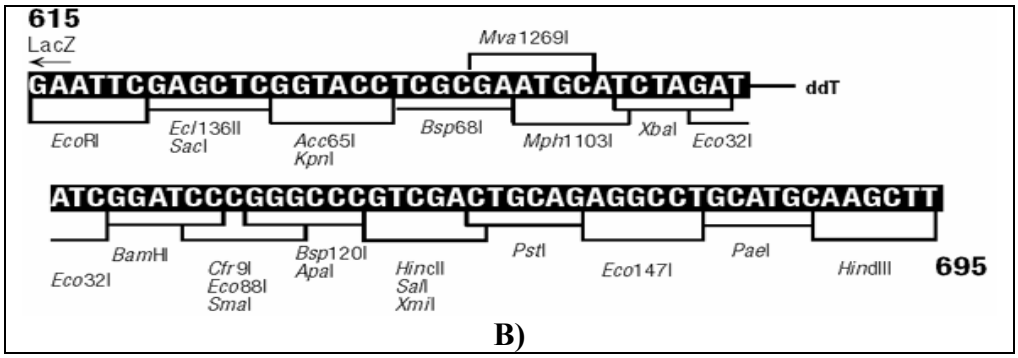

Figure 2.2: Continuing. Vector map **(A)** and, multiple cloning site of pTZ57R/T **(B)**

2.1.6. Protein and DNA Molecular Weight Markers

2.1.6.1. Protein Molecular Weight Marker

The Protein Molecular Weight Markers used in this study are presented below (Figure 2.3).

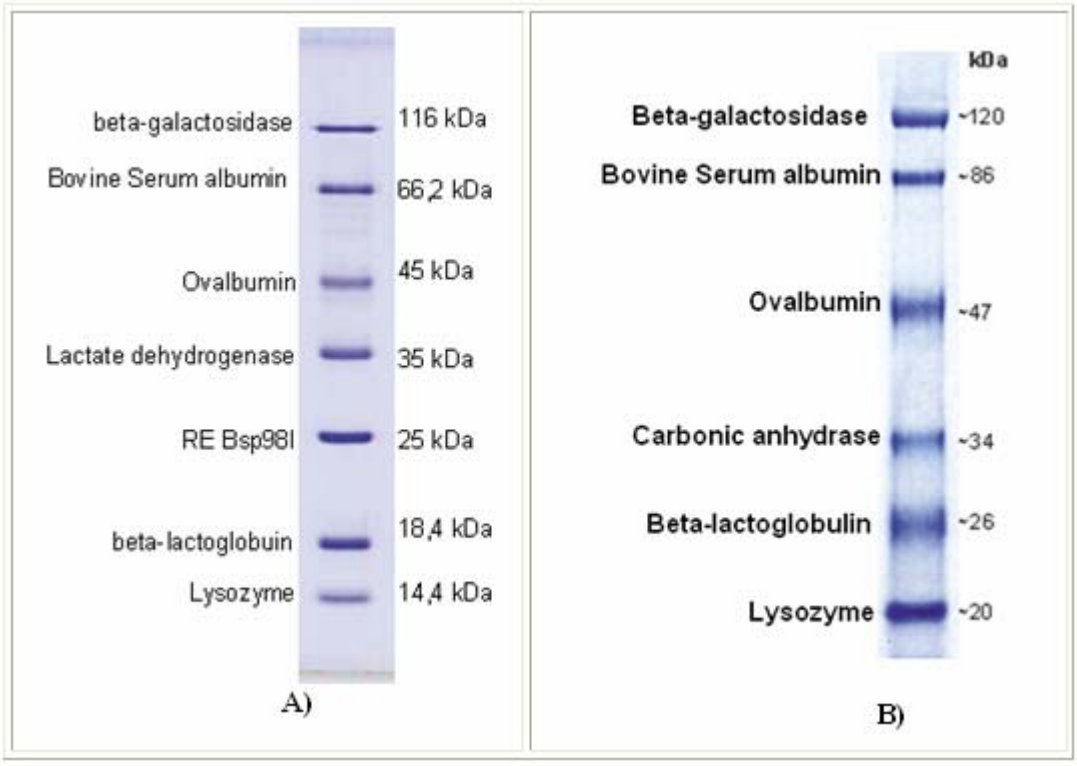

Figure 2.3: Protein molecular weight markers used in this study. **A)** Protein Molecular Weight Marker, 12% SDS-PAGE, Comassie Brilliant Blue R-250 stained. **B)** Prestained Protein Molecular Weight Marker, 8% SDS-PAGE. Source: http://www.fermentas.com.

2.1.6.2. DNA Molecular Weight Markers

The DNA Molecular Weight Markers used in this study are Lambda DNA/*EcoRI*+*HindIII* Marker 3 (Figure 2.5.a), MassRuler™ DNA Ladder, Mix, ready-to-use (Figure 2.5.b), FastRuler™ DNA Ladder, High Range (Figure 2.5.c), FastRuler™ DNA Ladder, Middle Range (Figure 2.5.d). They were purchased from Fermentas.

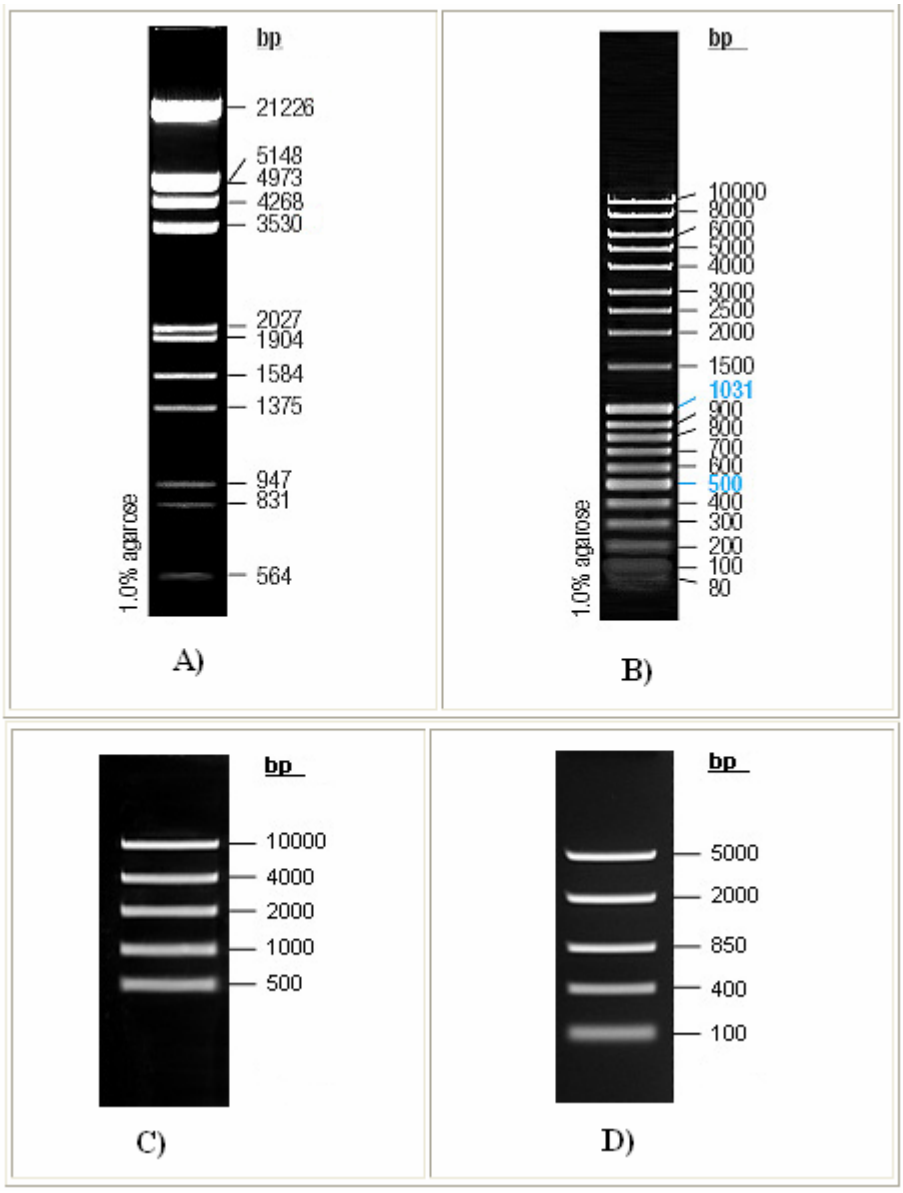

Figure 2.4: DNA markers used in this study. **A)** λ DNA *EcoRI* and *HindIII* digested marker, 1.0% agarose, 0.5µg/lane, 8cm length gel, 1X TAE, 7V/cm. **B)** MassRuler™ DNA Ladder, Mix, ready-to-use, 1.0% agarose, 0.5µg/lane, 8cm length gel, 1X TAE, 7V/cm Source: http://www.fermentas.com. **C)** FastRuler™ DNA Ladder, High Range, ready-to-use, 1.0% agarose, 1X TAE, 7V/cm. **D)** FastRuler™ DNA Ladder, Middle Range, ready-to-use, 1.0% agarose, 1X TAE, 7V/cm (http://www.fermentas.com.)

2.1.7. Oligonucleotide primers

The oligonucleotide primers were purchased from GIBCO-BR and IONTEK shown below. F1PH0876 and R2PH0876 are the first forward and reverse primers for ORF PH0876 respectively. CommonF2_primer is the second forward primer for both of the ORFs, PH0876 and PH1873, it carries *BamHI* restriction site. R2PH0876 is the second reverse primer for PH0876 and it carries *SacI* restriction site. RPH1873 is the second reverse primer for ORF PH1873 and it carries *SacI* restriction site. The restriction sites present on the primers are underlined.

Table 2.2: List of primers used in this study

F1PH0876	5'- GGG GAA TTC ATG CCT AAG CTT ATT AAT GAG-3'	30 mer
R1PH0876	5'- CCA AGC TTG TTA GGA ATT CTG ACC TCT CTT-3'	30 mer
CommonF2_primer	5'- CGC GGA TCC GCG GAT GCC TAA GCT TAT T -3'	28 mer
R2PH0876	5'- ACG CGA GCT CGT TAG GAA TTC TGA CCT C -3'	28 mer
R2PH1873	5'- CGC GAG CTC GTC AGG CAC TCT TTT TGC T -3'	28 mer

2.1.8. Buffers and Solutions

- **10x *EcoRI* Buffer:** 50mM Tris-HCl {pH:7.5}, 10mM $MgCl_2$, 100mM NaCl, 0.1 mg/ml BSA, 0.02 % TritonX-100.
- **10x *SacI* Buffer:** 10mM Bis-Tris Propane-HCl (pH:6.5), 10mM MgCl2, 0.1 mg/ ml BSA.
- **10x *BamHI* Buffer:** 10mM Tris-HCl (pH:8.0), 5mM MgCl2, 100mM KCl, 1mM 2-mercaptoethanol, 0.02%Triton X-100, 0.1mg/ml BSA.
- **10x O^+ Buffer:** 50mM Tris-HCl {pH:7.5}, 10mM $MgCl_2$, 100mM NaCl, 0.1 mg/ml BSA.
- **10x *Taq* polymerase Buffer:** 100mM Tris-HCl {pH:8.8 at 25^o C}, 500mM KCl, 0.8 % nonidet P40.
- **10X *Ex Taq* Buffer (Mg^{2+} free):** The full buffer composition of the *Ex Taq*™ buffer is proprietary.
- **10X *Pfu* Buffer with $MgSO_4$:** 200 mM Tris-HCl (pH:8.8), 20 mM $MgSO_4$, 100 mM KCl, 100 mM $(NH_4)_2SO_4$, 1% Triton® X-100, 1 mg/ml nuclease-free BSA
- **10x Ligation Buffer:** 400mM Tris- HCl, 100mM $MgCl_2$ 100mM DDT, 5mM ATP, pH 7.8 at 25^o C.

- **50x TAE (Tris, acetic acid, EDTA) buffer:** Stock solution containing 2.0 M Tris base, 5.71% v/v acetic acid, 10% v/v 0.5 M EDTA (pH 8.0). To make 1.0 L of 50X TAE, mix 242.2 g of Tris base, 57.1 ml glacial acetic acid, and 100 ml of 0.5 M EDTA (pH 8.0) stock solution in a one-liter container. Add MBG water to 1 liter. Store at room temperature.
- **1 % agarose:** 1 gram agarose is boiled to dissolve in 100 ml 1x TAE buffer.
- **Plasmid Purification - Cell resuspension solution:** 50mM Tris-HCl {pH 7.5}, 10mM EDTA, 100 µg/ml RNaseA.
- **Plasmid Purification - Cell lysis solution:** 0.2 N NaOH, 1 % sodium dodecyl sulfate (SDS).
- **Plasmid Purification - Cell neutralization solution:** 1.32 M potassium acetate, pH4.8.
- **DNA binding resin solution:** 4.2 M guanidine HCl.
- **DNA Elution buffer:** 10mM Tris-HCl (pH 8.5)
- **dNTP mix solution**: 2mM of each dATP, dCTP, dGTP, dTTP.
- **RF1 Buffer:** 100mM $RbCl_2$, 50 mM $MnCl_2$, 30mM KAc (pH: 7.5), 10mM $CaCl_2$, Glycerol 15 % (w/v); adjust pH to 5.8 with 0.2 M Acetic acid solution, sterilize with 0.22µm filter.
- **RF2 Buffer:** 10mM MOPS (0.5 M stock, pH: 6.9), 10mM $RbCl_2$,75 mM $CaCl_2$, Glycerol 15 % (w/v); adjust pH to 6.8 with NaOH, sterilize with 0.22µm filter.
- **5X sequencing buffer:** The full buffer composition is proprietary.
- **Cell solubilization buffer:** 50mM NaH_2PO4, 300 mM NaCl, pH=8 adjusted via NaOH
- **Ni-NTA Agarose Wash Buffer:** 50mM NaH_2PO4, 300 mM NaCl, 20 mM imidazole, pH=8 adjusted via NaOH
- **Ni-NTA Agarose Elution Buffer:** 50mM NaH_2PO4, 300 mM NaCl, 250 mM imidazole, pH=8 adjusted via NaOH
- **1X SDS-PAGE sample buffer:** 50 mM Tris·Cl (pH 6.8), 100 mM DTT, 2% SDS, 0.1% bromophenol blue, 10% glycerol

- **SDS-PAGE stain solution:** 10% Acetic acid, 45% Methanol, 0.2% g/ml CBB-R250 or CBB-G250 dissolved in 1 L dH_2O
- **SDS-PAGE Destain solution:** 10% Methanol and 10% Acetic acid mixed in dH_20
- **Transfer buffer for Western Blot Analysis:** 39 mM Glycine, 48 mM Tris, % 0.037 SDS, % 20 Methanol in deionized water.
- **Blocking Solution:** TBS containing 3% gelatin (w/v).
- **TBS for Western Blot Analysis:** 20 mM Tris, 500 mM NaCl, pH 7.5 in deionized water.
- **TTBS for Western Blot Analysis:** 0.05% Tween 20 containing TBS.
- **Antibody dissolving buffers**: 1% gelatin (w/v) containing TTBS.
- **AP color development buffer:** pH: 9.5 100 mM Tris-HCl.

2.1.9. Computer software

- **Homology search:** Basic Local Alignment Search Tool, BLAST. Standard protein-protein BLAST (blastp) (Altschul *et* al. 1990; Nakamura *et* al., 2000). Available at http://www.ncbi.nlm.nih.gov/BLAST/
- **Nucleotide alignments:** Multiple sequence alignment tool, ClustalW (Higgins *et* al., 1996). Available at http://www.ebi.ac.uk/clustalw/index.html
- **Translator tool:** JustBio Translator tool. Available at www.justbio.com.
- **Primer feasibility tool:** IDT BioTools Oligo Analyser 3.0. Available at http://207.32.43.70/analyzer/oligocalc.asp.
- **ProtCalc:** Tool for determining statistical, theoretical MW, pI and extinction data from protein sequence. Available at http:// www.justbio.com/ protcalc/index. php

2.2. Methods

2.2.1. Homology search with BLAST and alignment of sequences

Homology search of desired protein sequences with the protein databases was achieved via BLAST (Basic Local Alignment Search Tool) (Altschul *et* al. 1990; Nakamura *et* al., 2000). Multiple sequence alignments were performed via ClustalW (Higgins *et* al., 1996) in order to determine homologies.

2.2.2. PCR reactions

The following components were combined in each reaction tube and conditions of the thermal cycler were adjusted as shown below.

Table 2.3: Reaction mixture for PCR with TaKaRa Ex Taq Polymerase (total 50 µl)

	Stock	Volume	Final Conc.
TaKaRa Ex Taq™	5 units/µl	0.5 µl	2.5 u
10× *Ex Taq* Buffer (Mg^{2+} free)	10X	5 µl	1X
$MgCl_2$	25 mM	5 µl	2.5 mM
dNTP Mixture	2.5 mM	2 µl	0.1 mM
Template	variable	variable	50 ng
Primer 1	10 picomole/ µl	1 µl	0.1 picomole
Primer 2	10 picomole/ µl	1µl	0.1 picomole
Sterilized distilled water	-	upto 50 µl	-

Table2.4: Reaction mixture for PCR with Pfu DNA Polymerase (total 50 µl)

	Stock	Volume	Final Conc.
Pfu DNA Polymerase	2.5 units/µl	0.5 µl	1.25 u
10× *Pfu buffer with* $MgSO_4$	10X	5 µl	1X
dNTP Mixture	2.5 mM	2 µl	0.1mM
Template	variable	variable	50 ng
Primer 1	10 picomole/ µl	1 µl	0.1 picomole
Primer 2	10 picomole/ µl	1µl	0.1picomole
Sterilized distilled water	-	upto 50 µl	-

Table 2.5: Conditions of PCR reactions

94°C.	3 min.	
94°C	1 min.	35 cycle
58°C	1 min.	
72 °C	2 min	
72 °C	10 min	
4°C	∞	

2.2.3. Gel Extraction Procedure

The gel extraction was carried out via "QIAquick Gel Extraction Kit" (QIAGEN Inc.) protocol. The PCR fragment was excised from the gel and placed in a sterile Eppendorf tube. The gel slice is weighed and 3 volumes of Binding Buffer (QG, commercially available) was added into the tube. The mixture was incubated at 50°C for 10 min and the solution was vortexed 2 times during incubation period. After the gel is disolved completely, one volume of isopropanol was added and the sample was applied to the QIAquick column and centrifuged at 14000 x g for 1 minute. The flow through was discarded and the QIAquick column was placed back into the same collection tube. 0.5 ml of buffer QG was added to the column and centrifuged at 10000xg for 1 minute. The flow through was discarded and the column was washed with 0.75 ml of Column Wash Buffer (PE, commercially available). The column was then centrifuged at 14000 x g for 1 minute. In the end, the column was placed into a clean 1.5 ml microfuge tube and 30 µl of Elution Buffer (10 mM Tris·Cl, pH 8.5) was added to the centre of the QIAquick membrane within the column. After 1 min of incubation at room temperature, the column was centrifuged at 14000xg for 1 minute. The eluted DNA was run on 1 % agarose gel and analysed.

2.2.4. Ligation

2.2.4.1. Ligation of the PCR Products into T/A Cloning vector

Purified DNA fragments were inserted into the T/A cloning vector, pTZ57R. The ligation rections were set up as in the Table 2.8.

Table 2.6: Reaction ingredients for ligation of the PCR products into T/A Cloning vector

Plasmid Vector pTZ57R/T	(0.055µg, 0.06pmol ends) 1 µl
DNA	(approx. 0.18pmol ends) 2-4µl
10xBuffer	1.5 µl
Ligase (5u/ µl)	1 µl
Distilled Water	upto 15 µl
Total Volume	15 µl

Reaction mixture was incubated at 16^{o}C in thermal cycler for overnight then ligase was denatured at 65^{o}C for 10 minutes.

2.2.4.2. Ligation of the Insert into the Expression Vector

The desired inserts were cloned to an expression vector with a T4 DNA ligase. The ligation reaction ingredients are as shown in Table 2.9.

Table 2.7: Reaction ingredients for ligation of the insert into the expression vector

Vector (pET30b)	50-100ng
DNA	3–10 fold molar excess
10xBuffer	1 µl
Ligase	1 µl
Distilled Water	upto 10 µl
Total Volume	10 µl

The mixture was incubated overnight at 16°C in a thermal cycler. Then, T4 DNA Ligase was inactivated by incubation at 65°C for 10 minutes. Then, the mixture was used for transformation or kept at -20°C for later use.

2.2.5. Competent cell preparation

E. coli overnight inoculum was diluted 1:100 fold and used to inoculate 100 ml LB broth and incubated at 37^{o}C in water bath with 250 rpm shaking. When the OD_{600} (Optical Density at 600 nm) of the culture was between 0.2-0.3, cells were collected via centrifugation for 10 minutes at 4000x g at 4^{o} C. Supernatant was discarded and pellet was resuspended in 9 ml ice-cold RF1 solution (Section 2.1.8). Then, cells were again centrifuged for 10 minutes at 4000 x g at 4^{o} C. Supernatant was discarded and the cells were gently resuspended in 1 ml ice-cold RF2 solution (Section 2.1.8).

After keeping on ice for 1-2 hours, they were dispensed into aliquots of 30 µl into 1.5 ml Ependorf tubes. Aliquots were stored at -80^{o}C.

2.2.6. Transformation

5 µl of ligation mix was added to competent cells which were thawed on ice previously and were incubated on ice for 30 minutes. Heat pulse was applied for 42 seconds in 42^{o}C in water bath, then cells were again put on ice and incubated for further 10 minutes on ice. 0.5 ml of LB liquid medium was added to competent cells and was incubated at 37^{o} C for 45 minutes. The culture was then spread out onto LB plate containing appropriate antibiotics.

For the transformation of T/A cloning ligation mix, the incubated cultures were spread on a ampicillin (at a final concentration of 100µg/ml) containing LB plate onto which 40 µl 20 mg/ml X-Gal and 4 µl 20% (w/v) IPTG were spread previously. They were incubated overnight at 37°C.

2.2.7. Colony Screening

Plasmid minipreps were prepared for each colony which appeared on LB + antibiotic plates after overnight incubation at 37^{o}C. Restriction enzyme analysis was performed for further analysis.

Alpha-complementation test was used to select the recombinant colonies from LB Agar+Ampicillin plates onto which pTZ57R+gene_of_interest constructs containing cells were spread.

2.2.8. Plasmid DNA isolation (Mini-prep)

Plasmid DNA isolation was performed bu using Promega Wizard *Plus* miniprep DNA purification system. 1.5 ml of overnight culture was centrifuged at 10000 xg for 10 minutes. 200 µl Cell Resuspension Solution (Section 2.1.8) was used to resuspend the cell pellet after the supernatant was discarded. 200 µl of cell lysis solution (Section 2.1.8) was added and inverted 4 times. Then, 200 µl Neutralization Solution (Section 2.1.8) was added and mixed by inverting gently. The sample was incubated for 15 minutes on ice and then centrifuged at 10000 x g for 15 minutes. The supernatant was transferred to a new fresh tube. 1 ml DNA Purification Resin was added to the supernatant. The resin and supernatant mix was applied into the

minicolumn and vacuum was applied. The column was washed with 2 ml of Column Wash Solution (Section 2.1.8) and was dried by centrifugation for 30 sec. at 10000 x g. The column was transfered to a new microcentrifuge tube and 50 µl of deionized water (preheated to 70ºC) was added. It was left at room temperature for 1 minute. The column was centrifuged at 10000 x g for 30 seconds. The isolated DNA was run on 1 % agarose gel and the DNA was stored at -20ºC.

2.2.9. Restriction endonuclease digestions

Restriction enzyme buffer was supplied as 10X buffers and the final concentration of the 10X reaction buffer was adjusted as 1X or 2X according to the requirements of the used restriction enzyme. Final glycerol concentration in the digest mixture was adjusted to be less than 10% of the total digest volume. Moreover, one unit of enzyme is defined as the amount of enzyme required to digest 1 µg DNA. Therefore, previously determined amount of plasmid DNA was digested with appropriate amount of restriction enzyme according to this rule. The total reaction volume was brought to 20 µl to 40 µl with sterile deionized H_2O. The restriction enzyme digestion was performed at 37 °C for 4 hours.

2.2.10. Large scale plasmid DNA isolation (Midi-prep)

Promega Wizard Plus midiprep DNA purification system was used to obtain plasmid DNA in large scale. 100 ml of culture was centrifuged at 4000 x g for 10 minutes, at 4^{o} C. 3ml Cell Resuspension Solution was used to resuspend the pellet after the supernatant was discarded. 3ml of Cell Lysis Solution and 3ml of Neutralization Solution was added and the tubes were inverted 4 times to mix. Then, the tubes were centrifuged at 10000xg for 5 minutes and the supernatant was transferred to a new fresh tube. The transferred sample was mixed with 15 ml of resin solution. The solution was poured into midicolumn/syringe assembly on the vacuum manifold. Vacuum was applied in order to let the solution pass through the midicolumn. The column was washed with the Column Wash Solution and midicolumn was dried by centrifugation for 2 min. at 10000xG. The column was transfered to a new microcentrifuge tube and 300 µl of deionized water (preheated to 70ºC) was added.

It was left at room temperature for 1 minute. The column was centrifuged at 10000 x g for 30 seconds. The isolated DNA was run on 1 % agarose gel and the DNA was stored at -20ºC.

2.2.11. Preparation of the vector-target ORF constructs

The genomic clones including open reading frames PH0876 and PH1873 of *Pyrococcus horikoshii* were kindly provided by Dr. Yutaka Kawarabayasi of National Institute of Advanced Industry and Technology, Japan.

PH0876 was amplified from genomic clones of *Pyrococcus horikoshii* via PCR using the primers F1PH0876 and R1PH0876 (Section 2.1.7), and cloned into a T/A cloning vector pTZ57R/T. The construct (pTZ57R+ PH0876) was then digested with *SacI* and *SalI* restriction enzymes and inserted into *SacI* and *SalI* digested pET30b.

PH0876 was amplified from genomic clones of *Pyrococcus horikoshii* using CommonF2_primer and R2PH0876 (Section 2.2.1), PCR product was digested with *BamHI* and *Sal*I and ligated directly into pET30b. *E. coli* Rosetta(DE3)pLysS was transformed with this construct, pPH7630_Histag, and expression studies were carried out. The presence of protein was confirmed with Western Blotting.

PH1873 was amplified from a genomic clone of *Pyrococcus horikoshii* via PCR using the primers CommonF2_Primer and R2PH1873 (Section 2.2.1), PCR product was digested with *BamHI* and *Sal*I then ligated directly into pET30b by Assoc. Prof. Dr. Dinçtürk Botofte behind the N-terminal His•Tag. The construct was named as pPH7330_Histag. Cells of *E. coli* Rosetta(DE3)pLysS was transformed with this constructs and expression studies of this construct was carried out in this study. The presence of protein was confirmed with Western Blot.

Glutamate synthase β-subunit like region 3' region of NADH-GltS from *Medicago sativa* was amplified with appropriate primers and cloned by HBD from the monomeric full length cDNA clone provided by Carol Vance of University of Minnesota, USA. The construct was named as pGEM_alfa3'. In this study, the construct pGEM_alfa3' was digested with *EcoRI* and the product was then subcloned into *EcoRI* digested pET30b, behind the N-terminal His-Tag. Transformation into available expression host cell (RosettaDE3pLysS) was achieved and expression studies of the construct, pET_alfa3' were carried out in this study. To ensure that it

was a His-Tag fusion protein, Western Blot analysis was performed using His Tag monoclonal antibody as the first antibody.

2.2.12. DNA Sequencing

ABI 3100 Avant (PE, Applied Biosystem, CA) automated sequencer was used for DNA sequencing. The conditions for sequence PCR were as following.

Table 2.8: Sequencing PCR reaction mixture and PCR reaction conditions

PCR Reaction Mixture		**PCR Reaction Conditions**		
Big dye reaction mix	2µl	95 °C	2’	
5X sequencing buffer	1 µl	95 °C	10’’	25 cycle
Template dsDNA (200ng)	1 µl	55 °C (M13 forward primer) **or** 50 °C (T7 forward primer)	10’’	
Appropriate primer	3.2 µl			
dH_2O	2.8 µl			
Total volume	10 µl	60°C	4’	

2.2.13. Purification of Sequencing PCR products

A mixture of 1 µl of Sodium acetate (3M, pH 5.2) buffer and 25 µl of cold 95% ethanol was added to each sample and incubated on ice for 30 min. After the incubation, samples were centrifuged at 15000 x g for 30 min. Then, the supernatant was discarded and the pellet was washed with 250 µl 70% ethanol and centrifuged at 15000 x g for 30 min. The supernatant was again discarded and the residual ethanol was evaporated via incubation at 95 °C. DNA was dissolved in 20 µl diformamide and denatured by incubation at 95 °C for 5 min and -20 °C for 2 min, respectively.

2.2.14. Protein expression induction

5 ml LB medium containing appropriate antibiotic was inoculated from glycerol stocks of RosettaDE3pLysS which harbours the appropriate plasmid for induction to analyze expression of the target protein and its solubility. For the purification of the proteins, 50 ml LB in 250 ml Erlenmeyer flasks were inoculated with the overnight starter cultures. Cultures were grown at 37°C or 30°C with constant shaking until OD_{600} reaches 0.6. After that, cells were induced with 0.1-1 mM IPTG for 4 hours.

2.2.15. Cell Fractionation Analysis

2.2.15.1. Total cell protein analysis

1 ml of cell culture was harvested by centrifugation, 100 µl 1x SDS-PAGE sample buffer (Material Method Part, Section 2.1.8) was used to resuspend the pellet. Total cell protein samples were stored at -20°C until they were run on sodium dodecyl sulfate-polyacrylamide gel (SDS-PAGE).

2.2.15.2. Soluble total cell protein analysis

Pelleted (200 ml culture) and freeze-thawed cells were resuspended in 1 ml cold 20mM Tris-HCl solution, pH7.5. The sample was concentrated 10X. Cells were lysed by both Lyzozyme treatment (at a final concentration of 10µg/ml, incubation on ice for 30 min) and sonication. Sonication was applied by using three 20 seconds bursts at 200 Watt with a 1 min. cooling period between each bursts. After the sonication, the lysate was centrifugated at 14,000 × g for 10 min at 4°C to precipitate the cellular debris and the supernatant was saved. Then, an equal amount 2X SDS-PAGE sample buffer was added to the supernatant which would be analyzed by SDS-PAGE and remaining part of the soluble fraction was stored at – 20°C for the following purification procedure.

2.2.15.3. Insoluble total cell protein analysis

Insoluble cell fraction is the pellet fraction obtained during the separation of the soluble protein fraction. 250µl SDS sample buffer was added to this fraction and the sample was boiled for 3 min in water bath and the samples were run on SDS-PAGE or kept at –20°C or kept for later use.

2.2.16. SDS-PAGE

Table 2.9: Ingredients of separating and stacking gel for SDS-PAGE

SEPARATING GEL	
10% Gel	**5ml**
dH_2O (mL)	1.9 ml
30% acrylamide mix	1.7 ml
1.5M Tris (Hydroxymethyl) aminomethane (Tris) (pH 8.8)	1.3 ml
10% Sodium n-Dodecyl Sulfate (SDS)	0.05 ml
10% APS	0.05 ml
N,N,N',N'-Tetraethyl ethylenediamine (Temed)	0.002 ml
12% Gel	**5ml**
dH_2O (mL)	1.6 ml
30% acrylamide mix	2 ml
1.5M Tris (Hydroxymethyl) aminomethane (Tris) (pH 8.8)	1.3 ml
10% Sodium n-Dodecyl Sulfate (SDS)	0.05 ml
10% APS	0.05 ml
N,N,N',N'-Tetraethyl ethylenediamine (Temed)	0.002 ml
5% STACKING GEL	
	2ml
dH_2O (mL)	1.4 ml
30% acrylamide mix (g/ml)	0.33 ml
1.M Tris pH 6.8	0.25 ml
10% SDS	0.02 ml
10% APS	0.02 ml
TEMED	0.002 ml

SDS-PAGE protocol was performed with the BioRad Protean II electrophoresis apparatus. After the samples were loaded, the gel was run at 110 V until dye front is about 1 mm from bottom of gel. The gel was stained via Comassie Blue at room temperature for 30 min and destained overnight.

2.2.17. Protein purification under native conditions

Protein purification studies were performed under native conditions using Qiagen Nickel-Nitriloaceticacid (Ni-NTA). 100 µl of the 50% Ni-NTA slurry was added to 1 ml cleared lysate and mixed by mixing at 4°C for 60 min. Then, the lysate–Ni-NTA mixture was centrifuged at 14000 x g for 5min. The supernatant was discarded and

the pellet washed three times via 1 ml wash buffer (Section 2.1.8) The protein bound to the Ni-Ag was eluted 4 times with 100 µl elution buffer (Section 2.1.8) and analyzed by SDS-PAGE.

2.2.18. Western blotting

The proteins fractionated by SDS-PAGE were transferred to the PVDF membrane by electroblotting. In this transfer, a sandwich of gel and PVDF membrane was compressed in a cassette and immersed in buffer between two parallel electrodes. The system for the transfer from the SDS-gel containing the antigens to the PVDF membrane was set according to the following instructions. Firstly, PVDF transfer membrane was incubated in methanol for 3-4 sec. and then, in deionized water. The acrylamide gel was soaked for 5 minutes in transfer buffer without SDS prior to transfer. Also the filter papers and sponges were soaked in transfer buffer. Then, the transfer system containing gel and the membrane was assembled. All air bubbles between the gel and the membrane were removed. The separated polypeptides were transfered at 40 V at 4°C for 12-16 hours. After the transfer, the membrane was incubated in blocking solution (Material Methods Part, Section 2.1.8) for two hours. The membrane was then incubated in primary antibody solution (Anti His Tag Monoclonal Antibody, Novagen) for 2 hours at room temperature. Following incubation in primary antibody, the blot was washed three times with TTBS (Section 2.1.8). Then, the membrane was incubated in secondary antibody (Goat Anti-Mouse IgG, H & L Chain Specific Alkaline Phosphatase Conjugate, Novagen) for 1.30 hour at room temperature. Before signal detection step, membrane was washed in TBS for 5 minutes at RT. Detection step was achieved through the conversion of a colorimetric substrate (NBT/BCIP) to a colored precipitate. 25X AP color development buffer (Material Methods Part, Section 2.1.8), purchased from Bio-Rad Inc., and was diluted to obtain 1 X color development buffer. 200 µl NBT/BCIP (Bromochloroindolyl Phosphate-Nitro blue Tetrazolium) mixture (Section 2.1.8), which is purchased from Bio-Rad Inc. within the Immun-Blot Colorimetric Assay Kit, was added to the 1X AP color development buffer. The membrane was submerged in the freshly prepared color development buffer. The membrane was dried on filter paper and kept in dark for long term storage.

3. RESULTS

3.1. Determination of Putative Glutamate Synthase Small Subunit Coding Regions

Deduced amino acid sequences of PH0876 and PH1873 ORFs were analyzed with Comparative Domain Display (CDD) analysis (Figure 3.1), BLASTP (Figure 3.2 and Figure 3.3; summary of BLAST results) and ClustalW (Figure 3.4) alignment tools. They both showed highest homology to the GltD domain which is a conserved small glutamate synthase domain.

The CDD analysis revealed that PH1873 and PH0876 show highest homology to GltD type of protein family consisting of NADPH-dependent glutamate synthase beta chain and related oxidoreductases (Figure 3.2). The second high homology sharing protein family was pyridine nucleotide-disulphide oxidoreductase protein family (PyR_redox) which includes both class I and class II oxidoreductases and also NADH oxidases and peroxidases.

As a result of the BLAST N analysis of the ORFs which are present upsream and downstream of the PH0876 and PH1873, it was seen that upstream and downstream regions of PH0876 and PH1873 contain several putative oxidoreductase- and hydrogenase-like genes (Figure 3.3 and Figure 3.4). For instance, PH0878 shows high homology with oxidoreductase of *Pyrococcus abyssi* and hydrogenase of *Pyrococcus furiosus* whereas PH0874 showed high homology with beta lactamase of *Pyrococcus abyssi*. In addition, there is not any region showing significant homology to *GltB* upstream or downstream of these ORFs PH0876 and PH1873. (Figure 3.3 and Figure 3.4).

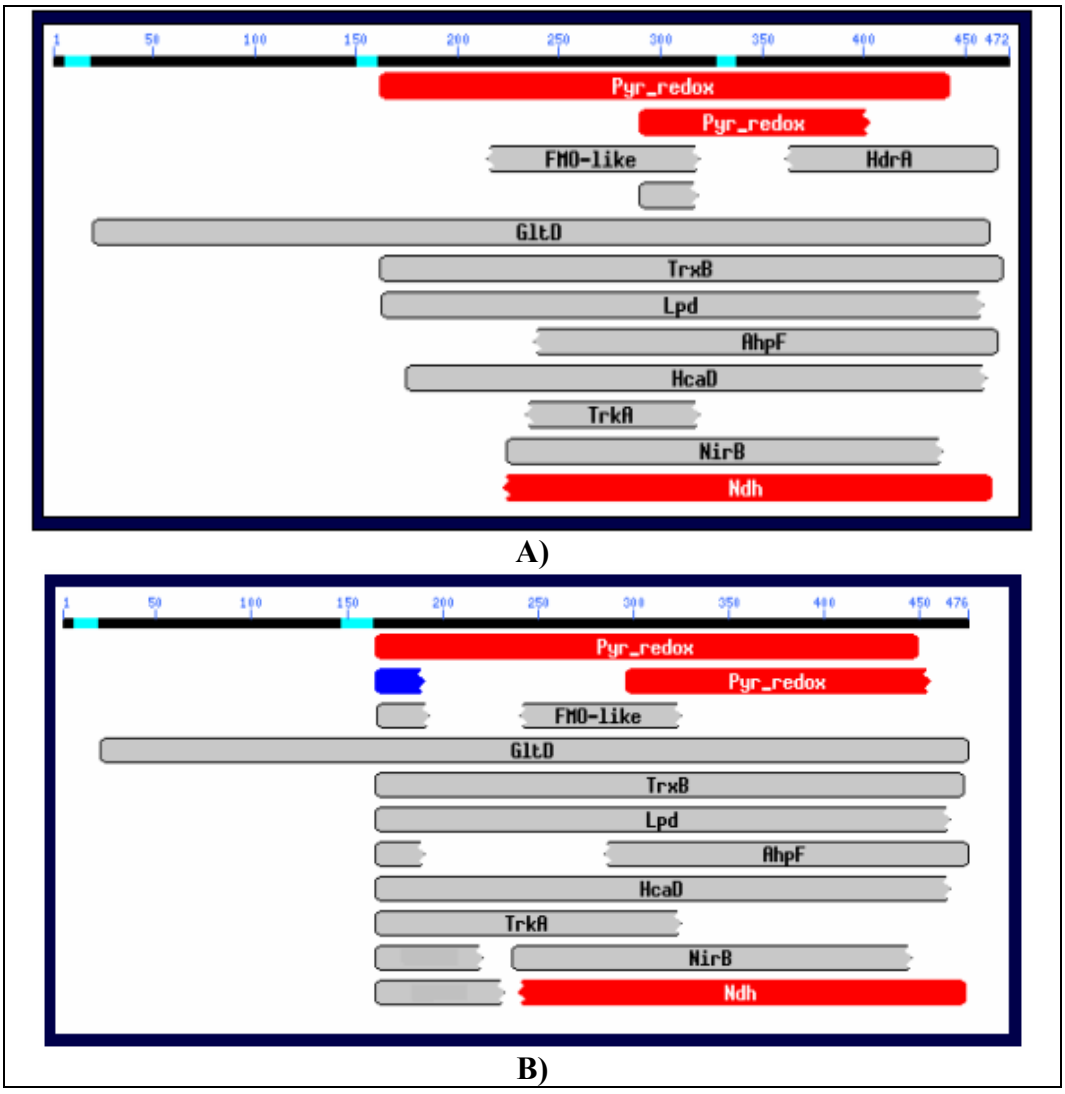

Figure 3.1: Comparative Domain Display analysis of deduced amino acid sequences of PH0876 and PH1873. **a)** CDD analysis of deduced amino acid sequence of ORF PH0876. **b)** CDD analysis of deduced amino acid sequence of ORF PH1873.

In Figure 3.1 the nomenclature is as following. PyR_redox: pyridine nucleotide-disulphide oxidoreductase protein family; FMO-like: Flavin-binding monooxygenase -like; TrxB: Thioredoxin reductase; Lpd: Pyruvate/2-oxoglutarate dehydrogenase complex, dihydrolipoamide dehydrogenase (E3) component, and related enzymes; HcaD: Uncharacterized NAD(FAD)-dependent dehydrogenases; TrkA: Predicted flavoprotein involved in K+ transport; NirB, NAD(P)H-nitrite reductase; Ndh: NADH dehydrogenase, FAD-containing subunit .

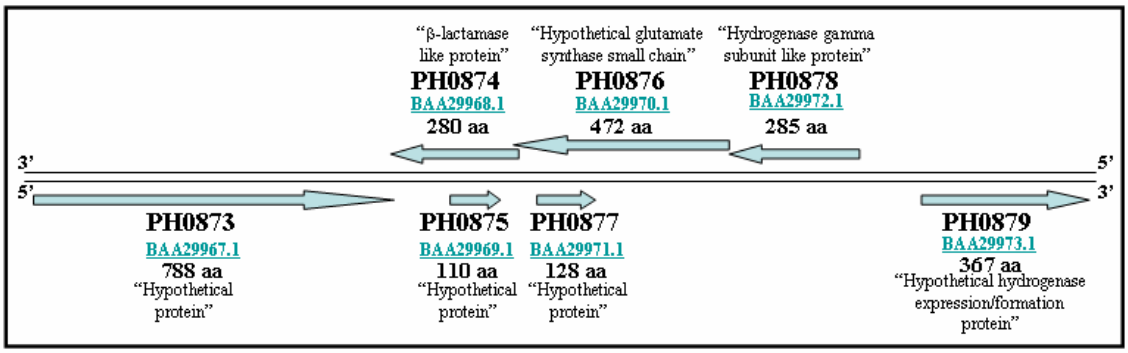

Figure 3.2: The figure presents the upstream and downstream regions of PH0876. The proteins are placed according to their protein sizes and the relative positions of ORFs encoding them on the genome.

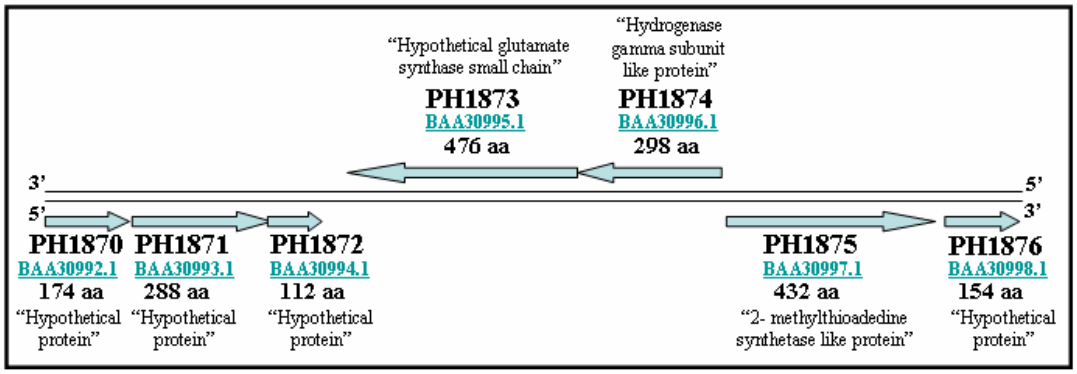

Figure 3.3: The figure presents the upstream and downstream regions of PH1873. The proteins are placed according to their protein sizes and the relative positions of ORFs encoding them on the genome.

The small subunits (β subunit) of the NADPH-dependent bacterial glutamate synthase, the C terminal regions of NADH-dependent glutamate synthases share two conservative ADP binding folds one of which is for NAD(P)H and the other is for flavin adenine dinucleotide (FAD) (Vanoni et al., 1996). In order to identify potential flavin cofactor binding and NAD(P)H binding regions, CLUSTAL W multiple amino acid sequence alignment of PH0876 and PH1873 with some of the small subunits of the NADPH-dependent bacterial glutamate synthase (*E. coli* and *Azospirillium brasilense*) and C terminal region of NADH-dependent glutamate synthase from *Medicago sativa and Synechosystis sp. PCC 6803* was performed (Figure 3.4).

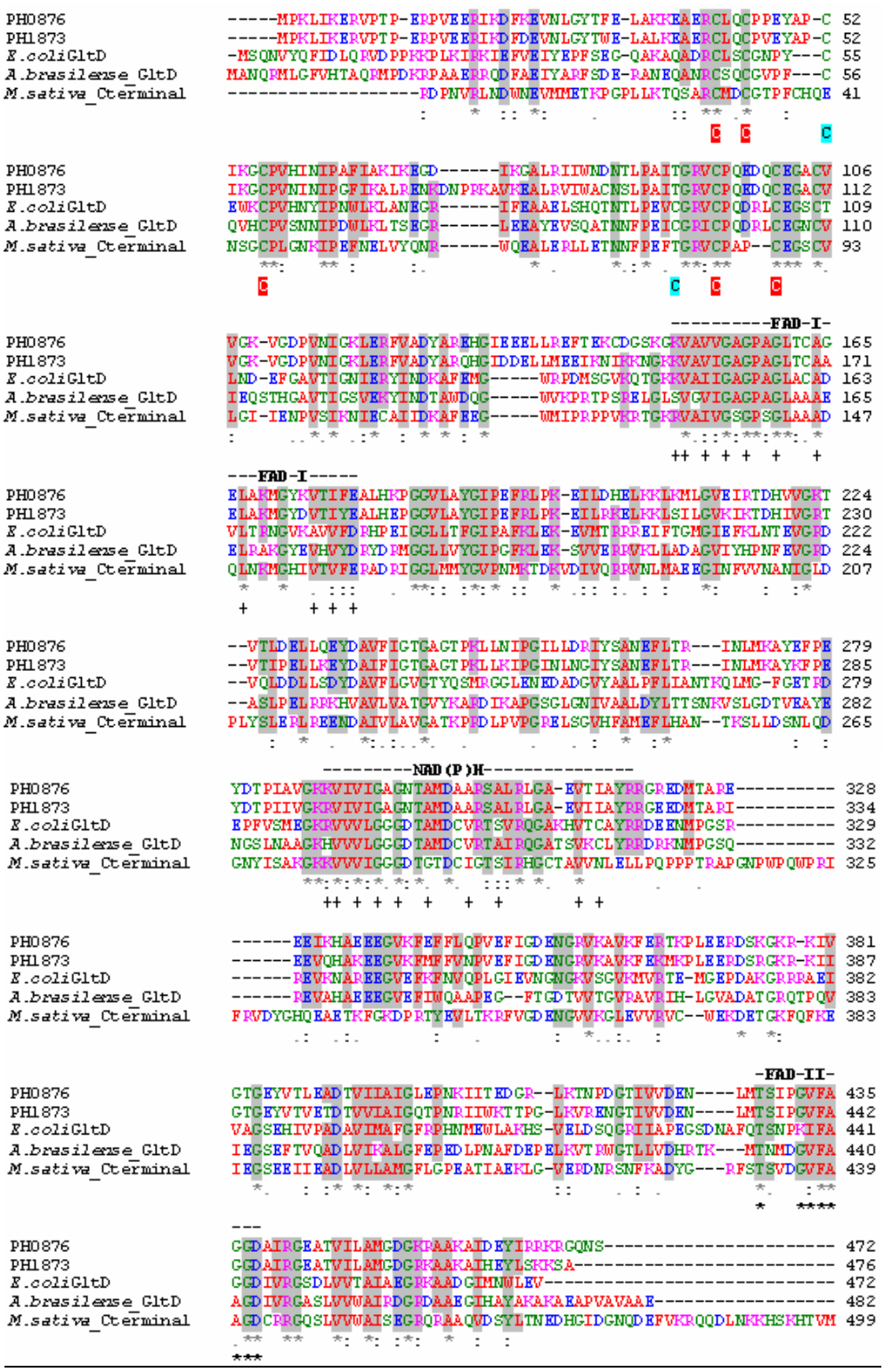

Figure 3.4: CLUSTAL W multiple amino acid sequence alignment of PH0876 and PH1873 with some of the other GltS β subunit proteins. (+) is used to indicate the consensus sequence matching regions required for an adenylate binding fold formation. (*) is used to show the second consensus sequence matching region.

In Figure 3.4, the gray shading represent residues conserved in >70% of the sequences aligned and the Cys residues that may be responsible for 4Fe-4S clusters are showed with the letter (C).

There are also some proteins containing the conservative sites of the glutamate synthase β subunit, and therefore called as GltS β subunit like proteins. The ORFs which are encoding GltS β subunit like proteins are *DsrL* from *Allochromatium vinosum* (Dahl et al., 2005), *SudA* from *P. furiosus* (Schut *et al*., 2003), *GltA* from *Thermococcus kodakaerensis* (Jongsareejit et al., 1997), *GltX* from *C. saccharobutylicum* NCP262 (Stutz et al., 2004). CLUSTAL W multiple amino acid sequence alignment of PH0876 and PH1873 was also performed with GOGAT β subunit-like proteins found in various organisms (Figure 3.5).

```
Pyrococcus_horikoshii_PH1873        MP--KLIKERVPTPERPVEERIKDFDEVNLGYTWELA-LKEAERCLQCPV 47
T_kodakarensis_GltA                 MPRRKLIKERVPTPERPPEERIKDFKEVNLGYTFELA-VKEAERCLQCPY 49
Pyrococcus_horikoshii_PH0876        MP--KLIKERVPTPERPVEERIKDFKEVNLGYTFELA-KKEAERCLQCPP 47
Pyrococcus_furiosus_SudA            MP--RLIKDRVPTPERSVGERVRDFGEVNLGYSWELA-LREAERCLQCPV 47
C_saccharobutylicum_GltX            ----------------------MTCNDIQL--------LDEADRCLLC-- 18
Allochromatium_vinosum_DsrL         -----MATSSDEMKMKPTWRRFEDGEHVWDNLTDKIFNQDRSHKCPTYVH 45
                                                          .:            .:.:*
                                                                          C  C

Pyrococcus_horikoshii_PH1873        EYAPCIKGCPVNINIPGFIKALRENKDNPR--KAVKEALRVIWACNSLPA 95
T_kodakarensis_GltA                 EYAPCIKGCPVHINIPGFISKLVEYRDDPD--KAVKEALNVIWACNSLPA 97
Pyrococcus_horikoshii_PH0876        EYAPCIKGCPVHINIPAFIAKIKE--------GDIKGALRIIWNDNTLPA 89
Pyrococcus_furiosus_SudA            EYAPCIKGCPVKINIPGFIKALRENRDNPS--KAVREALRIIWRDNTLPA 95
C_saccharobutylicum_GltX            KKPRCKENCPIQTSIPEIISLYKENR--------LREAGEILFNNNPLSA 60
Allochromatium_vinosum_DsrL         KTPPCQGSCPSGEDIRGWLQIVRGMEKPPQGMDWQEYAFRRSTDANPFPA 95
                                    : . *  .**   .*   :                . * .     *.:.*
                                        C   C

Pyrococcus_horikoshii_PH1873        ITGRVCPQEDQCEGACVVGKVGDPVNIGKLERFVADYARQHGIDDELLME 145
T_kodakarensis_GltA                 TTGRVCPQEDQCEMNCVMGKVGDKINIGKLERFVADYAREKGIDEELLFE 147
Pyrococcus_horikoshii_PH0876        ITGRVCPQEDQCEGACVVGKVGDPVNIGKLERFVADYAREHGIEEELLRE 139
Pyrococcus_furiosus_SudA            ITGRVCPQEEQCEGACVVGKVGDPINIGKLERFVADYAREHGIDDELLLE 145
C_saccharobutylicum_GltX            VCSLVCIHEDQCKGNCIKGIKGEPIRFHDIE-----YEISMKYLEEVRFE 105
Allochromatium_vinosum_DsrL         MMGRVCP--APCQDGCNRNELEDFVGINSVEQFIGDTAIANGYTFEAPEL 143
                                      . **     *:  *  .   : : : .:*             *
                                         C     C  C

                                                 ----------FAD-I-------------
Pyrococcus_horikoshii_PH1873        EIKNIKKNGKKVAVIGAGPAGLTCAAELAKMGYDVTIYEALHEPGGVLAY 195
T_kodakarensis_GltA                 IIPKIEKKGQKVAIIGAGPAGLTAAGELAKLGYDVTIYEALHEPGGVLMY 197
Pyrococcus_horikoshii_PH0876        FTEKCDGSKGKVAVVGAGPAGLTCAGELAKMGYKVTIFEALHKPGGVLAY 189
Pyrococcus_furiosus_SudA            EIKGIKRNGKKVAIIGAGPAGLTCAADLAKMGYEVTIYEALHQPGGVLIY 195
C_saccharobutylicum_GltX            NLP---KDKDRIAIIGGGPAGITIAFILANKGYDVTIFDAHVKIGGVLRY 152
Allochromatium_vinosum_DsrL         DTG------KRIAIVGGGPAGLAAAYQLRRKGHSCTIFEANDGLGGMFRF 187
                                           ::*::*.****:: *  * . *:. **::*    **:: :
```

Figure 3.5: CLUSTAL W multiple sequence alignment of GltS β subunit-like proteins. (NAD(P)H and FAD binding regions containing part of CLUSTAL W result). The Cys residues that may be responsible for 4Fe-4S clusters are showed with the letter (C). (+) is used to indicate the consensus sequence matching regions required for an adenylate binding fold formation. (*) is used to show the second consensus sequence matching region.

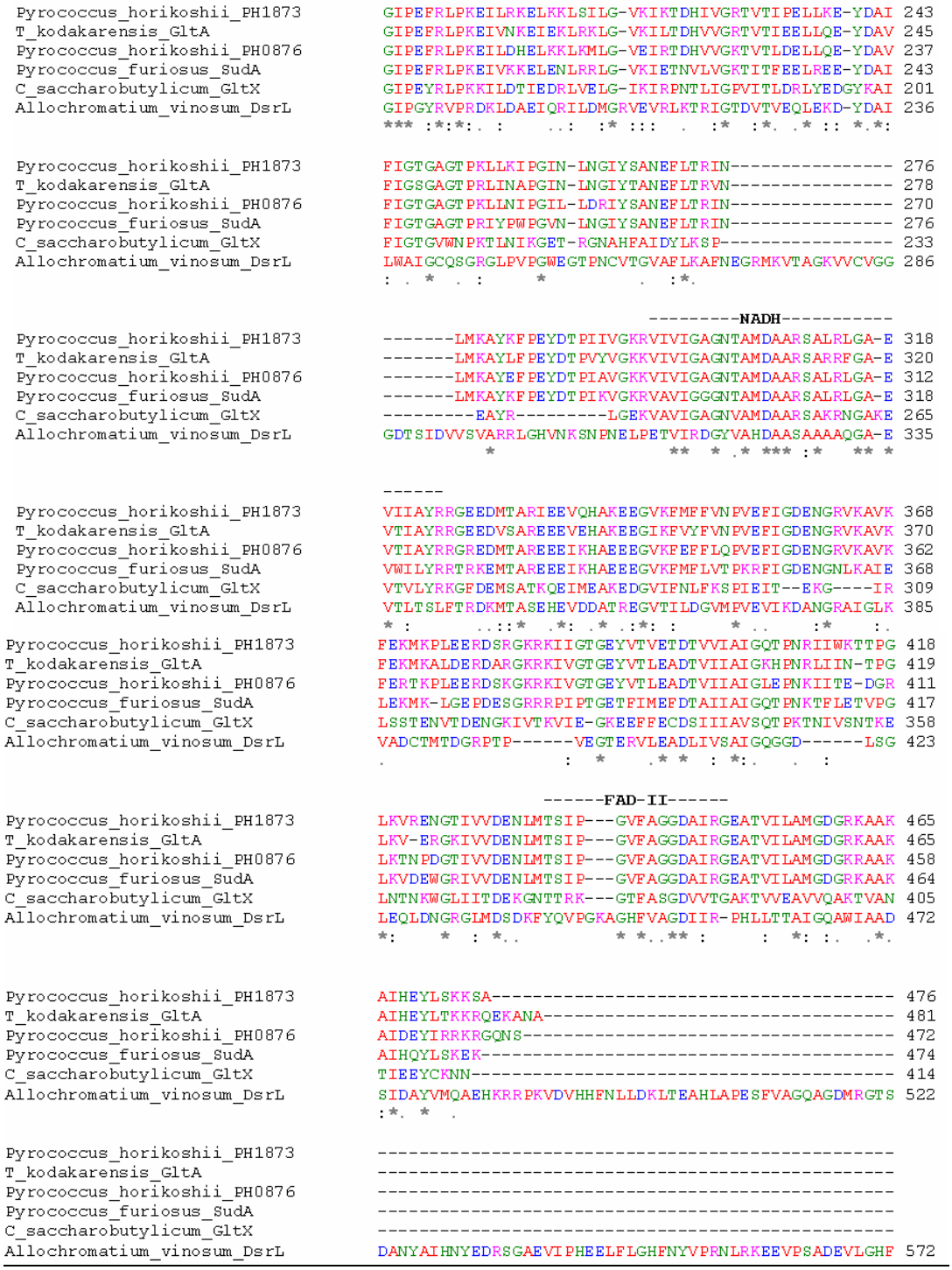

Figure 3.5: Continuing. CLUSTAL W multiple sequence alignment of GltS β subunit-like proteins. (NAD(P)H and FAD binding regions containing part of CLUSTAL W result).

3.2. Cloning

ORFs PH0876 and PH1873 were amplified from two genomic clones of *Pyrococcus horikoshii,* which were kindly provided by Dr. Yutaka Kawarabayasi of National Institute of Advanced Industry and Technology, Japan. Beta- subunit like 3' region

of glutamate synthase was cloned into pGEM easy cloning vector by HBD from the monomeric full length cDNA clone provided by Carol Vance of University of Minnesota, USA. In this study, it was subcloned into pET30b expression vector in order to be used as control in activity analysis.

3.2.1. Cloning of PH0876 in the Native Form

PH0876 was amplified from a genomic clone of *Pyrococcus horikoshii* via PCR using the primers F1_PH0876 and R1_PH0876 (Figure 3.7.a) as indicated in Materials and Methods (Section 2.2.2), and cloned into a T/A cloning vector pTZ57R/T (Figure 3.7.b).

```
  1 - ATGCCTAAGCTTATTAAGGAGAGAGTTCCAACTCCCGAGAGGCCCGTTGAGGAAAGGATT - 60
    - M  P  K  L  I  K  E  R  V  P  T  P  E  R  P  V  E  E  R  I
 61 - AAGGATTTCAAGGAGGTGAACTTGGGTTATACCTTTGAGCTTGCCAAGAAGGAAGCAGAG - 120
    - K  D  F  K  E  V  N  L  G  Y  T  F  E  L  A  K  K  E  A  E
```

Figure 3.6: The nucleotide sequence of the DNA encoding the 5' end of native form of PH0876 small subunit-like region and the translated sequence of the protein.

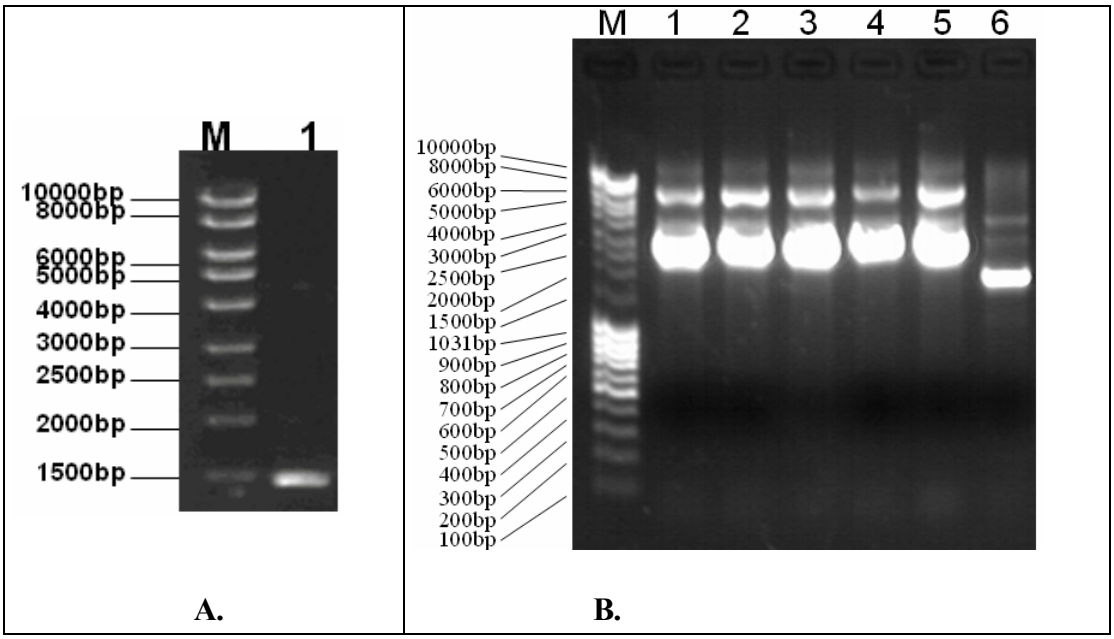

Figure 3.7: 1% agarose gel analysis of amplified PCR product of ORF PH0876 and potential recombinant colony minipreps containing pTZ57R_PH0876 construct.

In the Figure 3.7, the lane ingredients on the first gel are as follows: M: Fermentas Mass Ruler Mix Range Marker, Lane 1; Amplified PCR product of ORF PH0876 (~1445 bp). The lane ingredients on the second gel are as follows: M; Fermentas Mass Ruler Mix Range Marker, Lane1-5; Potential recombinant colony minipreps of pTZ57R_PH0876, Lane 6; Undigested pTZ57R.

The construct (pTZ57R+ PH0876) was then digested with *SacI* and *SalI* restriction enzymes (Figure 3.8.b) and inserted into *SacI* and *SalI* digested pET30b (Figure 3.8.a). The obtained DNA fragment to be ligated in Figure 3.8.b was expected to be ~1484 bp with the sequences coming from pTZ57R and primers.

The ligation mixture was used to transform *E. coli* strain XL1Blue competent cells and transformants were selected on LB agar plates containing kanamycin to a final concentration of 50 μg/ml.

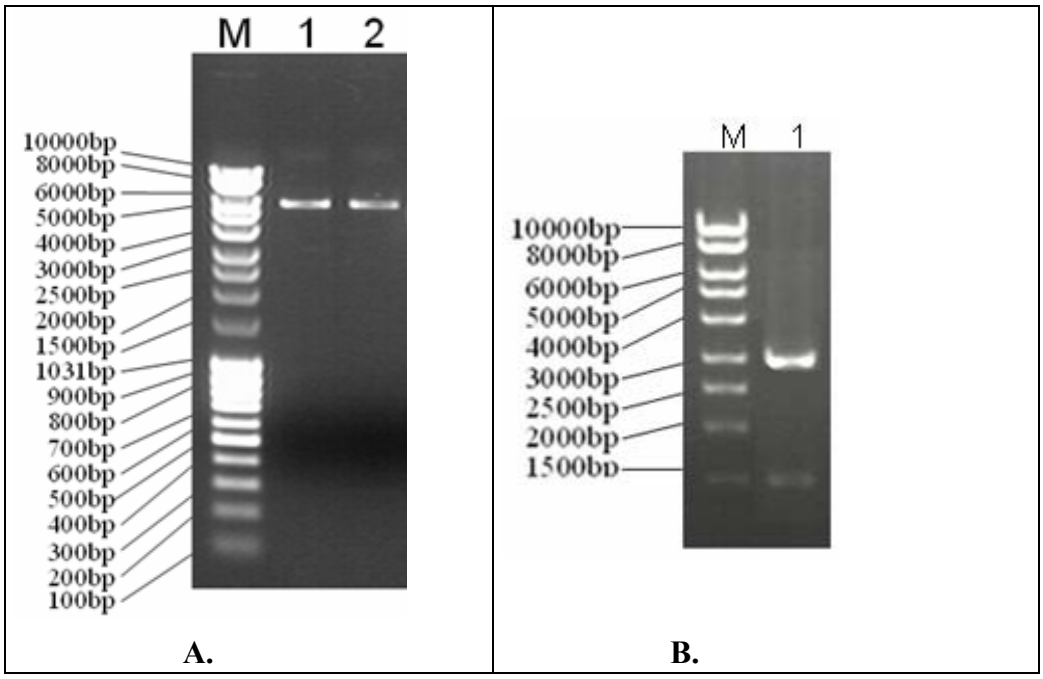

Figure 3.8: 1% agarose gel analysis of *SalI & SacI* digested pET30b vector and pTZ57R_PH0876 construct.

In the Figure 3.8, the lane ingredients on the first gel are as follows: M; Fermentas Mass Ruler Mix Range Marker, Lane 1-2; Linearized pET30b after *SacI* and *SalI* digestion, and the lane ingredients on the second gel are as follows: M; Fermentas Mass Ruler High Range Marker, *SacI*I and *Sal*I digested pTZ57R_PH0876.

The transformant colonies were inoculated into LB broth containing Kanamycin to a final concentration of 50 μg/ml and incubated overnight at 37°C. DNA minipreps were done from the overnight cultures of individual transformants (Figure 3.9). Recombinants were screened by digestion with *SacI* and *SalI* restriction enzymes (Figure 3.10). Positive clones were sequenced to confirm the 5' end of the vector and insert joining region. The construct was then named as pPH7630_Native, and used in expression studies.

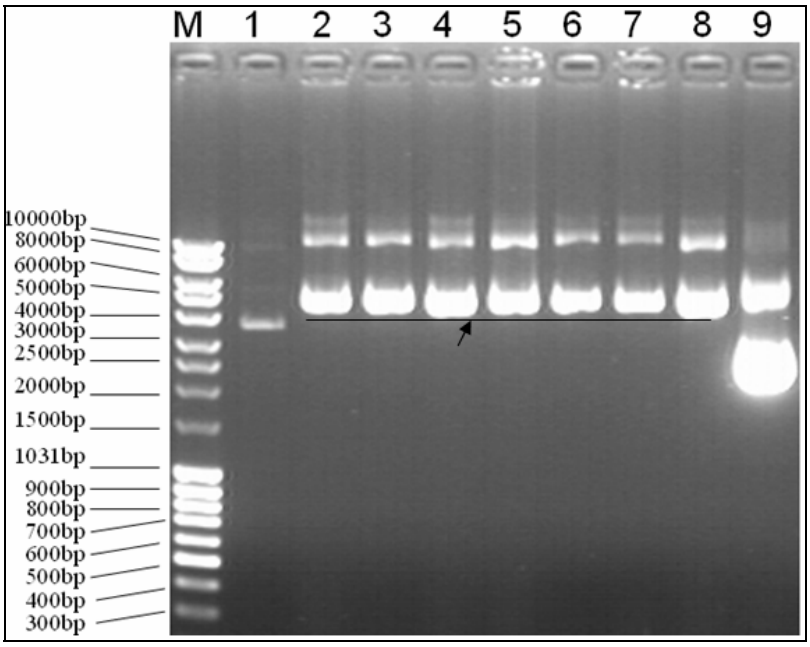

Figure 3.9: 1% agarose gel analysis of potential recombinant colony minipreps for PH0876 cloning into pET30b in its native form. M; Fermentas Mass Ruler Mix Range Marker. Lane 1; Undigested pET30b. Lane2-8; Potential recombinant colony minipreps of pET30b_ PH0876.

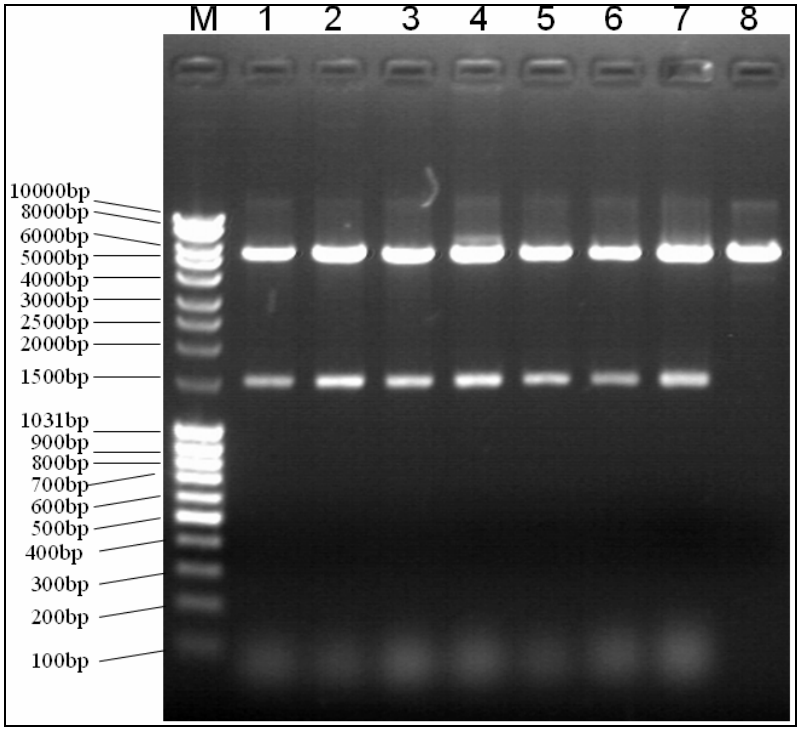

Figure 3.10: 1% agarose gel analysis of the restriction screen of the colony minipreps for PH0876 cloning in its native form. M; Fermentas Mass Ruler Mix Range Marker. Lane 1-7; *SacI* and *SalI* digestion of the recombinant colony minipreps of pET30b_PH0876. Lane 8; *SacI* and *SalI* digested pET30b.

3.2.2. Cloning of PH0876 in His-Tagged form into pET30b with *BamHI* and *SacI* sites

This time, PH0876 was amplified from genomic clones of *Pyrococcus horikoshii*, using the primers CommonF2_Primer and R2_PH0876 which harbor *BamHI* and *SacI* restriction sites, respectively (Figure 3.11).

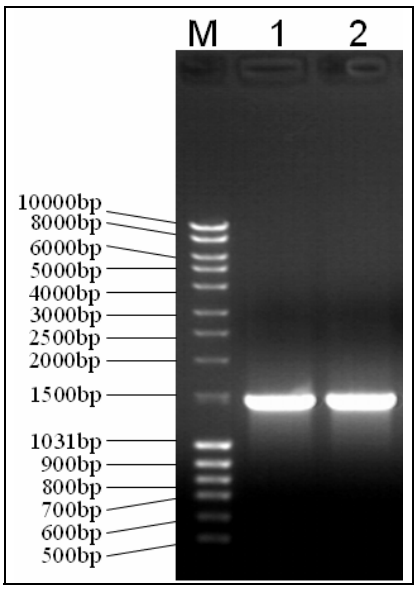

Figure 3.11: 1% agarose gel analysis of the resulting PH0876 ORF PCR products of PCR reaction done by using *Pfu* DNA polymerase. M: Fermentas Mass Ruler Mix Range Marker. Lane 1-2; Amplified ORF PH0876 (~1443 bp)

In order to clone PH0876, the obtained PCR fragment was digested with *SacI* and *BamHI* restriction enzymes (Figure 3.12.b.) and ligated directly from the PCR product into pET30b digested with the same enzymes (Figure 3.12.a.). The ligation mixture was used to transform *E. coli* strain XL1Blue competent cells and transformants were selected on LB agar plates containing kanamycin to a final concentration of 50 μg/ml.

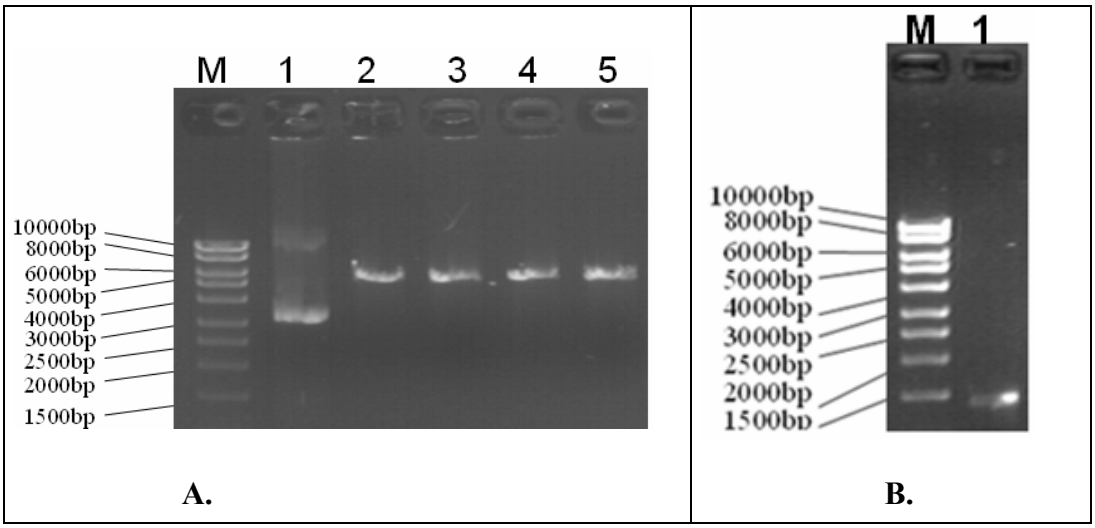

Figure 3.12: 1% agarose gel analysis of *BamHI & SacI* digested and gel extracted pET30b vector and PH0876 PCR product.

In the Figure 3.12, the lane ingredients on the first gel are as follows: M; Fermentas Mass Ruler High Range Marker, Lane 1; Undigested pET30b, Lane 2-5: *BamHI & SacI* digested and gel extracted pET30b, and the lane ingredients on the second gel are as follows: M; Fermentas Mass Ruler High Range Marker, Lane 1; *BamHI & SacI* digested and gel extracted PH0876 PCR product.

The transformant colonies were inoculated into LB broth containing Kanamycin to a final concentration of 50 μg/ml and incubated overnight at 37°C. DNA minipreps were done from the overnight cultures of individual transformants (Figure 3.13). Recombinants were screened by *HindIII* restriction enzyme digestion. The fragments that should be appearing after *HindIII* digestion of recombinant colony minipreps would be 815bp, 612bp and 5412bp and the restriction of colony minipreps gave DNA fragments with expected sizes (as seen in Figure 3.14, on Lane 1-2). Positive clones were sequenced to confirm the 5' end of the vector and insert joining region. The construct was then named as pPH7630_Histag and used in expression studies.

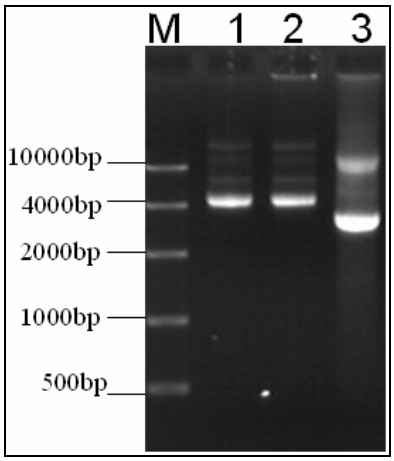

Figure 3.13: 1% agarose gel analysis of colony minipreps for PH0876 cloning in His-Tagged form. M; Fermentas Fast Ruler High Range Marker. Lane 1-2; Potential recombinant colony minipreps of pET30b_PH0876. Lane 3; Undigested pET30b.

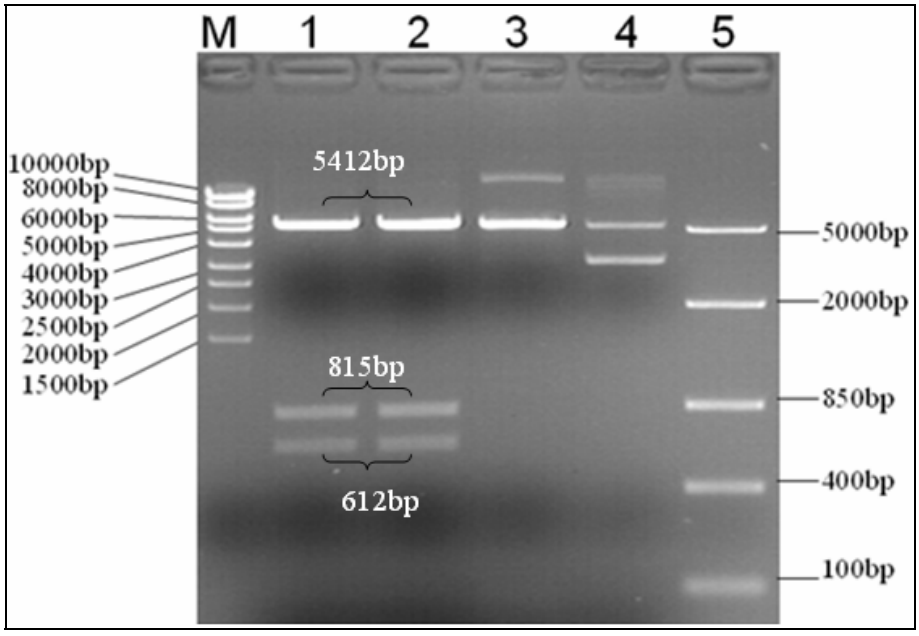

Figure 3.14: 1% agarose gel analysis of the *HindIII* digestion screen of the colony minipreps for PH0876 cloning in His-Tagged form.

The explanation of the lane ingredients in the Figure 3.14 are as follows: M; Fermentas Mass Ruler High Range Marker, Lane 1-2; *HindIII* digestion of the recombinant colony minipreps of pET30b_PH0876, Lane 3; *HindIII* digested pET30b, Lane 5; Fast Ruler Middle Range.

3.2.3. Cloning of PH1873

PH1873 was amplified from a genomic clone of *Pyrococcus horikoshii* via PCR using the primers CommonF2_Primer and R2PH1873. The resulting PCR product was then

digested with *BamHI* and *SacI* and subcloned into *Bam*HI and *Sac*I digested pET30b by HBD. The final construct was named pPH7330_Histag.

3.2.4. Cloning of Glutamate synthase β subunit-like 3' region of NADH-GltS from *Medicago sativa*

Glutamate synthase β-subunit like region 3' region of NADH-GltS from *Medicago sativa* was amplified with appropriate primers and cloned by HBD from the monomeric full length cDNA clone provided by Carol Vance of University of Minnesota, USA. The construct was named as pGEM_alfa3'.

In order to clone the 3' region of NADH-GltS from *Medicago sativa* into pET30b expression vector, the pGEM_alfa3' construct and pET30b was separately digested by *Eco*RI restriction enzyme (Figure 3.15) and pET30b was further treated with CIAP in order to prevent recircularization of the pET30b during cloning. As a result, β-subunit like 3' region of NADH-GltS from *Medicago sativa* was cloned into pET30b.

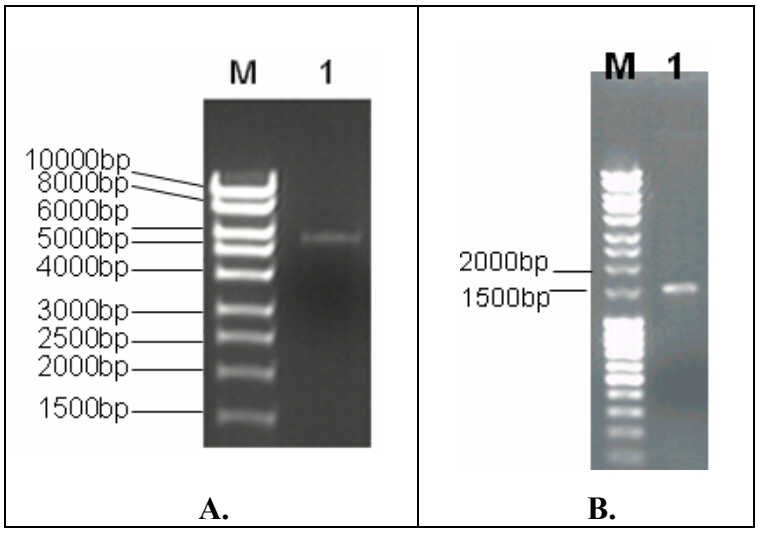

Figure 3.15: 1% agarose gel analysis of the *EcoRI* digestion of pET30b and the gel extracted DNA fragment after *EcoRI* digestion of pGEM_alfa3' construct**.**

In the Figure 3.15, the lane ingredients on the first gel are as follows: M; Fermentas Mass Ruler High Range Marker, Lane 1; *EcoRI* digested and CIAP treated pET30b, and the lane ingredients on the second gel are as follows: Gel extracted DNA fragment after *EcoRI* digestion of pGEM_alfa3' construct.

Ligation mixture was used to transform *E. coli* strain XL1Blue competent cells and transformants were selected on LB agar plates containing kanamycin to a final concentration of 50 μg/ml. The transformants were inoculated and DNA minipreps

were performed from the overnight cultures of individual transformants (Figure 3.16). As a result of the 1% agarose gel analysis of the potential recombinant colony minipreps for cloning of β subunit-like 3' region of NADH-GltS from *Medicago sativa,* the colonies whose minipreps were loaded to Lane 2, 4 and 9 were chosen for further analysis (Figure 3.16).

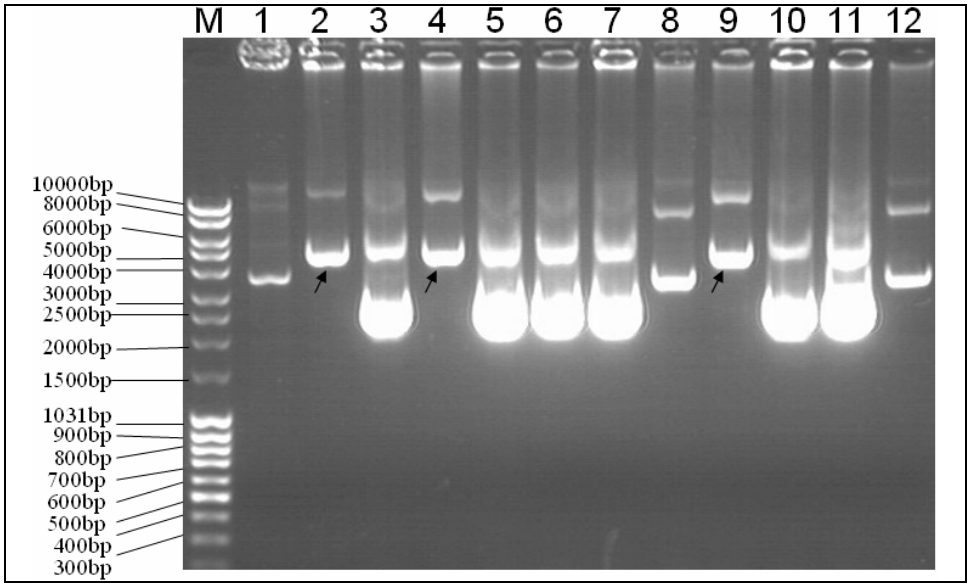

Figure 3.16: 1% agarose gel analysis of screening the potential recombinant colonies of pET_alfa3'. M; Fermentas Mass Ruler Mix Range Marker. Lane 1; Undigested pET30b. Lane 2-12; Colony minipreps of pET_alfa3'.

Recombinants were screened by digestion with some restriction enzymes, separately, to select the clone with correct orientation. The restriction sites for the selected enzymes (*XbaI, PstI and EcoRI*) which are used in determination of the correct orientation of *M. sativa* clone and the expected fragments after digestion are shown in Figure 3.17. *PstI* digestion was done in order to prove the presence of insert since only the insert contains *PstI* restriction site, there is not any *PstI* site on the pET30b vector. Therefore, it was expected to linearize the construct (as seen in Figure 3.18; on Lane 3, 6 and 9). Furthermore, *EcoRI* digestion of the colony minipreps gave the whole insert which was cloned (as seen in Figure 3.18; on Lane 4, 7 and 10). In addition, *XbaI* digestion would determine whether the gene was inserted in its correct orientation. If the gene was inserted into pET30b in its correct orientation, digestion with *XbaI* should give 5827 bp and 1101 bp DNA fragments (Figure 3.17). However, if it was not in its correct orientation, digestion with *XbaI* should give 786bp+6142bp DNA fragments (Figure 3.17). According to the result of the *XbaI* digestion of the selected colony minipreps, it can be concluded that two of the colonies includes the

insert in correct orientation (Lane 2 and 5 in Figure 3.18). Positive clones were sequenced to confirm the 5' end of the vector and insert joining region. The new construct was named as pET_alfa3'.

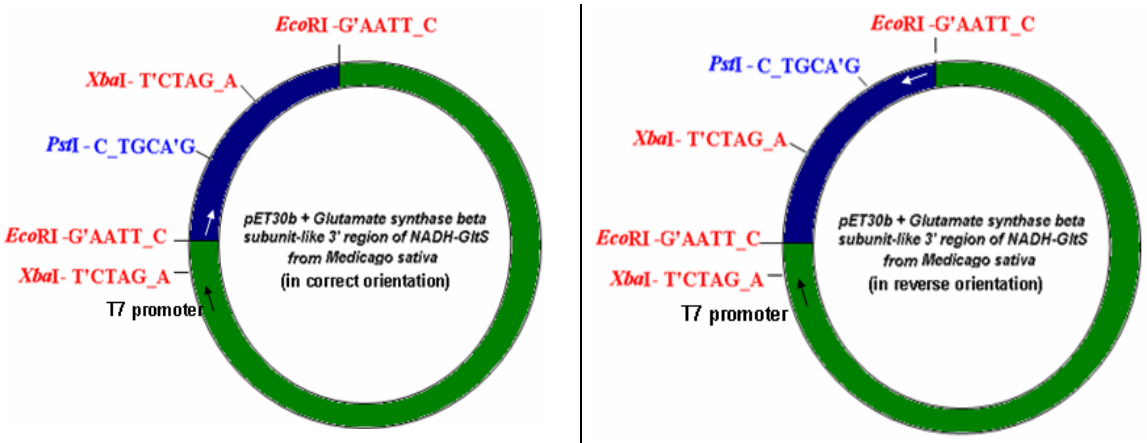

	Fragments after *XbaI* digestion
Correct orientation	5827 bp+1101 bp
Reverse orientation	786bp+6142bp

Figure 3.17: Maps of pET_alfa3' constructs containing the insert in correct orientation and in reverse orientation, respectively.

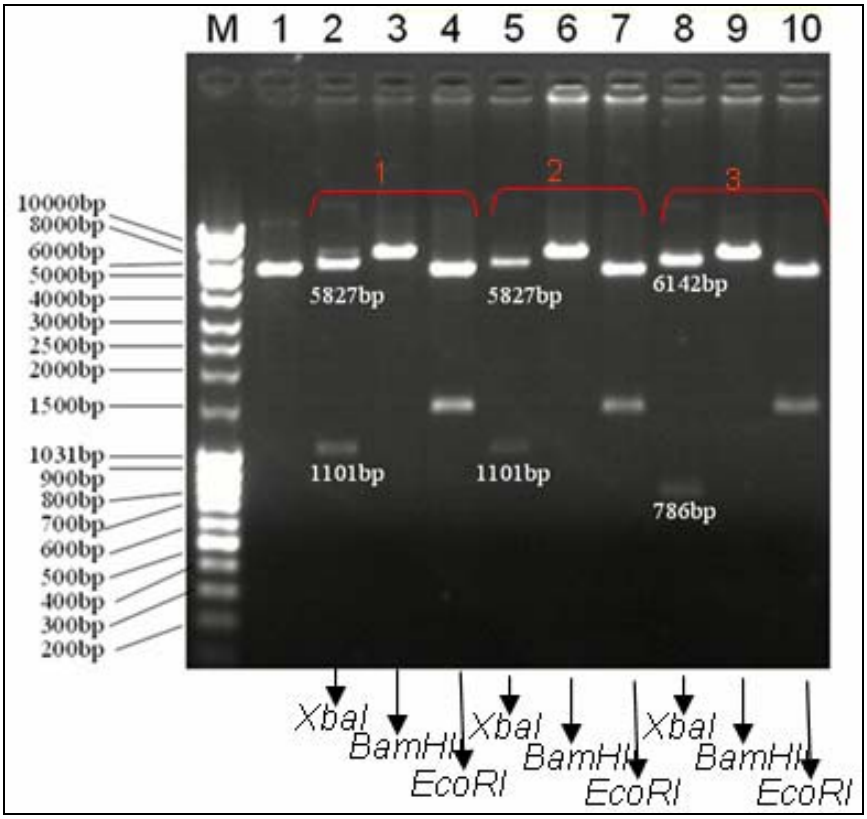

Figure 3.18: 1% gel analysis for determination of the correct orientation of *M. sativa* clone.

The explanation of the lane ingredients in the Figure 3.18 is as follows: M; MassRuler DNA Ladder, Mix, ready-to-use, Lane 1; pET30b digested with *EcoRI*, Lane2-5-8; Colony Minipreps digested with *XbaI,* Lane 3-6-9; Colony Minipreps digested with *Pst,* Lane 4-7-10; Colony Minipreps digested with *EcoRI.*

3.3. Expression Studies

Rosetta (DE3) pLysS, derivative of BL21 (DE3), was chosen as an expression host cell because it contains rare tRNA genes on the pLysSRARE plasmid which overcomes the codon usage bias difference between *P. horikoshii* and *E. coli* (Novy et al., 2001). Therefore, the usage of Rosetta (DE3) pLysS can prevent possible amino acid misincorporation, translation termination, translation frame-shifting during protein expression. This strain of *E.coli* also includes the *lon,* cytoplasmic protease and *omp*T, periplasmic protease deficiencies which increase protein stability. In addition, before using Rosetta series *E. coli* expression strains, *E. coli* BL21 (DE3) expression strain was tested by our group. However, expression of the archaeal protein could not be obtained using this strain (Demir and Dincturk, 2006).

The constructs, pPH7630_Native, pPH7630 and pPH7330 gave high or very high expression when Rosetta (DE3) pLysS cells were used as host cell. In addition, all of the expressed proteins were all found in the soluble part of the cell.

3.3.1. Construction and the expression of PH0876 native protein

A stop codon downstream of the His-tag region of pET30b and 19 bp of the pTZ57R, followed by a purine rich sequence prior to the initiator ATG, resulted in a construct, which successfully produced the native PH0876 protein (Figure 3.19)

"ATG CAC CAT CAT CAT CAT CAT TCT TCT GGT CTG GTG CCA CGC GGT TCT GGT ATG AAA GAA ACC GCT GCT GCT AAA TTC GAA CGC CAG CAC ATG GAC AGC CCA GAT CTG GGT ACC GAC GAC GAC GAC AAG GCC ATG GCG ATA TCG GAT CCG AAT TCG AGC TCG GTA CCT CGC GAA TGC ATC (TAG) ATT GGG GAA TTC ATG CCT AAG CTT ATT AAG GAG AGA GTT CCA ACT CCC GAG.."

Figure 3.19: Construction of the pPH7630_Native.

In the figure 3.19, black sequences are the fusion part encoding region of pET30b. Pink sequences are the *SacI* restriciton site used for cloning. Blue sequences come from the initial cloning into pTZ57R. The green region represents the EcoRV site of pTZ57R. Gray T is the extra sequence in the TA vector. Yellow region shows the primer sequence. Underlined black sequence shows the coding region of the native protein. The location of the stop codon is indicated between two parentheses.

Rosetta (DE3) pLysS was transformed by the resulting plasmid pPH7630_Native to express PH0876_Native protein. A single colony of the transformed strain Rosetta (DE3) pLysS was used to check the expression of the proteins, 4 h after the addition of 0.1 mM IPTG (isopropyl-β-D-thiogalactopyranoside) (Figure 3.20). The approximate molecular weights of the protein PH0876_Native was calculated via the ProtCalc bioinformatic tool as 51.9 kDa. The bacterial strain which harbours only pET30b vector was used as the negative expression control. Also uninduced cultures were analyzed via SDS-PAGE as a control of induced cultures. LB broth was used as growth medium and induction of Rosetta (DE3) pLysS *E. coli* strain containing plasmid pPH7630_Native was performed at 37ºC.

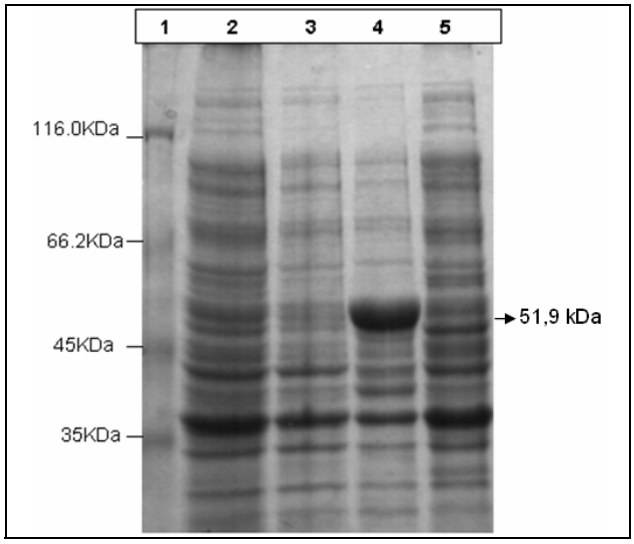

Figure 3.20: 10% SDS-PAGE analysis of induction of pET30b + PH0876 (pPH7630_Native).

The explanation of the lane ingredients in the Figure 3.18 is as follows: Lane1; Protein Molecular Weight Marker, Lane 2; Total cell protein harbouring vector only (uninduced), Lane 3; Total cell protein harbouring vector only (induced), Lane 4; Total cell protein harbouring pPH7630_Native (induced), Lane 5; Total cell protein harbouring pPH7630_Native (uninduced).

In order to check if overexpressed PH0876_Native protein is in the soluble fraction, cells were disrupted both by lysozyme treatment and sonication. Soluble and insoluble fractions were separated by centrifugation (Section 2.2.15) and samples were analyzed with SDS-PAGE. The electrophoresis of the collected fractions reveal that the overexpressed protein is in the soluble fraction of the cell lysate (Figure 3.21). An overexpressed band of ~51,9 kDa was observed at the soluble cell fraction after seperation of soluble and insoluble parts of the cell lysate.

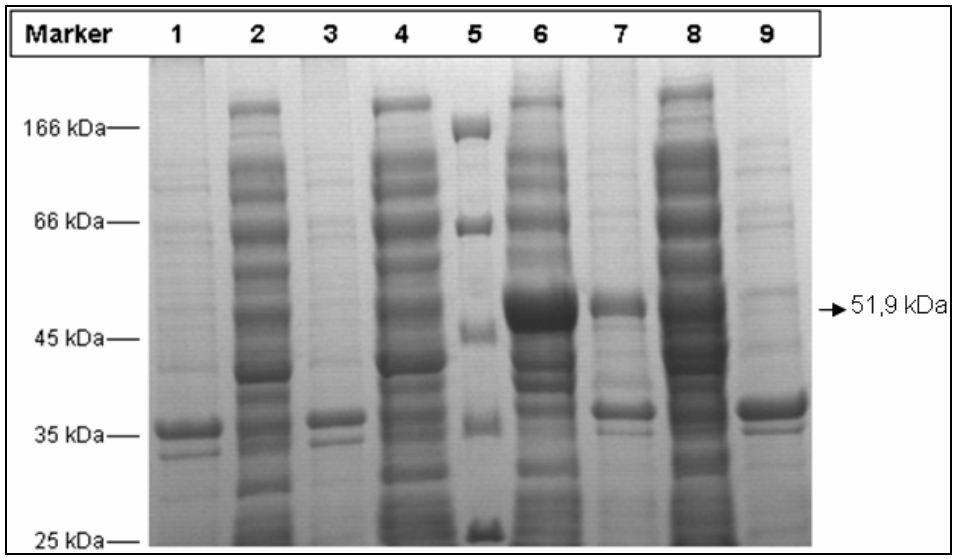

Figure 3.21: 10% SDS-PAGE analysis of soluble and insoluble fraction after induction of pPH7630_Native.

The explanation of the lane ingredients in the Figure 3.21 is as follows: Lane 1; Soluble fraction of lysate of *E. coli* harbouring vector only (uninduced), Lane 2; Insoluble fraction of lysate of *E. coli* harbouring vector only (uninduced), Lane 3; Soluble fraction of lysate of *E. coli* harbouring vector only (induced), Lane 4; Insoluble fraction of lysate of *E. coli* harbouring vector only (induced), M; Protein molecular weight marker, Lane 6; Soluble fraction of lysate of *E. coli* harbouring pPH7630_Native (induced), Lane 7; Insoluble fraction of lysate of *E. coli* harbouring pPH7630_Native (induced), Lane 8; Soluble fraction of lysate of *E. coli* harbouring pPH7630_Native (uninduced), Lane 9; Insoluble fraction of lysate of *E. coli* harbouring pPH7630_Native (uninduced).

To determine the N-terminal protein sequence of the protein, the overexpressed band was excised from the SDS-PAGE (HBD). The N-terminal sequencing was kindly performed in Université Mons-Hainaut, Belgium (in Dr. Ruddy Wattiez laboratory) by Edman degradation (Edman, 1950), and I would like to acknowledge Dr.

Raymond Cunin (in Vrije Universitet, Brussel) for providing the possibility of this experiment. The data showed that the overexpressed band represents the N-terminal of the native PH0876 product (Figure 3.22).

N-Terminal Protein Sequence Result for PH0876_native	PH0876 N-Terminal Protein Sequence
N'- MPKLIKERVPTPERPVEER	N'-MPKLIKERVPTPERPVEERIKDFK

Figure 3.22: Comparison of the N-Terminal Protein Sequence Result with the actual PH0876 N-Terminal Protein Sequence.

PH0876 native protein was succesfully expressed using pET expression system in *E. coli* in spite of the presence of a stop codon downstream of the His-tag region of pET30b (Figure 3.19). The protein initiation site upstream of the PH0876 coding region on the pPH7630_Native construct was analyzed.

"AUG CAC CAU CAU CAU CAU CAU UCU UCU GGU CUG GUG CCA CGC GGU UCU GGU AUG AAA GAA ACC GCU GCU GCU AAA UUC GAACGC CAG CAC AUG GAC AGC CCA GAU CUG GGU ACC GAC GAC GACGAC AAG GCC AUG GCG AUA UCG GAU CCG AAU UCG AGC UCG GUA CCU CGC GAA UGC AUC (UAG) AUU GG G GAA UUC #AUG# CCU AAG CUU AUU AAG GAG AGA GUU CCA ACU CCC GAG…"

Figure 3.23: Deduced mRNA sequence transcribed from the pPH7630_Native. Blue sequences are the transcribed region which is coming from the easy cloning vector pTZ57R. Gray regions may act as conservative nucleotides for the protein initiation site. Underlined black sequence shows the coding region of the native protein. The stop codon is indicated by two parentheses.

The sequence belongs to first 234 nucleotide sequence of the deduced mRNA sequence transcribed from the pPH7630_Native (Figure 3.23). The components of the transcription and translation machinery of *E. coli* are used during expression of this native protein. Therefore, this deduced mRNA sequence was compared with some of the initiation sites for protein synthesis found in *E. coli*. In bacterial mRNA, ribosome binding site plays an important role for translation initiation. Ribosome binding site containing purine rich sequence is where the 30S small subunit of bacterial ribosome binds first on mRNA (Figure 3.24). This site is called Shine-Dalgarno (SD) sequence (Shine and Dalgarno, 1975). There is a region on 5' side of the initiator codon of the PH0876 which is marked by grey color seems to have acted as a Shine-Dalgarno sequence (Berg et al., 2002). The efficiency of Shine-Dalgarno sequence depends on the length of the complementarity and the distance between the

Shine-Dalgarno sequence and the initiator codon. When the interaction involves the most favored region of 16S rRNA (GGAGG), a three-base-pair interaction is enough(complete SD 5'-UAA**GGAGG**U-3') The deduced mRNA sequence transcribed from the pPH7630_Native contains for GGGG nucleotide on the 5' region of the start codon in an appropriate distance from the start codon. This part is complementary to the most favored region of Shine-Dalgarno sequence (GGAGG) except the missing A nucleotide between the G nucleotides. Since this is the most important part of the Shine-Dalgarno sequence, the missing A nucleotide may be compensated.

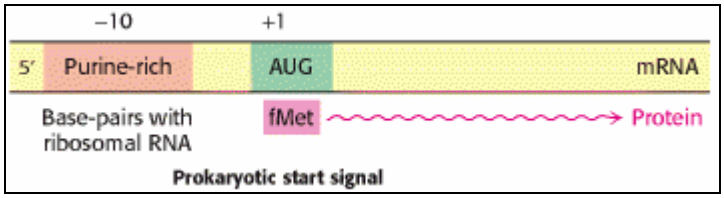

Figure 3.24: Initiation of protein synthesis in prokaryotes (Berg et al., 2002).

3.3.2. Expression of PH0876_HisTag and PH1873 proteins

Rosetta (DE3) pLysS was transformed by the resulting plasmids pPH7630_Histag and pPH7330 to express proteins PH0876_HisTag and PH1873. A single colony of each of the transformed strain Rosetta (DE3) pLysS was used to check the expression of the proteins, 4 h after the addition of 1 mM IPTG (isopropyl-β-D-thiogalactopyra noside). The bacterial strain which harbours only pET30b vector was used as the negative expression controls. Also uninduced cultures were analyzed via SDS-PAGE as a control of induced cultures.

LB broth was used as the growth medium and induction of Rosetta (DE3) pLysS *E. coli* strains containing plasmids pPH7630_Histag and pPH7330 were performed at 30ºC. Induction at 30ºC slows down the generation speed of cells and providing sufficient time for the proper folding of the protein.

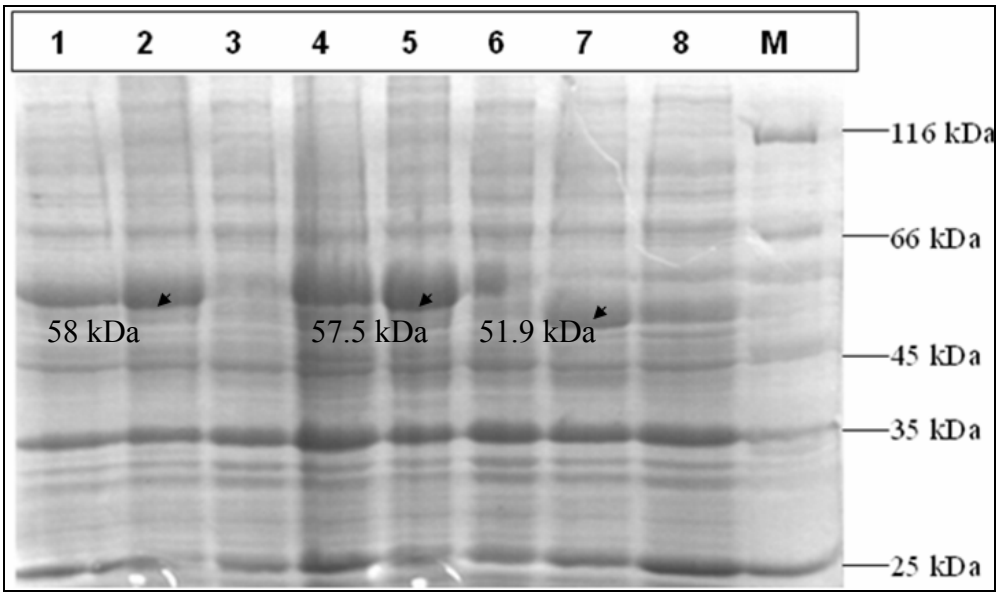

Figure 3.25: 10% SDS-PAGE analysis of induction of pET30b + PH0876_native (pPH7630_native), pET30b+PH0876_with_HisTag (pPH7630_HisTag) and pET30b +PH1873 (pPH7330).

The explanation of the lane ingredients in the Figure 3.25 is as follows: Lane1; Total cell protein harbouring pPH7330 (uninduced), Lane 2; Total cell protein harbouring pPH7330 (induced), Lane 3; Total cell protein harbouring vector only (induced), Lane 4; Total cell protein harbouring pPH7630_HisTag (uninduced). Lane 5; Total cell protein harbouring pPH7630_HisTag (induced), Lane 6; Total cell protein harbouring vector only (induced), Lane 7; Total cell protein harbouring pPH7630_ Native (induced), Lane 8;Total cell protein harbouring pPH7630_Native (uninduced), M; Protein Molecular Weight Marker. Arrows indicate expressed proteins.

"ATG CAC CAT CAT CAT CAT CAT TCT TCT GGT CTG GTG CCA CGC GGT TCT GGT ATG AAA GAA ACC GCT GCT GCT AAA TTC GAA CGC CAG CAC ATG GAC AGC CCA GAT CTG GGT ACC GAC GAC GAC GAC AAG GCC ATG GCG ATA TCG GAT CCG CGG ATG CCT AAG CTT ATT AAG GAG AGA GTT CCA ACT CCC GAG AGG CCC GTT GAG GAA AGG ATT AAG GAT"

Figure 3.26: Construction of the pPH7630_HisTag. Black sequences are the fusion protein part encoding region of pET30b. Red sequence is the *BamHI* restriciton site used for cloning. Yellow region shows the primer sequence. The forward primer is same for both PH0876 and PH1873. Underlined black sequence shows the coding region of the native protein.

“ATG CAC CAT CAT CAT CAT CAT TCT TCT GGT CTG GTG CCA CGC GGT TCT GGT ATG AAA GAA ACC GCT GCT GCT AAA TTC GAA CGC CAG CAC ATG GAC AGC CCA GAT CTG GGT ACC GAC GAC GAC GAC AAG GCC ATG GCG ATA TCG GAT CCG CGG ATG CCT AAG CTT ATT AAG GAG AGA GTT CCA ACT CCC GAG AGG CCC GTT GAG GAG AGA ATA AAA GAT TTT GAT GAA GTT AAT CTT GGT TAC ACC TGG GAG CTA GCT TTA A”

Figure 3.27: Construction of the pPH7330_HisTag. Black sequences are the fusion protein part encoding region of pET30b. Red sequence is the *BamHI* restriciton site used for cloning. Yellow region shows the primer sequence. The forward primer is same for both PH0876 and PH1873. Underlined black sequence shows the coding region of the native protein.

The approximate molecular weights of the PH0876 and PH1873 protein products were calculated via the ProtCalc bioinformatic tool as 51.9 kDa and 52.4 kDa, respectively. However, because of the extra sequences which comes from pET30b vector, their molecular weights rise to 57.5 kDa for PH0876_HisTag and 58 kDa for PH1873 Histag fusion protein (Figure 3.26 and Figure 3.27). The expressed protein bands were at expected molecular weights with respect to the protein marker on the gel (Figure 3.25 and Figure 3.28). In addition, the basal expression was observed in uninduced cultures which indicates that the expression was not tightly regulated by the addition of IPTG.

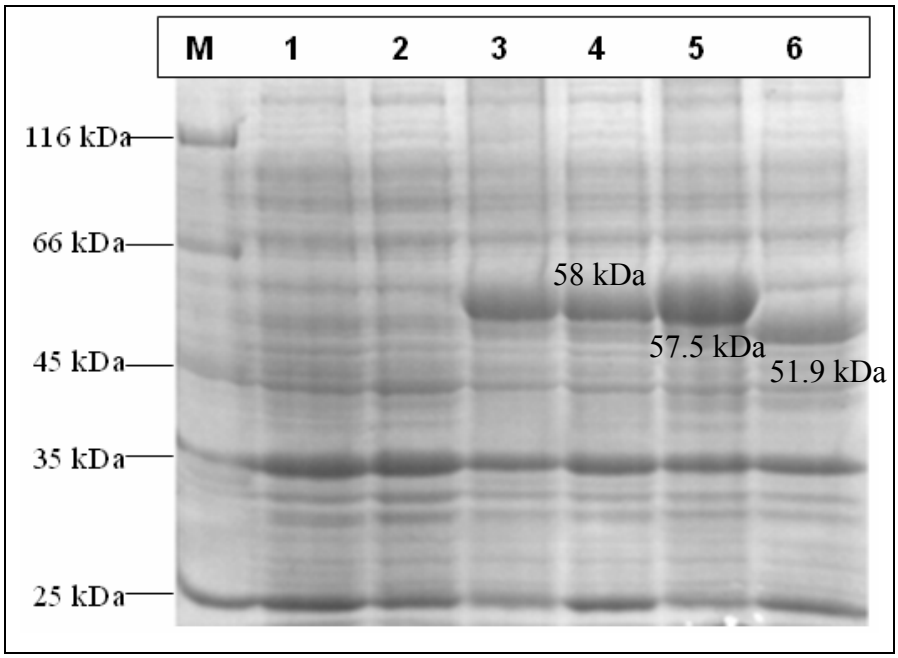

Figure 3.28: Comparison of the molecular weights among the proteins, PH0876_native, PH0876 _HisTag and PH1873 via 10% SDS-PAGE analysis.

The explanation of the lane ingredients in the Figure 3.28 is as follows: M; Protein Molecular Weight Marker, Lane 1; Total cell protein harbouring vector only (uninduced), Lane 2; Total cell protein harbouring vector only (induced), Lane3; Total cell protein harbouring pPH7330 (uninduced), Lane 4; Total cell protein harbouring pPH7330 (induced), Lane 5; Total cell protein harbouring pPH7630_HisTag (induced), Lane 6; Total cell protein harbouring pPH7630_Native (induced).

All of the constructs in Rosetta (DE3) pLysS, which were tested, gave high expression. In order to check if overexpressed PH0876 and PH1873 His Tag fusion proteins are in the soluble fraction, cells were disrupted both by lysozyme treatment and sonication. Soluble and insoluble fractions were separated by centrifugation (Section 2.2.15) and samples were analyzed with SDS-PAGE. Electrophoresis of the collected fractions reveals that the PH0876 and PH1873 His Tag fusion proteins were found in the soluble fraction (Lane2 and Lane3) of the cell lysate (Figure 3.29).

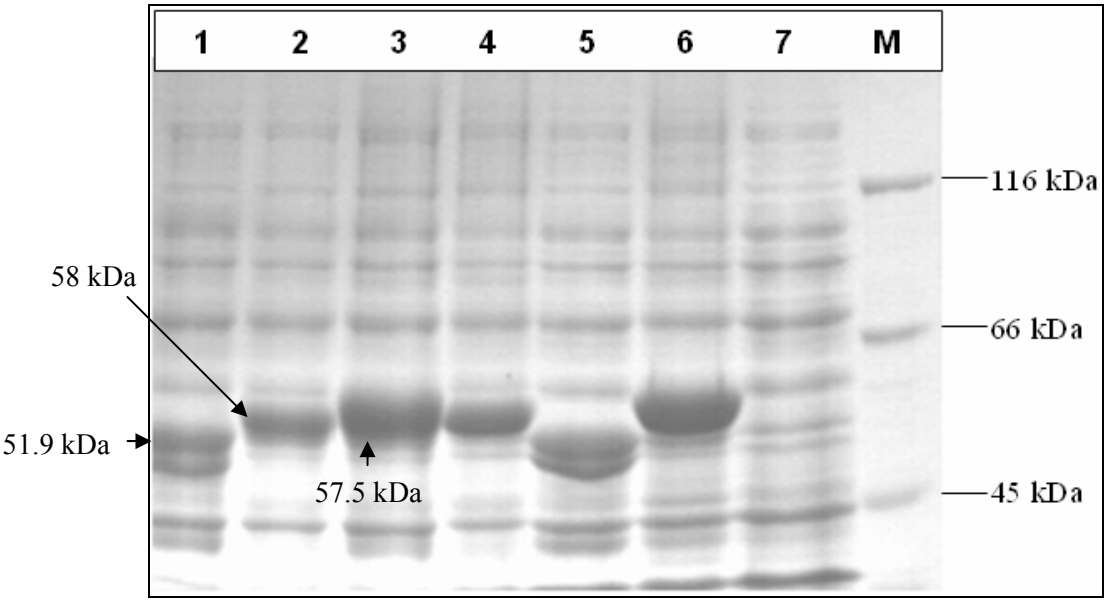

Figure 3.29: 10% SDS-PAGE analysis of soluble fraction after induction of pPH7630_Native and pPH7630_Histag and pPH7330. The proteins were run longer in order to observe the molecular weight difference of proteins more easily.

The explanation of the lane ingredients in the Figure 3.29 is as follows: Lane 1; Soluble fraction of lysate of *E. coli* harbouring pPH7630_Native (induced), Lane2; Soluble fraction of lysate of *E. coli* harbouring pPH7330 (induced), Lane3; Soluble fraction of lysate of *E. coli* harbouring pPH7630_Histag (induced), Lane4; Total cell

protein harbouring pPH7330 (induced), Lane 5; Total cell protein harbouring pPH7630_Native (induced), Lane 6; Total cell protein harbouring pPH7630_HisTag (induced), Lane 7; Total cell protein harbouring vector only (induced).

3.3.3. Expression of C terminal region of NADH-dependent Glutamate Synthase from *Medicago sativa*

Rosetta (DE3) pLysS was transformed by the resulting plasmid pPET30alfa to express β subunit-like C terminal region of NADH-dependent glutamate synthase from *Medicago sativa.* A single colony of the transformed strain Rosetta (DE3) pLysS was used to check the expression of the proteins, 4 h after the addition of 1 mM IPTG. The bacterial strain which harbours only pET30b vector was as the negative expression control. Also uninduced cultures were analyzed via SDS-PAGE as a control of induced cultures. LB broth was used as growth medium and induction of Rosetta (DE3) pLysS *E. coli* strain containing plasmid pPET30alfa was performed at 30ºC. Induction at 30ºC slows down the generation speed of cells for efficient folding of the recombinant protein.

The approximate molecular weight of the β-subunit like C terminal region of NADH-dependent glutamate synthase from *Medicago sativa* was calculated via the ProtCalc bioinformatic tool as 55.4 kDa. However, because of the extra sequences that come from pET30b vector, its molecular weights rise to ~60.5 kDa. The expressed protein bands were at expected molecular weights with respect to the protein marker on the gel (Figure 3.30).

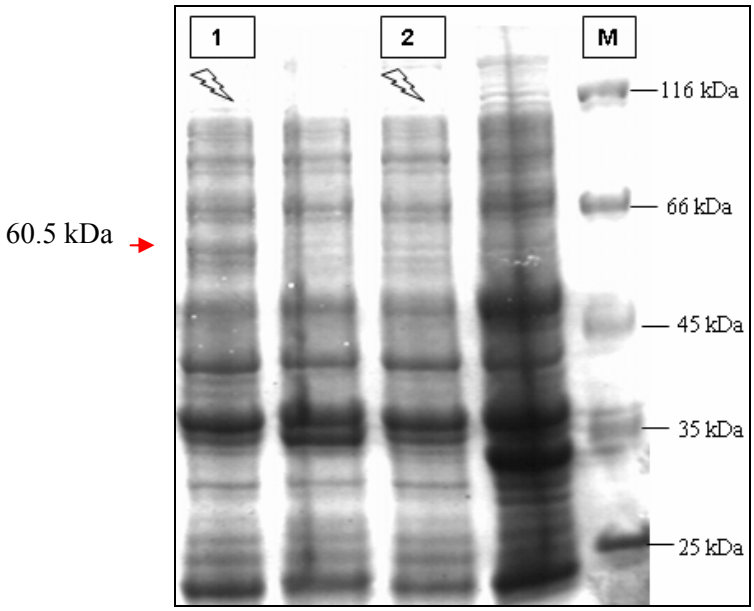

Figure 3.30: 10% SDS-PAGE analysis of induction of pET30b + β-subunit like C terminal region of NADH-dependent glutamate synthase from *Medicago sativa*. Red arrow indicates the location of the expressed protein on the gel. ⇘ is used to mark the lanes.

The explanation of the lane ingredients in the Figure 3.30 is as follows: Lane 1; Total cell protein harbouring pET30b + β-subunit like C terminal region of NADH-dependent glutamate synthase from *Medicago sativa* (induced), Lane 2; Total cell protein harbouring vector only (induced), M; Protein Molecular Weight Marker.

3.4. Purification of proteins under native conditions

Nucleotide sequencing of each plasmid have confirmed that the 6-residue histidine tag of pET30b, are in the correct frame upstream of the ORFs of interest. Successful purification of intact fusion proteins from total culture extracts was achieved using slurry nickel resin (Ni-NTA) which binds histidine residues. During the purification of the proteins PH0876 and PH1873, Ni-NTA became yellow in color. This may because of the FAD binding to these proteins if these proteins are flavoproteins as expected.

3.4.1. Purification of His Tag fusion protein PH0876 under native conditions with Ni-NTA

A concentration range varying from 20 mM to 350 mM imidazole was used during purification. The amount of purified proteins on Lanes 6, 7 and 8 are relatively higher than others (Figure 3.31). Therefore, the yield of proteins increase when there

is 200-300 mM imidazole is present in the elution buffer. This result is in agreement with the suggested concentration which is 250 mM (The QIAexpressionist catalogue).

Although the protein content bound on the resin decreases during each elution step, it was seen that elution with 300 mM imidazole concentration yielded a lot amount of protein. This indicates a strong binding of the fusion protein to the Ni-NTA with its His Tag region. It may be suggested that the folding of the protein enables His Tags to bind to the Ni-NTA freely or almost freely.

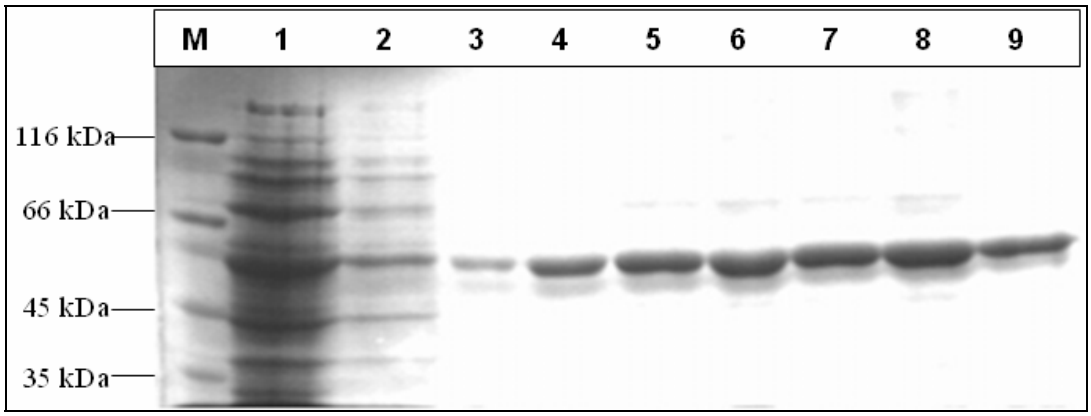

Figure 3.31: 10% SDS-PAGE analysis of protein purification of PH0876_HisTag (57.5 kDa) under native conditions with Ni-NTA.

The explanation of the lane ingredients in the Figure 3.31 is as follows: M; Protein Molecular Weight Marker, Lane 1; Flow-through of unbound proteins to Ni-NTA, Lane 2; Elution with 20 mM imidazole concentration, Lane 3; Elution with 50 mM imidazole concentration, Lane 4; Elution with 100 mM imidazole concentration, Lane 5; Elution with 150 mM imidazole concentration, Lane 6; Elution with 200 mM imidazole concentration, Lane 7; Elution with 250 mM imidazole concentration, Lane 8; Elution with 300 mM imidazole concentration, Lane 9; Elution with 350 mM imidazole concentration.

3.4.2. Purification of His Tag fusion protein PH1873 under native conditions with Ni-NTA

A concentration range varying from 20 mM to 350 mM imidazole was used during purification. The amount of purified proteins on Lanes 4, 5 and 6 are relatively higher than others (Figure 3.32). Therefore, sufficient amount of the PH1873 fusion protein can be obtained when there is 150-200 mM imidazole is present in the elution

buffer. This indicates a moderate binding of the fusion protein to the Ni-NTA with its His Tag region. It may be suggested that the folding of the protein interferes with the His Tag binding to the Ni-NTA.

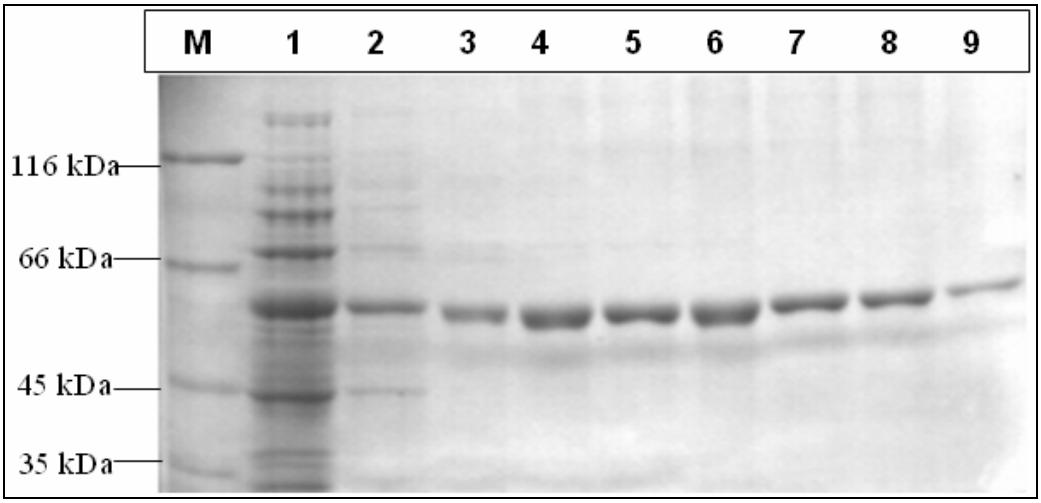

Figure 3.32: 10% SDS-PAGE analysis of protein purification of PH1873_HisTag (58 kDa) under native conditions with Ni-NTA.

The explanation of the lane ingredients in the Figure 3.32 is as follows: M; Protein Molecular Weight Marker, Lane 1; Flow-through of unbound proteins to Ni-NTA, Lane 2; Elution with 20 mM imidazole concentration, Lane 3; Elution with 50 mM imidazole concentration, Lane 4; Elution with 100 mM imidazole concentration, Lane 5; Elution with 150 mM imidazole concentration, Lane 6; Elution with 200 mM imidazole concentration, Lane 7; Elution with 250 mM imidazole concentration, Lane 8; Elution with 300 mM imidazole concentration, Lane 9; Elution with 350 mM imidazole concentration.

3.5. Western-Blotting of the expressed proteins

For Western blotting total cell protein fractions from induced cultures of cells which harbour pPH7630 and pPH7330 were used. HisTag monoclonal antibody was used as primary antibody. Electro-blotting membrane transfer was applied to transfer proteins from SDS-PAGE. The total protein cell samples, which were disrupted by SDS sample buffer, were used for Western blotting of the proteins.

3.5.1. Western Blotting of PH0876_Histag and PH1873_HisTag Proteins

Rosetta (DE3) pLsyS cells containing constructs pPH7630 and pPH7330 were induced with 1 mM IPTG at OD_{600}=0.6 for four hours, using LB broth as the growth media at

37ºC. Duplicate gels were run on SDS-PAGE in order to compare the antibody signals with the protein bands (Figure 3.33). While one gel was stained with Coomassie Blue, the other one was used for immunoblotting.

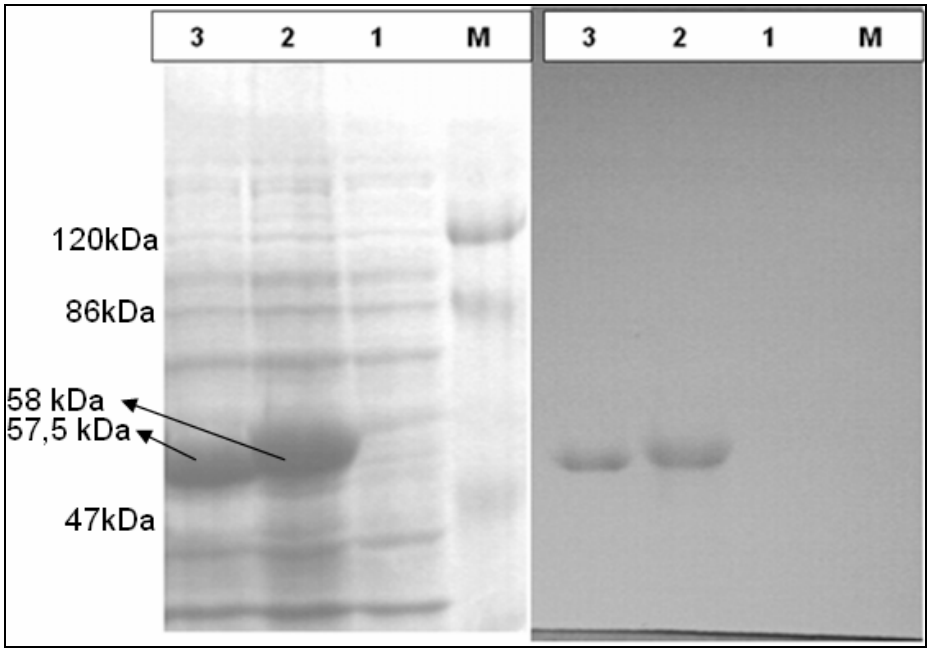

Figure 3.33: Western-blot of PH0876 and PH1873 proteins.

The explanation of the lane ingredients of the SDS-PAGE in the Figure 3.33 is as follows: Lane1; Total cell protein harbouring vector only (induced), Lane2; Total cell protein harbouring pPH7630_Histag (induced), Lane 3; Total cell protein harbouring pPH7330 (induced), M; Prestained Protein Molecular Weight Marker. Observed signals can be seen for PH0876 (Lane 3) and PH1873 (Lane2), respectively. Marker bands were not transfered to the membrane.

Membrane was treated firstly with His Tag monoclonal antibody and then treated with Goat Anti-Mouse AP (Alkaline Phosphatase) Conjugate, as the second antibody. Two positive signals for the induced bands of PH0876 (Lane3) and PH1873 (Lane 2) were obtained on the membrane (Figure 3.33).

3.5.2. Western Blotting of β-subunit like C terminal region of NADH-dependent glutamate synthase from *Medicago sativa*

Rosetta (DE3) pLsyS cells containing construct pET_alfa3' were induced with 1 mM IPTG at OD_{600}=0.6 for four hours, using LB broth as the media at 37ºC. Duplicate gels were run on SDS-PAGE in order to compare the signal bands with protein bands (Figure 3.34). One of the gels was stained with Coomassie Blue while the other one

was used for immunoblotting. Membrane was treated first with anti-Histag monoclonal antibody and then treated with anti- His-tag mAb (Novagen) conjugated to alkaline phosphatase, as second antibody. There is a signal on Lane 5 at the region corresponding to the area between 66 kDa and 45 kDa protein marker bands (Figure 3.34). The signal is on the same line with expressed protein band of the β-subunit like C terminal region of NADH-dependent glutamate synthase from *Medicago sativa* in lane 5 on SDS-PAGE which is ~60.5 kDa (Figure 3.34). The overexpressed protein bands observed on Lane 1 and 2 belongs to proteins expressed from the constructs named as pET30b+MJ1351 and pET30b+MJ1350, respectively for another project on *M. jannaschii* glutamate synthases in our laboratory (Figure 3.34). These proteins were used as positive controls and as markers for determination of the accurate molecular weight of the protein expressed from pET_alfa3' (Figure 3.34).

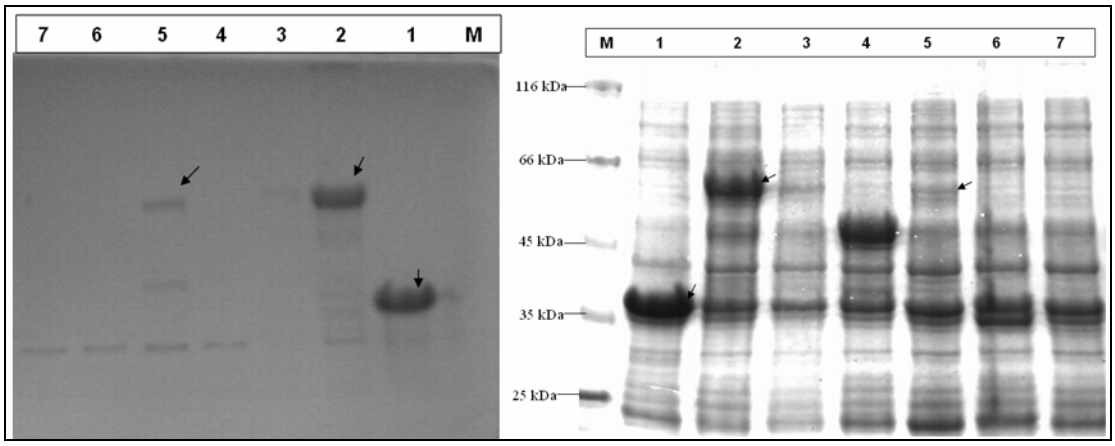

Figure 3.34: Western-blot of β-subunit like C terminal region of NADH-dependent glutamate synthase from *Medicago sativa.* **a)** Membrane treated with His tag antibody. **b)** Duplicate SDS-PAGE gel.

The explanation of the lane ingredients of the SDS-PAGE in the Figure 3.34 is as follows: Lane 1; Total cell protein harbouring pET30b+MJ1351 (induced), Lane 2; Total cell protein harbouring pET30b+MJ1350 (induced), Lane4; Total cell protein harbouring pPH7630_Native (induced), Lane 5; Total cell protein harbouring pET_alfa3' (induced), Lane 6-7; Total cell protein harbouring vector only (induced).

3.6. Thermal Stability of the PH0876 and PH1873 Proteins from *Pyrococcus horikoshii*

To examine the thermal stability of the PH0876 and PH1873, heat inactivation tests were carried out. After lysozyme treatment and sonication, soluble total cell proteins

of induced cultures were heat denaturated for 15 minutes at 85ºC. Heat treatment denaturated most of the host proteins and caused them to precipitate. PH0876 and PH1873 were obtained in the soluble part after heat denaturation for 15 minutes at 85ºC as expected since *P. horikoshii* proteins are thermostable (Figure3.35 and 3.36, respectively).

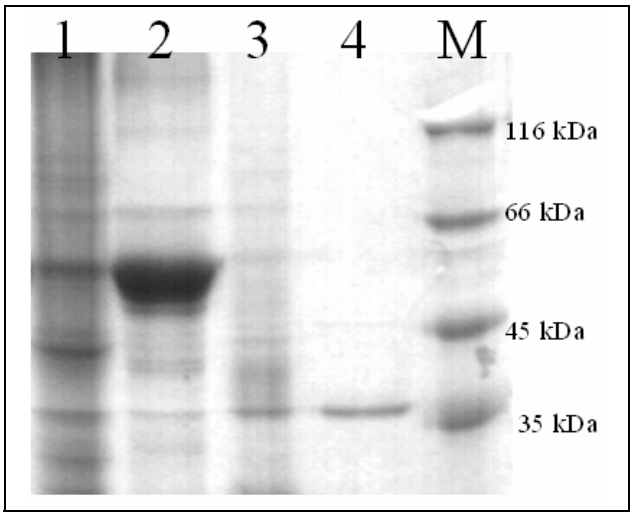

Figure 3.35: Heat inactivation test result for PH0876. The test was performed using soluble fraction of cell lysate.

The explanation of the lane ingredients in the Figure 3.35 is as follows: Lane 1; Insoluble protein fraction of cell protein harbouring pPH0876-His Tag after heat inactivation test (induced), Lane 2; Soluble fraction of cell protein harbouring pPH0876-His Tag after heat inactivation test (induced), Lane 3; Insoluble fraction of cell protein harbouring only vector after heat inactivation test (induced), Lane 4; Soluble fraction of cell protein harbouring only vector after heat inactivation test (induced), M; Protein Molecular Weight Marker.

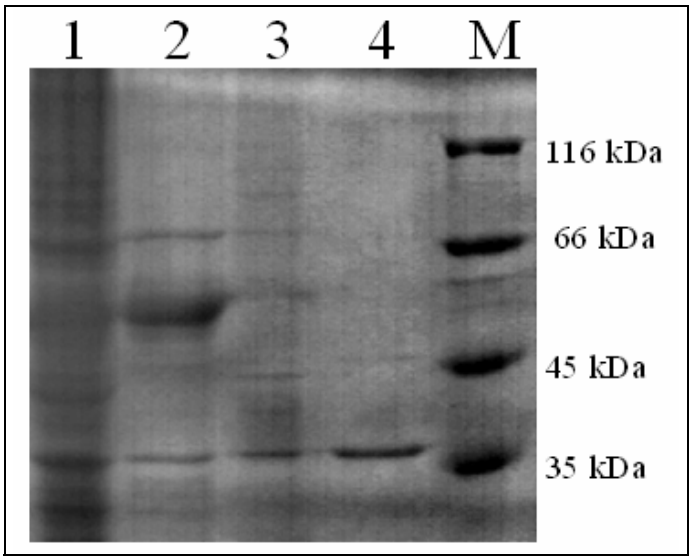

Figure 3.36: Heat inactivation test result for PH1873. The test was performed using soluble fraction of cell lysate.

The explanation of the lane ingredients in the Figure 3.36 is as follows: Lane 1; Insoluble fraction of cell protein harbouring pPH1873 after heat inactivation test (induced), Lane 2; Soluble fraction of cell protein harbouring pPH1873 after heat inactivation test (induced), Lane 3; Insoluble fraction of cell protein harbouring only vector after heat inactivation test (induced), Lane 4; Soluble fraction of cell protein harbouring only vector after heat inactivation test (induced), M; Protein Molecular Weight Marker.

4. DISCUSSION

The availability of the whole genome sequence of several hyperthermophilic archaea, provide a large mass of data which requires a long time for processing. The overall information is valuable not only for the commercialization of industrially important enzymes with high temperature stability, but, at the same time, from many perspectives such as the elucidation of metabolisms of these organisms in such heavy selective pressures and reveal information about important evolutionary turns. However, sequence information alone can be misleading when such ancient organisms are concerned as the evolution of new genes raise from mutations and gene duplications of the existing ones as well as the transfer of genes via insertion elements.

Glutamate synthase is an interesting enzyme to work on to solve such puzzles as several subunits of the enzyme are found as separate ORFs in archaeal genomes. To elucidate the role, activity and evolutionary importance of archaeal glutamate synthase small- subunit-like genes, which show high homology to small subunit of bacterial glutamate synthases and the C-terminal regions of the monomeric NADH-dependent glutamate synthases, it was necessary to clone and express them in *Escherichia coli* so that a large quantity was available for activity analyses.

The two open reading frames PH0876 and PH1873 of the hypertermophilic archaea, *Pyrococcus horikoshii*, which show very high homology to the glutamate synthase small subunits from many bacterial species, have been cloned and successfully expressed in *E. coli*. The hyperthermophile characteristic of the organism and the difficulty of culturing conditions was also one of the reasons for cloning and expressing the proteins in a heterologous system, as well as the requirement for large quantities in a purified form. Both proteins are expressed in soluble fractions and purified via His-tag purification systems.

These small subunit-like ORFs are interesting from three major perspectives. The first one is that, there are no open reading frames which may be coding for a large

subunit which is responsible for the glutamate formation neither upstream nor downstream of these ORFs and neither anywhere else in the genome of *P. horikoshii* (Figure 1.11). Although there is a very high sequence homology, the activity of the protein may be different. As archaea are earlier in evolution in comparison to bacteria and plants, such an ORF can well be initially coding for a different enzyme, which may later be adapted as a subunit to glutamate synthases. The second perspective is that, these two putative GOGAT small subunit-like regions show above 90% homology to one another, which raises the possibility of gene duplication (Figure 1.17). As an important mechanism for the evolution of new genes, gene duplication may enhance the likeliness of the argument above. Therefore, many copies of the gene are present in different parts of the genome and such a domain may have been used by several different proteins for a similar purpose, such as being an electron transfer domain.

The third perspective raise from an interesting observation of three *Methanocaldococcus jannaschii* ORFs (MJ1350-MJ1351- MJ1351.1) which may be coding for the large subunit of GOGAT while no ORF has been detected for a small subunit homologue. However, the genomes of three *Pyrococcus* species, *P. horikoshii*, and *P. abyssi* harbour two, *P. furiosus* three open reading frames which show homology with the small subunit of GOGAT. This brings the possibility of lateral gene transfer via the combination of two subunits in the higher organisms (Dinçtürk, 2001, Andersson & Roger, 2002). It seems likely that these open reading frames are the early forms of an electron transfer domain in archaea which may have later contributed to many electron transfer enzymes. There are other enzymes where the role as an electron transfer domain is likely such as sulphide dehydrogenase (Hagen et.al, 2000) as well as PH0876 and PH1873 presented in this work.

The electron transfer between a reduced pyridine nucleotide and a second protein or protein domain is probably the role of putative β subunits and β subunit-like proteins as they contain conservative sites for ADP binding folds and Fe/S cluster(s). Both NAD(P)H and FAD binding regions are also conserved in PH0876 and PH1873 (Figure 3.4). The cystein-rich domains forming Fe-S clusters which provide reducing elements for oxidation-reduction reaction are also conserved in both PH0876 and PH1873. Thus, observation of an NAD(P)H dependent oxidoreductase activity can be a probable expected result for these proteins.

In addition, Morandi et al. (2000) investigated potential ADP binding region responsible for NADPH binding in the β subunit of *Azospirillum brasilense* glutamate synthase by a G298A substitution. This substitution was introduced in the second glycine of the presumed NADPH binding site motif GXGXXA. This change affected the binding of the pyridine nucleotide substrate negatively (Morandi et al., 2000). As a result, ADP binding fold at the C terminal of the GltS β subunit was found to be the NADPH binding site (Morandi et al., 2000). This ADP binding fold involved in NAD(P)H binding is also present in both PH0876 and PH1873 (Figure 3.4). Moreover, the C-terminal pyridine nucleotide binding glycine-rich regions of PH0876 and PH1873 are differing from that of the C-terminal consensus sequence of NADH-GltS beta subunit amino acid sequences (Figure 3.5). The existence of an A instead of G in the last position of the motif GXGXX(G/A/P) which is proposed to be involved in NADPH binding (Morandi et al., 2000) is also valid for PH0876 and PH1873 (Figure 3.5). This may suggest that the proteins encoded by these open reading frames may utilize NADPH as pyridine nucleotide. However, these have to be confirmed experimentally. Activity analyses of the His-tag purified PH0876 and PH1873 and native PH0876 are on progress.

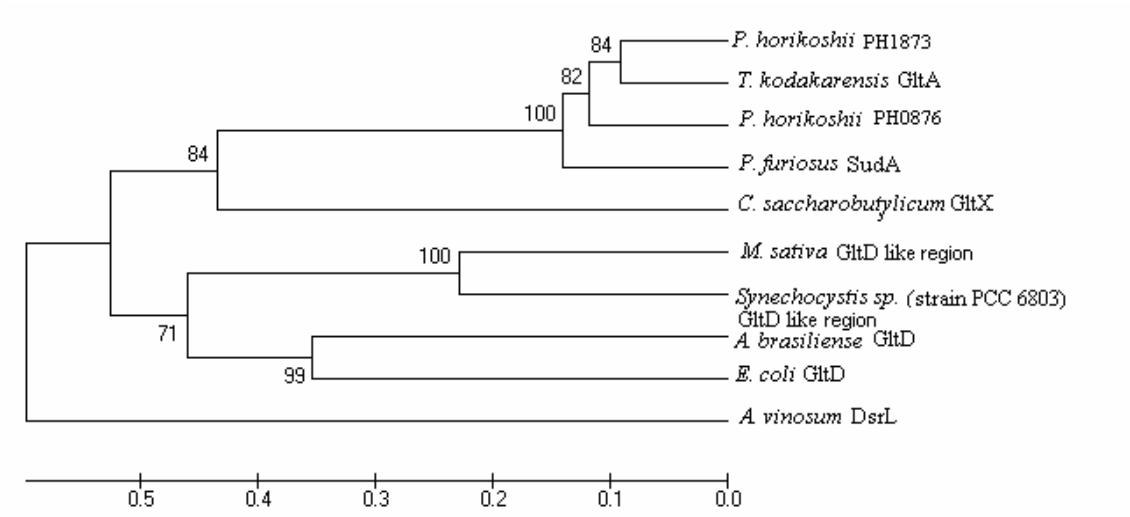

Figure 4.1: Phylogenetic tree of glutamate synthase small subunits and small subunit-like regions drawn by MEGA 3.1 (Kumar et.al, 2004). The bar represents changes per amino acid.

Parsimony analysis of glutamate synthase small subunits and small subunit-like ORFs showed three major branches. *A. vinosum* DsrL which harbours a C-terminal extension followed by a CXXC motif formed an outgroup. It is interesting to observe that the characterized bacterial glutamate synthases and the plant C-terminal small

subunit-like regions and yet uncharacterized small subunit homologues from archaea and a *Clostridium* species formed two distinct groups. In the latter one, comparatively different *Clostridium* species may be considered as an outgroup for the archael species. None of the species in this group has a large subunit homologue which harbours an amidotransferase domain upstream or downstream of the gene. Neither SudA of *P. furiosus* (Hagen et.al., 2000) nor GltX of *C. saccharobutylicum* (Stutz and Reid, 2004) from this branch showed any GOGAT activity.

It is not surprising that two NADH dependent forms, cyanobacterial and plant GOGAT C-terminal regions branched with a 100% of bootstrap value. This is also valid for the NADPH dependent two bacterial GOGAT small subunits.

The phylogenetic tree shows that the species in both of the major branches are similar but yet sufficiently different from one another. It seems like they may have had similar evolutionary origins but have differed to serve for different functional roles, possibly by means of gene duplication. The similarity of NADPH binding regions and the presence of flavins show that they are still involved in electron transfer.

REFERENCES

Adams M. W.W., Holden J. F., Menon A., , Schut G. J., Grunden A. M., Hou C., Hutchins A. M. Jenney E. F., JR., Kim C. , Ma K., Pan G. , Roy R., Sapra R., Story S. V. , AND Verhagen M. J. M., 2001. Key Role for Sulfur in Peptide Metabolism and in Regulation of Three Hydrogenases in the Hyperthermophilic Archaeon *Pyrococcus furiosus, Journal of Bacteriology*, **183,** 716–724.

Altschula, S.F., Gisha, W., Millerb, W., Meyersc, E.W., Lipmana, D.J., 1990. Basic Local Alignment Search Tool, *Journal of Molecular Biology*, **215,** 403-410.

Alberts B., Alexander J., Lewis J., Raff M., Roberts K., Walter P., 2002. Molecular Biology of the Cell, p. 349, GS Garland Science. New York.

Amend J. P., Shock E. L., 2001. Energetics of overall metabolic reactions of thermophilic and hyperthermophilic Archaea and Bacteria, *FEMS Microbiology Reviews,* **25**, 175-243.

Andersson J.O. and Roger A.J., 2002. Evolutionary Analyses of the Small Subunit of Glutamate Synthase: Gene Order Conservation, Gene Fusions, and Prokaryote to Eukaryote Lateral Gene Transfers, *Eukaryotic Cell*, **1**, 304-310.

Anderson, M.P., Vance, C.P., Heichel, G.H., Miller, S.S., 1989. Purification and characterization of NADH-glutamate synthase from alfalfa root nodules, *Plant Physiol,* **90**, 351-358.

Atomi H. Matsumi R. Imanaka T., 2004. Reverse gyrase is not a prerequisite for hyperthermophilic life, *J. Bacteriol.,* **186**, 4829–4833.

Bell S. D., Jackson S. P., 2001. Mechanism and regulation of transcription in archaea, *Current Opinion in Microbiology*, **4**, 208–213.

Berg J., Tymoczko J., Stryer L., 2002. Biochemistry, Fifth Edition. W. H. Freeman and Company, New York.

Binda, C., Bossi, R. T., Wakatsuki, S., Arzt, S., Coda, A., Curti, B., Vanoni, M. A., and Mattevi, A., 2000. Cross Talk and Ammonia Channeling between Active Cnters in the Unexpecxted Domain Arrangement of Glutamate Synthase, *Struct. Fold. Des.,* **8**, 1299–1308

Chavez S, Lucena JM, Reyes JC, Florencio FJ, Candau P., 1999. The presence of glutamate dehydrogenase is a selective advantage for the cyanobacterium *Synechocystis* sp. strain PCC 6803 under nonexponential growth conditions, *Journal of Bacteriology.,* **181**, 808-813.

Cogoni C., Valenzuela L., Halphen D.D.L., Olivera H., Macino G., Ballario P., Gonzalez A., 1995. *Saccharomyces cerevisiae* Has a Single Glutamate Synthase Gene Coding for a Plant-Like High-Molecular-Weight Polypeptide, *Journal of Bacteriology*, **177**, 792–798.

Cohen, G. N. , Barbe V., Flament D., Galperin M., Heilig R., Lecompte O., Poch O., Prieur D., Querellou J., Ripp R., Thierry J.-C., Van der Oost J., Weissenbach J., Zivanovic Y., Forterre P., 2003. An integrated analysis of the genome of the hyperthermophilic archaeon *Pyrococcus abysii*., *Molecular Microbiology, 47*, 1495-1512.

Coshigano KT, Melo-Oliveita R, Lim J, Coruzzi M., 1998. Arabidopsis gls mutants and distinct Fd-GOGAT genes: implications for photorespiration and primary nitrogen assimilation, *Plant Cell*., **10**, 741–752.

Curti B, Vanoni MA, Verzotti E, Zanetti G., 1996. Glutamate synthase: a complex iron-sulphur flavoprotein, *Biochem. Soc. Trans.,* **24**, 95-99.

Dahl C.,Engels S.,Pott-Sperling A. S.,Schulte A.,Sander J.,Lübbe Y.,Deuster O., and Brune D. C. , 2005. Novel Genes of the *dsr* Gene Cluster and Evidence for Close Interaction of Dsr Proteins during Sulfur Oxidation in the Phototrophic Sulfur Bacterium *Allochromatium vinosum, Journal of Bacteriology*, **187**, 1392-1404.

Deckert G., Warren P. V., Gaasterland T., Young W. G., Lenox A. L., Graham D. E., Overbeek R., Snead M. A., Keller M., Aujay M., Huber R., Feldman R. A., Short J. M., Olsen G. J., Swanson R. V., 1998. The complete genome of the hyperthermophilic bacterium Aquifex aeolicus, *Nature*, **392**, 353–358.

Dinçtürk H.B., 2001. Glutamate synthase: An archaeal horizontal gene transfer?, *Journal of Biosciences*, **26**, 13-14.

Demir V, Dincturk H.B., 2006. Semi-anaerobic growth conditions are favoured by some Escherichia coli strains during heterologous expression of some archaeal proteins, *Molecular Biology Reports*, **33**, 59-63.

Dinçtürk H.B. & Knaff D. B., 2000. The evolution of glutamate synthase, *Molecular Biology Reports,* **27,** 141–148.

DiRuggiero J. , Dunn D., Maeder D. L., Holley-Shanks R., Chatard J., Horlacher R., Robb F. T., Boos W. , and Weiss R. B., 2000. Evidence of recent lateral gene transfer among hyperthermophilic Archaea., *Molecular Microbiology* **38**, 684-693.

Doolittle, W.F., 1999. Lateral genomics, *Trends Cell Biol.,* **9**, 5-8.

Edman P., 1950. Method for determination of the amino acid sequence in peptides, Acta Chem. Scand, **4**, 283-293.

Erauso G., 1993. *Pyrococcus abyssi* sp. nov., a new hyperthermophilic archaeon isolated from a deep-sea hydrothermal vent, *Arch Microbiol,* **160**, 338-349.

Forterre P., 1995. The reverse gyrase of hyperthermophilic archaeobacteria: origin of life and thermophily, *Microbiologia SEM,* **11,** 225–32**.**

Forterre P., 2002. A hot story from comparative genomics: reverse gyrase is the only hyperthermophile-specific protein*, Trends in Genetics,* **18**, 236-238.

Fukui T., **Atomi H**., **Kanai T**., **Matsumi R**., **Fujiwara S**., **Imanaka T**., 2005. Complete genome sequence of the hyperthermophilic archaeon Thermococcus kodakaraensis KOD1 and comparison with Pyrococcus genomes, *Genome Res.,* **15**, 352-63.

Galván, F., Márquez, A.J. and Vega, J.M., 1984. Purification and molecular properties of ferredoxin-glutamate synthase from *Chlamydomonas reinhardii,. Planta,* **162**, 180-187.

Gregerson R. G., Miller S. S., Twary N. S., Gantt J. S. and Vance C. P., 1993. Molecular Characterization of NADH-Dependent Glutamate Synthase from Alfalfa Nodules, *The Plant Cell*, **5**, 215-226.

Gonzales J. M., Masuchi Y., Robb F.T., Ammerman J. W. Maeder D. L., Yanagibayashi M., Tamaoka J. and Kato C., 1998. Pyrococcus horikoshii sp. Nov., a hyperthermophilic archaeon isolated from a hydrothermal vent at the Okinawa Trough, *Extromophiles,* **2**, 123-130.

Gosset, G., Merino, E., Recillas, F., Oliver, G., Becerril, B., Bolivar, F., 1989. Amino acid sequence analysis of the glutamate synthase enzyme from *Escherichia coli* K-12, *Protein Sequence Data Analysis*, **2**, 9-16.

Hagen W.R., Silva P.J., Amorim M.A., Hagedorn P.L., Wassink H., Haaker H., Robb F.T., 2000. Novel structure and redox chemistry of the prostetic groups of the iron-sulfur flavoprotein sulfide dehydrogenase from *Pyrococcus furiosus*; evidence for a [2Fe-2S] cluster with $Asp(Cys)_3$ ligands, *Journal of Biological Inorganic Chemistry*, **5**, 527-534.

Hamilton-Brehm S.D., Schut G.J., Adams M.W.W., 2005. Metabolic and evolutionary relationships among *Pyrococcus* species: Genetic exchange within a hydrothermal vent environment, *Journal of Bacteriology*, **187**, 7492-7499.

Heuvel R.H.H., Ferrari D., Bossi R.T., Ravasio S., Curti B., Vanoni M.A., Florencio F.J., Mattevi A., 2002. Structural Studies on the Synchronization of Catalytic Centers in Glutamate Synthase, *The Journal of Biological Chemistry,* **277**, 24579–24583.

Heuvel R.H.H., Svergun D.I., Petoukhov M.V., Coda A, Curti B., Ravasio S., Vanoni M.A., Mattevi A., 2003. The active conformation of glutamate synthase and its binding to ferredoxin, *J. Mol. Biol.*, **330**, 113-128.

Higgins D., Thompson J., Gibson T.Thompson J.D., Higgins D.G., Gibson T.J., 1994. CLUSTAL W: improving the sensitivity of progressive multiple sequence alignment through sequence weighting, position-specific gap penalties and weight matrix choice. *Nucleic Acids Res.,* **22**, 4673-4680.

Hirasawa M., Hurley J.K., Salamon Z., Tollin G., Knaff D.B., 1996. Oxidation-reduction and transient kinetic studies of spinach ferredoxin-dependent glutamate synthase, *Arch Biochem Biophys.*, **330**, 209-215.

Hirayama C, Saito H, Konno K, Shinbo H., 1998. Purification and characterization of NADH-dependent glutamate synthase from the silkworm fat body (*Bombyx mori*), *Insect Biochem. Mol. Biol.*, **28**, 473-482.

Hummelt, G., Mora, J., 1980. Regulation and function of glutamate synthase in *Neurospora crassa*, *Biochemical and Biophysical Reviews Communication*, **96**, 1688-1694.

Ishiyama K., Hayakawa T., Yamaya T., 1998. Expression of NADH-dependent glutamate synthase protein in epidermis and exodermis of rice roots in response to the supply of nitrogen, *Planta*, **204**, 288-294.

Jannasch, H. W., C. O. Wirsen, S. J. Molyneaux, and T. A. Langworthy, 1992. Comparative physiological studies on hyperthermophilic archaea isolated from deep-sea hot vents with emphasis on *Pyrococcus* strain GB-D. *Appl. Environ. Microbiol*., **58**, 3472-3481.

Jongsareejit B., Rahman R.N.Z. A., Fujiwara S., Imanaka T., 1997. Gene cloning, sequencing and enzymatic properties of glutamate synthase from the hyperthermophilic archaeon, *Pyrococcus* sp. KOD1, *Mol Gen Genet*., **254**, 635-642.

Kawarabayasi Y., Sawada M., Horikawa H., Haikawa Y., Hino Y., Yamamoto S., Sekine M., Baba S., Kosugi H., Hosoyama A., Nagai Y., Sakai M., Ogura K., Otsuka R., Nakazawa H., Takamiya M., Ohfuku Y., Funahashi T., Tanaka T., Kudoh Y., Yamazaki J., Kushida N., Oguchi A., Aoki K. and Kikuchi H., 1998. Complete sequence and gene organization of the genome of a hyper-thermophilic archaebacterium, *Pyrococcus horikoshii* OT3, *DNA Res.,* 55–76.

Knaff D. B., Hirasawa M., Ameyiborp E., Fu W., and Johnsonell M. K., 1991. Spectroscopic Evidence for a [3Fe-4S] Cluster in Spinach Glutamate Synthase, *The Journal of Biological Chemistry*, **2661**, 5080-15084.

Kumar, S., Tamura, K., Nei, M., 2004. MEGA3: Integrated software for Molecular Evolutionary Genetics Analysis and sequence alignment. *Briefings in Bioinformatics*, **5**, 150-163.

Lawrence, J.G., and Ochman, H., 1998. Molecular archaeology of the Escherichia coli genome, *Proc Natl Acad Sci*, USA, **95**, 9413-9417.

Lea PJ, Ireland RJ., 1999. Nitrogen metabolism in higher plants. *In* BK Singh, ed, Plant Amino Acids: Biochemistry and Biotechnology. Marcel Dekker, New York, pp 1-47.

Lea P.J. and Miflin B.J., 2003. Glutamate synthase and the synthesis of glutamate in plants, *Plant physiology and Biochemistry*, **41**, 555-564.

Madigan M., Martinko J. M., Parker J., 2003.Brock Biology of Microoorganisms. Pearson Education Inc.

Maeder D. L., Weiss R. B., Dunn D. M., Cherry J. L., Gonzales J. H., DiRuggiero J., and Robb F. T., 1999. Divergence of the Hyperthermophilic Archaea *Pyrococcus furiosus* and *P. horikoshii* Inferred From Complete Genomic Sequences, *Genetics,* **152**, 1299–1305.

Marqués S, Florencio FJ, Candau P., 1992. Purification and characterization of the ferredoxin-glutamate synthase from the unicellular cyanobacterium *Synechococcus* sp. PCC 6301, *Eur J Biochem.,* **296**, 69–77.

Miflin, B.J., Lea, P.J., Wallsgrove, R.M., 1980. The role of glutamine in ammonium assimilation and reassimilation in plants, Academic Press, New York.

Miller, R. E. & Stadtman, E. R., 1972. Glutamate synthase from *Escherichia coli*. An iron–sulfide flavoprotein, *J Biol Chem,* **247**, 7407-7419.

Morandi P., Valzasina B., Colombo C., Curti B. and Vanoni M. A., 2000. Glutamate synthase: identification of the NADPH-binding site by site-directed mutagenesis, *Biochemistry,* **39**, 727–735.

Nagradova N., 2003. Interdomain Communications in Bifunctional Enzymes: How Are Different Activities Coordinated?, *IUBMB Life*, **55**.

Nakamura, Y., Gojobori, T., Ikemura, T., 2000. Codon usage tabulated from the international DNA sequence databases: status for the year, Nucleic Acids Research, **28**, 292.

Navarro F., Chavez S., Candau P., Florencio F. J., 1995. Existence of two ferredoxin-glutamate synthases in the cyanobacterium Synechocystis sp. PCC 6803. Isolation and insertional inactivation of gltB and gltS genes, *Plant Mol. Biol.,* **27,** 753– 767.

Navarro F., Eugenio M.F., Candau P., Florencio F.J., 2000. Ferredoxin-Dependent Iron-Sulfur Flavoprotein Glutamate Synthase (GlsF) from the Cyanobacterium *Synechocystis* sp. PCC 6803: Expression and Assembly in *Escherichia coli*, *Archives of Biochemistry and Biophysics*, **379**, 267–276.

Nelson, K.E., Clayton, R.A., Gill, S.R., Gwinn, M.L., Dodson, R.J., Haft, D.H., 1999. Evidence for lateral gene transfer between Archaea and bacteria from genome sequence of Thermotoga maritima, *Nature*, **399**, 323-329.

Novy, R., Drott, D., Yaeger, K., Mierendorf, R., 2001. Overcoming the codon bias of *E. coli* for enhanced protein expression, News Letter of Novagen, Inc. Advanced Products and Protocols for Molecular Biology Research, **12.**

Pelanda R., Vanoni A., Peregoe M., Piubelli L., Galizziell A., Curti B., Zanetti G., 1993. Glutamate synthase genes of the diazotroph Azospirillum brasilense. Cloning, sequencing, and analysis of functional domains, *Journal of Biological Chemistry*, **268**, 3099-3106.

Petoukhov M.V., Svergun D. L.,Konarev P. V., Ravasio S., van den Heuvel R. R. H., Curti B., and Vanoni M. A.,, 2003. Quaternary Structure of *Azospirillum brasilense* NADPH-dependent Glutamate Synthase in Solution as Revealed by Synchrotron Radiation X-ray Scattering, *The Journal of Biological Chemistry,* **278**, 29933–29939.

Ravasio, S., Curti, B., and Vanoni, M. A., 2001. Determination of Midpoint Potential of thebFAD and FMN Flavin Cofactors and of the 3Fe-4S Cluster of Glutamate Synthase, *Biochemistry,* **40**, 5533–5541.

Ratti, S., Curti, B., Zanetti, G. & Galli, E., 1985. Purification and characterization of glutamate synthase from *Azospirillum brasilense*, *J Bacteriol,* **163**, 724-729.

Reitzer, L., 2003. Nitrogen assimilation and global regulation in Escherichia coli, *Annu. Rev. Microbiol,*. **57**, 155–176.

Rosenbaum, K., Jahnke, K., Curti, B., Hagen, W. R., Schnackerz, K., and Vanoni, M. A., 1998. Porcine Recombinant Dihydropyrimidine Dehydrogenase: Comparison of the Spectroscopic and Catalytic Properties of the Wild-Type and C671A Mutant Enzymes, *Biochemistry, **37,*** 17598- 17609.

Sambrook, J., Maniatis, T., Fritsch, E. F., 1989. Molecular Cloning. A Laboratory Manual. Cold Spring Harbor, NY: Cold Spring Harbor Laboratory Press.

Saitou, N., Nei, M., 1987. The neighbor-joining method: A new method for reconstructing phylogenetic trees, *Molecular Biology and Evolution*, **4**, 406-425.

Sakakibara H., Watanabe M., Hase T., Sugiyama T., 1991. Molecular cloning and characterization of complementary DNA encoding for ferredoxin-dependent glutamate synthase in maize leaf, *J. Biol. Chem.*, **266**, 2028–2035.

Scrutton, N. S., A. Berry, and R. N. Perham, 1990. Redesign of the coenzyme specificity of a dehydrogenase by protein engineering, *Nature*, **343**, 38-43.

Schut, G.J., Brehm, S.D., Datta, S., Adams, W.W.M., 2003. Whole-Genome DNA Microarray Analysis of a Hyperthermophie and an Archaeon: *Pyrococcus furiosus* Grown on Carbohydrates or Peptides, *Journal of Bacteriology,* **185**, 3935-3947.

Senior, P.J., 1975. Regulation of nitrogen metabolism in *Escherichia coli* and *Klebsiella aerogenes*: studies with the continuous-culture technique, *Journal of Bacteriology*, **123**, 407-418.

Shine J and Dalgarno L., 1975. Determinant of cistron specificity in bacterial ribosomes, *Nature*, **254**:34-38.

Silva, P.J., d. B.E.C., Wassink, H., de Haaker, H.C.B., Robb, F.T., and Hagen, W.R., 2000. Enzymes of hydrogen metabolism in *Pyrococcus furiosus*, *Eur J Biochem.,* **267**, 6541–6551.

Stabile H, Curti B, Vanoni MA, 2000. Functional properties of recombinant Azospirillum brasilense glutamate synthase, a complex iron-sulfur flavoprotein, *Eur. J. Biochem.*, **267**, 2720-2730.

Stutz, H. E., Reid, S. J., 2004. GltX from *Clostridium saccharobutylicum* NCP262: glutamate synthase or oxidoreductase?, *Biochimica et Biophysica Acta*., **1676**, 71-82.

Temple S.J., Vance C.P., Gantt J.S., 1998. Glutamate synthase and nitrogen assimilation, *Trends in Plant Science*, **3**, 51–56.

Tempest DW, Meers JL, Brown CM, 1970. Synthesis of glutamate in *Aerobacter aerogenes* by a hitherto unknown route, *Biochem. J.*, **117**, 405-407.

Tobin A.K., Yamaya T., 2001. Celular compartmentation of ammonium assimiltaion in rice and barley, *J. Exp. Bot.*, **52**, 591-604.

Vanoni M. A., Curti B., 1999. Glutamate synthase: a complex iron-sulfur flavoprotein, *Cellular and Molecular Life Sciences (CMLS)*, **55**, 617-638.

Vanoni B. A. Curti B., 2005. Structure–function studies on the iron–sulfur flavoenzyme glutamate synthase: an unexpectedly complex self-regulated enzyme, *Archives of Biochemistry and Biophysics*, **433**, 193–211.

Vanoni M. A., Edmondson D. E., Zanetti G., Curti B., 1992. Characterization of the flavins and the iron-sulfur centers of glutamate synthase from Azospirillum brasilense by absorption, circular dichroism, and electron paramagnetic resonance spectroscopies, *Biochemistry*, **31**, 4613–4623.

Vanoni M. A., Fischer F.,Ravasio S.,Verzotti E.,Edmondson E. D., Hagen W. R.,Zanetti G.,and Curti B., 1998. The Recombinant α Subunit of Glutamate Synthase: Spectroscopic and Catalytic Properties, *Biochemistry,* **37***,* 1828-1838 (1998)

Vanoni M. A., Verzotti E., Zanetti G., Curti B., 1996. Properties of recombinant β subunit of glutamate synthase, *Eur. J. Biochem.*, **236**, 937-946.

Verhees, C.H., Kengen, S.W.M., Tuininga, J.E., Schut, G.J., Adams, M.W.W., de Vos, W.M. and van der Oost, J., 2003. The unique features of glycolytic pathways in Archaea., *Biochem. J.,* **375**, 231-246.

Zalkin, H., & Smith, J. L., 1998. Enzymes utilizing glutamine as an amide donor. *Advances in Enzymology,* **72***,* 87-144.

Zivanovic Y., **Lopez P., Philippe H., and Forterre P.,** 2002. *Pyrococcus* genome comparison evidences chromosome shuffling-driven evolution, *Nucleic Acids Res*., **30**: 1902 - 1910.

----, http://biology200.gsu.edu/houghton/4595%20'04/lecture25.html, May 6, 2006.

----, http://www.bio. nite.go.jp/dogan/MicroTop?GENOME_ID=ot3, May 6, 2006.

----, http://www.ucmp. berkeley.edu/ archaea/archaeasy.html, May 6, 2006.

----, http://nai.arc.nasa.gov/news_stories/news_ detail. c fm?article =old/ understanding_life.htm, May 6, 2006.

APPENDIX

Hyperthermophilic Archaea

Genus	Species	T_{MAX} (°C)	Hetero/auto	Aerobe/anaerobe
Acidianus	*infernus*	96	A	FAN
Aeropyrum	*pernix*	100	H	AE
Archaeoglobus	*fulgidus*	95	FA	AN
	profundus	90	A	AN
Caldivirga	*maquilingensis*	92	H	FAN
Caldococcus	*litoralis*	100	H	AN
	noboribetus	96	H	AN
Desulfurococcus	*amylolyticus*	97	H	AN
	mobilis	97	H	AN
	mucosus	97	H	AN
Ferroglobus	*placidus*	95	FA	AN
Hyperthermus	*butylicus*	108	H	AN
Methanococcus	*fervens*	92	A	AN
	igneus	91	A	AN
	infernus	91	A	AN
	jannaschii	94	A	AN
Methanopyrus	*kandleri*	110	A	AN
Methanothermus	*fervidus*	97	A	AN
	sociabilis	97	A	AN
Pyrobaculum	*aerophilum*	104	FA	FAN
	islandicum	102	FA	AN
	organotrophum	102	H	AN
Pyrococcus	*abyssi*	108	H	AN
	endeavori (ES4)	110	H	AN
	furiosus	103	H	AN
	horikoshii	102	H	AN
	woesei	104	H	AN
Pyrodictium	*abyssi*	110	H	AN
	brockii	110	A	AN
	occultum	110	A	AN
Pyrolobus	*fumarii*	113	A	FAN
Staphylothermus	*marinus*	98	H	AN
Stetteria	*hydrogenophila*	102	H	AN
Sulfophobococcus	*zilligii*	95	H	AN

Figure A: Taxonomy of hyperthermophilic organisms and their metabolic properties (Amend and Shock, 2001).

Sulfurisphaera	*ohwakuensis*	92	H	FAN
Thermococcus	*acidaminovorans*	93	H	AN
	aggregans	94	H	AN
	alcaliphilus	90	H	AN
	barophilus	100	H	AN
	barossi	92	H	AN
	celer	93	H	AN
	chitonophagus	93	H	AN
	fumicolans	103	H	AN
	gorgonarius	95	H	AN
	guaymasensis	90	H	AN
	hydrothermalis	100	H	AN
	litoralis	98	H	AN
	pacificus	95	H	AN
	peptonophilus	100	H	AN
	profundus	90	H	AN
	siculi	93	H	AN
	stetteri[b]	98	H	AN
Thermodiscus	*maritimus*	98	H/A[c]	AN
Thermofilum	*pendens*	100	H	AN
Thermoproteus	*neutrophilus*	85[a]	A	AN
	tenax	96	FA	AN
	uzoniensis	102	H	AN
Thermosphaera	*aggregans*	90	H	AN

Figure A: Continuing. Taxonomy of hyperthermophilic organisms and their metabolic properties (Amend and Shock, 2001).

RESUME

Hande Akçe was born in Bursa, in 1981. Following her graduation from Bursa Milli Piyango Anatolian High School, in 1999, she started her studies in Department of Molecular Biology and Genetics, Istanbul Technical University (ITU). She received her Bachelor degree in 2003. She was accepted to Molecular Biology-Genetics and Biotechnology Program in Department of Molecular Biology and Genetics at the same year where she continues her studies.